Chapter 7

GEOMECHANICS

GEOTECHNICAL DESIGN MANUAL

January 2022

Table of Contents

List of Tables

List of Figures

CHAPTER 7

GEOMECHANICS

7.1 INTRODUCTION

This Chapter presents the geotechnical design philosophy of SCDOT. This philosophy includes the approach to the geotechnical investigations of the project and the correlations that link the field and laboratory work that precedes this Chapter to the engineering analysis that is subsequent to this Chapter. The approach to the geotechnical investigation of transportation projects entails the use of preliminary and final explorations and reports. The development of an understanding of the regional and local geological environment and the effect of seismicity on the project is required. The geotechnical approach provided in this Chapter is not meant to be the only approach, but a representative approach of the thought process expected to be used on SCDOT projects. The GEOR shall develop a design approach that reflects both the requirements of this Manual as well as a good standard-of-practice. While there is some flexibility in the approach to the design process, the correlations provided in this Chapter shall be used unless written permission is obtained in advance. All requests for changes shall be submitted to the OES/GDS for review and approval. These correlations were adopted after a review of the geotechnical state-of-practice within the United States and the experience of SCDOT.

7.2 GEOTECHNICAL DESIGN APPROACH

Geotechnical engineering requires the use of science, art, and economics to perform analyses and designs that are suitable for the public use. The science of geotechnical engineering consists of using the appropriate theories to interpret field data; develop geologic profiles; select foundation types; perform analyses; develop designs, plans and specifications; construction monitoring; maintenance; etc.

The art of geotechnical engineering is far more esoteric and relies on the judgment and experience of the engineer. This is accomplished by knowing the applicability and limitations of the geotechnical analytical theories and assessing the uncertainties associated with soil properties, design methodologies, and the resulting impact on structural performance. The engineer is required to evaluate the design or analysis and decide if it is "reasonable" and whether it will meet the performance expectations that have been established. Reasonableness is a subjective term that depends on the engineer's experience, both in design and construction. If the solution does not appear reasonable, the engineer should make the appropriate changes to develop a reasonable solution. In addition, the engineer should document why the first solution was not reasonable and why the second solution is reasonable. This documentation is an important part of the development of the design approach. If the solution appears reasonable, then the design proceeds to the economics of geotechnical engineering.

The economics of geotechnical engineering assesses the effectiveness of the solution from a cost perspective. Sometimes geotechnical engineers get caught up in the science and art of geotechnical engineering and do not evaluate other non-geotechnical solutions that may be cost effective both in design and construction. For example, alternate alignments could be explored to avoid poor soils, decreasing vertical alignment to reduce surface loads, placing alternate designs on the plans to facilitate competitive bidding, etc. The science, art, and economics are not sequential facets of geotechnical engineering but are very often intermixed throughout the design process.

7.3 DEVELOPMENT OF SUBSURFACE PROFILES

The SCDOT geotechnical field exploration process indicated in Chapter 4, allows for a preliminary and a final geotechnical exploration program for all projects. The primary purpose of the preliminary exploration is to provide a first glance at the project, while the final exploration is to provide all of the necessary geotechnical information to complete the final design.

It is incumbent upon the GEOR to understand the geology of the project site and determine the potential effects of the geology on the project. The GEOR should also have knowledge of the regional geology that should be used in the development of the exploration program for the project. In addition to the geologic environment, the GEOR shall be aware of the seismic environment (see Chapters 11 and 12). The GEOR is also required to know and understand the impacts of the design earthquake event on the subsurface conditions at the project site (see Chapters 13 and 14 for the impacts and designs, respectively). The geologic formation and local seismicity may have a bearing on the selection of the foundation type and potential capacity. For example, for driven piles bearing in the Cooper Marl formation of the Charleston area, prestressed concrete piles should penetrate the formation approximately 5 feet, with most of the capacity being developed by steel H-pile extensions, penetrating into the Marl.

The GEOR shall develop a subsurface profile for both the preliminary and final geotechnical subsurface explorations. The subsurface profile developed shall take into consideration the site variability as indicated in Section 7.5. The profile should account for all available data and is normally depicted along the longitudinal axis of the structure or roadway. The bridge profile shall extend from 100 feet from either end of the bridge, inclusively. However, in some cases, cross-sectional subsurface profiles transverse to the axis of the structure or roadway may be required to determine if a formation is varying (i.e., sloping bearing strata) along the transverse axis.

7.4 SITE VARIABILITY

Keeping in mind the geologic framework of the site, the GEOR shall evaluate the site variability (SV) or site uniformity. The SV is used in determining the resistance factor, φ, and the required amount of load testing for deep foundations (see Chapter 9). A site with “Low” SV is more uniform than a site with “High” SV. A “High” SV shall not be allowed except with review and approval by the OES/GDS. All “High” variability, unless previously approved, sites shall be subdivided into smaller “sites” such that the SV is either “Low” or “Medium”. All “sites” shall be geologically continuous (i.e., shall contain similar soils). The SV shall be determined using energy corrected SPT N-values (N_{60}) (see Section 7.8.1.6 and Equation 7-6), or the corrected tip resistance (q_t) from the CPT or the RQD for rock cores. Other site factors such as undrained shear strength, etc., may be used to determine the SV, only with the prior written permission of the OES/GDS. The Coefficient of Variation (COV) shall be determined on the bearing stratum at each testing location using the following equation.

$$\boldsymbol{COV = \frac{\sigma}{\bar{x}}}$$ **Equation 7-1**

Where,

σ = Standard deviation

$\bar{x}$ = Mean (average) value

The σ and $\overline{x}$ shall be determined using statistical equations that are generally recognized. An average COV ($\overline{COV}$) shall be developed based on the results of the individual test location COVs. The $\overline{COV}$ shall be used to determine the SV using Table 7-1.

Table 7-1, Site Variability Defined By $\overline{COV}$

Site Variability (SV)	$\overline{COV}$
Low	< 25%
Medium	$25\% \leq \overline{COV} < 40\%$
High	40% ≤

7.5 PRELIMINARY GEOTECHNICAL SUBSURFACE EXPLORATION

Prior to the commencement of the preliminary exploration, the GEOR shall visit the site and conduct a GeoScoping. The GeoScoping consists of the observation of the project site to identify areas that may impact the project from the geotechnical perspective. These areas shall be selected for exploration during the preliminary exploration if the site is located within the existing SCDOT ROW. If the areas of concern are located outside of the existing SCDOT ROW, then these areas shall be investigated as early as possible in the project development process. For projects conducted by SCDOT, the results of the GeoScoping shall be reported on the appropriate forms (see Appendix A). For non-in-house projects, the GEC shall use the form developed and approved by the GEC firm. The form shall be included in the Appendix to the preliminary geotechnical report. An engineering professional with experience in observing and reviewing sites for potential geotechnical concerns shall be responsible for conducting the GeoScoping.

The preliminary exploration requirements are detailed in Chapter 4, while the contents of the preliminary geotechnical report are detailed in Chapter 21. The primary purpose of the preliminary exploration is to provide an initial assessment of the project. Typically, there will be few project details available prior to conducting the preliminary exploration; however, the most important details that will be known are what type of project it is (i.e., bridge replacement, new road, intersection improvement, etc.) and where the project is located. In many cases, the final alignment and structure locations may not be known. The primary purpose of this type of exploration is not to provide final designs, but to determine if there are any issues that could significantly affect the project. These issues should be identified and the potential impacts and consequences of these design issues should be evaluated by the project design team. Design issues should be identified and documented for additional exploration during the final geotechnical exploration. If the project is located completely within the SCDOT ROW, then the entire exploration may be performed during the preliminary exploration phase of the project; however, the report prepared shall be a preliminary report that meets the requirements of Chapter 21.

7.6 FINAL GEOTECHNICAL SUBSURFACE EXPLORATION

The final geotechnical exploration shall conform to the requirements detailed in Chapter 4, while the contents of the final geotechnical report shall conform to the requirements detailed in Chapter 21. The final exploration shall be laid out to use the testing locations from the preliminary exploration to the greatest extent possible without compromising the results of the final exploration. The final exploration shall include those areas identified during the preliminary exploration or during the GeoScoping as requiring additional investigation. If these areas impact the performance of the project, these impacts shall be brought to the immediate attention of the Design/Program Manager or the project team leader for consultant designed projects. In addition, the GEOR shall also include recommended mitigation methods.

7.7 FIELD DATA CORRECTIONS AND NORMALIZATION

In-situ testing methods such as the SPT, the CPTu, and the DMT may require corrections or adjustments prior to using the results for soil property correlation or for direct use in design. These in-situ testing methods are described in Chapter 5. The SPT and CPTu field data are most commonly corrected or normalized to account for overburden pressure, energy, rod length, non-standard sampler configuration, borehole diameter, fines content, and the presence of thin very stiff layers. The data obtained from the DMT is corrected for the effects of the instrument operation on the results of the testing. All corrections for in-situ testing methods that are used in geotechnical design and analyses shall be documented in the geotechnical report. The following sections discuss corrections and adjustments in greater detail.

7.7.1 SPT Corrections

Many correlations exist that relate the corrected N-values to relative density (D_r), peak effective angle of internal friction (ϕ'), undrained shear strength (S_u), and other parameters; therefore it is incumbent upon the designer to understand the correlations being used and the requirements of the correlations for corrected N-values. Design methods are available for using N-values directly in the design of driven piles, embankments, spread footings, and drilled shafts. These corrections are especially important in soil Shear Strength Loss (SSL) potential assessments (Chapter 13). Design calculations using SPT N-value correlations should be performed using corrected N-values; however, only the actual field SPT N_{meas}-values should be plotted on the soil test boring logs and profiles depicting the results of SPT borings. Each of the corrections is discussed in greater detail in the following Sub-sections.

7.7.1.1 Energy Correction (C_E)

The type of hammer used to collect split-spoon samples shall be noted on the boring logs. Typically correlations used between soil parameters and N-values are based on a hammer system having a transferred energy of 60 percent of the theoretical maximum. A split-spoon sampler advanced with a manual safety hammer has historically been assumed to have an approximate transferred energy of 60 percent (ER ≈ 60%); although, the relatively recent ability to make actual energy measurements has indicated that this assumption is not necessarily valid. The energy ratio (ER) is the measured energy divided by the theoretical maximum (i.e., 140-pound hammer dropping 30 inches or 4,200 inch-pounds). The measured energy is determined as discussed in Chapter 5.

The split-spoon sampler is also advanced with either an automatic hammer (measured ER is typically greater than 60%); a manual safety hammer (measured ER is typically 60%); or a manual donut hammer (measured ER is typically less than 60%) **[<u>Reminder:</u>** ***The use of the donut hammer is not permitted*****]**. The corrections for the donut hammer are provided for information only since some past projects were performed using the donut hammer. N-values obtained using either the automatic or the manual safety hammer will require correction prior to being used in engineering analysis. As indicated in Chapter 5, the measured transferred energy (ER) for each drill-rig and hammer shall be determined. The energy correction factor (C_E) shall be determined using the following equation.

$$C_E = \frac{ER}{60} \qquad \textbf{Equation 7-2}$$

$$ER = \frac{E_{meas}}{E_{theor}} = \frac{E_{meas}}{4{,}200} \qquad \textbf{Equation 7-3}$$

Where,

E_{meas} = Measured energy (see Chapter 5 for determination)

ER is expressed as an integer (i.e., 90 percent energy is ER = 90) in Equation 7-2. The C_E values provided in Table 7-2 for each hammer type shall only be used on boring logs where the hammer energy transfer ratio is not provided. In addition, if the hammer type is not indicated and the boring was obtained prior to the year 2000, the hammer shall be assumed to be a manual safety hammer.

Table 7-2, Assumed Energy Ratio by Hammer Type (C_E)

Hammer Type	Energy Ratio (ER) %	C_E
Automatic	80	1.33
Safety	60	1.00
Donut	45	0.75

7.7.1.2 Overburden Correction (C_N)

N_{meas}-values in Sand-Like soils will increase with depth due to increasing overburden pressure. The overburden correction is used to standardize all N-values to a reference overburden pressure. The reference overburden pressure is 1 ton per square foot (tsf) (1 atmosphere). The overburden correction factor (C_N) (Liao and Whitman (1986)) for coarse-grained soils is provided below. A C_N of 1.0 shall be used for Clay-Like soils.

$$C_N = \left(\frac{1}{\sigma'_v}\right)^{0.5} \leq 1.7 \qquad \textbf{Equation 7-4}$$

Where,

σ'_v = Effective overburden stress, tsf

7.7.1.3 Rod Length Correction (C_R)

N_{meas}-values measured in the field should be corrected for the length of the rod used to obtain the sample. The original N_{60}-value measurements were obtained using long rods (i.e., rod length greater than 33 feet); therefore, a correction to obtain "equivalent" N_{60}-values for short rod length (i.e., rod length less than 33 feet) is required. Typically, the rod length will be the depth of the sample (d) plus an assumed 5 feet of stick up above the ground surface. The rod length correction factor (C_R) equation is provided below with typical values presented in Table 7-3 (McGregor and Duncan (1998)).

$$C_R = e^{-e^{(-0.11d-0.55)}}$$ **Equation 7-5**

Where,

d = Depth of sample, ft

Table 7-3, Rod Length Correction (C_R)

Rod Length (feet)	C_R
< 13	0.75
13 – 20	0.85
20.1 – 33	0.95
> 33	1.00

7.7.1.4 Sampler Configuration Correction (C_S)

The sampler configuration correction factor (C_S) (Cetin et al. (2004)) is used to account for samplers designed to be used with liners, but the liners are omitted during sampling. If the sampler is not designed for liners or if the correct size liner is used no correction is required (i.e., C_S = 1.0). When liners are omitted there is an increase to the inside diameter of the sampler; therefore, the friction between the soil and the sampler is reduced. The sampler configuration correction factor is presented in Table 7-4.

Table 7-4, Sampler Configuration Correction (C_S)

Sampler Configuration	C_S
Standard Sampler not designed for liners	1.0
Standard Sampler designed for and used with liners	1.0
Standard Sampler designed for liners and used without liners:	
$N_{meas} \leq 10$	1.1
$11 \leq N_{meas} \leq 29$	$1 + N_{meas}/100$
$30 \leq N_{meas}$	1.3

7.7.1.5 Borehole Diameter Correction (C_B)

The borehole diameter affects the N_{meas}-value if the borehole diameter is greater than 4.5 inches. Large diameter boreholes allow for stress relaxation of the soil materials. This stress relaxation can be significant in Sand-Like soils, but has a negligible effect in Clay-Like soils. Therefore, for Clay-Like soils use C_B equal to 1.0. Listed in Table 7-5 are the borehole diameter correction factors (C_B) for Sand-Like soils (McGregor and Duncan (1998)).

Table 7-5, Borehole Diameter Correction (C_B)

Borehole Diameter (inches)	C_B
2-1/2 – 4-1/2	1.00
6	1.05
8	1.15

7.7.1.6 Corrected N-values

As indicated previously, the N-values measured in the field (N_{meas}) require corrections or adjustments prior to being used for the selection of design parameters or in direct design methods. The N-value requirements of the correlations or the direct design methods should be well understood and known to the GEOR. Please note that the correction for fines content has been intentionally left out of this Section. The correction for fines content is used only in the determination of soil SSL (see Chapter 13). Corrections typically applied to the N_{meas}-values are listed in the following equations.

$$N_{60} = N_{meas} * C_E \quad \textbf{Equation 7-6}$$

$$N_{1,60} = N_{60} * C_N \quad \textbf{Equation 7-7}$$

$$N^*_{60} = N_{60} * C_R * C_S * C_B \quad \textbf{Equation 7-8}$$

$$N^*_{1,60} = N^*_{60} * C_N \quad \textbf{Equation 7-9}$$

7.7.2 CPTu Corrections

The CPTu corrected tip resistance (q_t, see Chapter 6) and sleeve resistance (f_s) require corrections to account for the effect of overburden on the tip and sleeve resistance. The tip resistance may also be corrected to account for thin stiff layers located between softer soil layers. These corrections are discussed in the following Sub-sections.

7.7.2.1 Effective Overburden Normalization

The corrected CPTu tip resistance (q_t) and sleeve resistance (f_s) in Sand-Like soils are influenced by the effective overburden stress. This effect is accounted for by normalizing the measured resistances to a standard overburden stress of 1 tsf (1 atm). The normalized and corrected CPTu tip resistance ($q_{t,1}$) and sleeve resistance ($f_{s,1}$), for Sand-Like soils are provided below. A C_N of 1.0 shall be used for Clay-Like soils.

$$q_{t,1} = C_N * q_t \quad \textbf{Equation 7-10}$$

$$f_{s,1} = C_N * f_s \quad \textbf{Equation 7-11}$$

Where,

q_t = Corrected CPTu tip resistance, tsf (1 MPa ≅ 10.442 tsf) (see Chapter 6 for correction)

f_s = Measured CPTu sleeve resistance, tsf (1 MPa ≅ 10.442 tsf)
C_N = Overburden normalization factor is the same for $q_{t,1}$ and $f_{s,1}$ as indicated in Equation 7-4.

7.7.2.2 Thin Layer Correction

When the corrected CPTu tip resistance (q_t) is obtained in a thin layer of Sand-Like soil that is embedded between softer surrounding soils, the corrected tip resistance (q_t) will be reduced due to the effects of the underlying softer soils. This commonly occurs in fluvial environments where Sand-Like soils are interbedded between layers of Clay-Like soils. Sand-Like soils that are affected by this reduction in corrected tip resistance (q_t) are typically Sand-Like layers that are less than 3-1/2 feet (~1,074 mm) thick and where the ratio of the corrected tip resistance of the Sand-Like soil (q_{tA}) is twice the corrected tip resistance of the Clay-Like soil (q_{tB}) (see Figure 7-1). This correction only applies to thin Sand-Like layers (i.e., less than 3-1/2 feet thick). The CPTu tip resistance for this special case is normalized and corrected for the thin layer ($q_{t,1,Thin}$) and is computed as indicated in the following equation.

$$q_{t,1,Thin} = C_{Thin} * (q_{t,1}) \qquad \textbf{Equation 7-12}$$

Where,

$q_{t,1}$ = Normalized and corrected CPTu tip resistance, MPa (1 MPa ≅ 10.442 tsf)
C_{Thin} = Thin layer correction factor and is determined from the following equation and is depicted in Figure 7-2.

$$\mathrm{C_{Thin}} = 1.0 + 0.25\left[\left(\frac{\left(\frac{H}{d_c}\right)}{17}\right) - 1.77\right]^2 \qquad \textbf{Equation 7-13}$$

Where,

H = Thickness of the soil layer less than or equal to 1,074 mm, millimeters (mm)
d_c = diameter of cone, mm (35.7 mm for a standard 10 cm^2 cone)

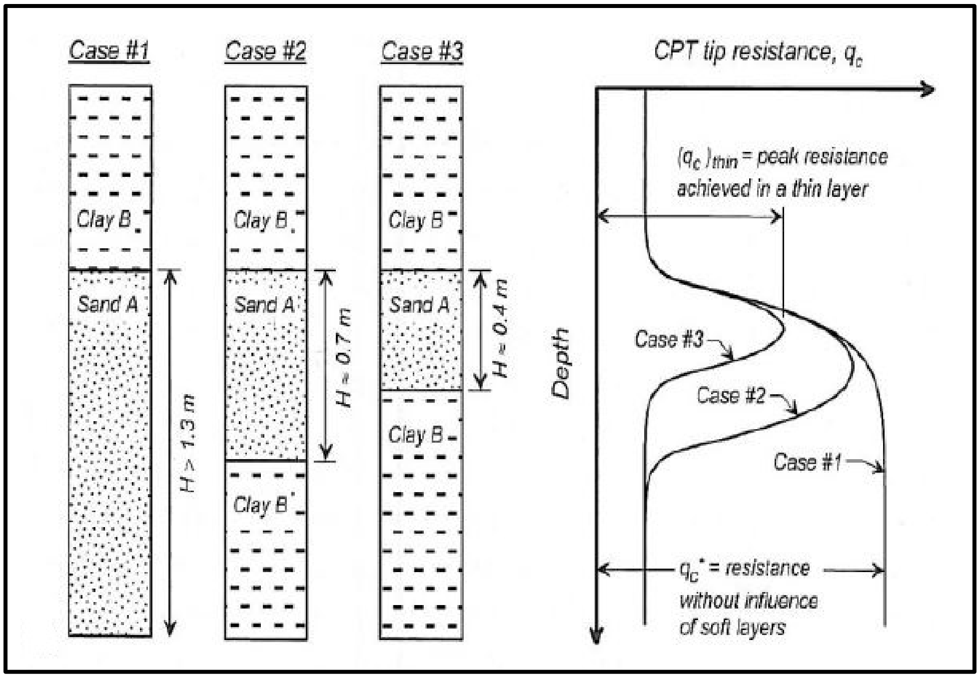

Figure 7-1, Schematic of Thin Layer Effects (Idriss and Boulanger (2008))

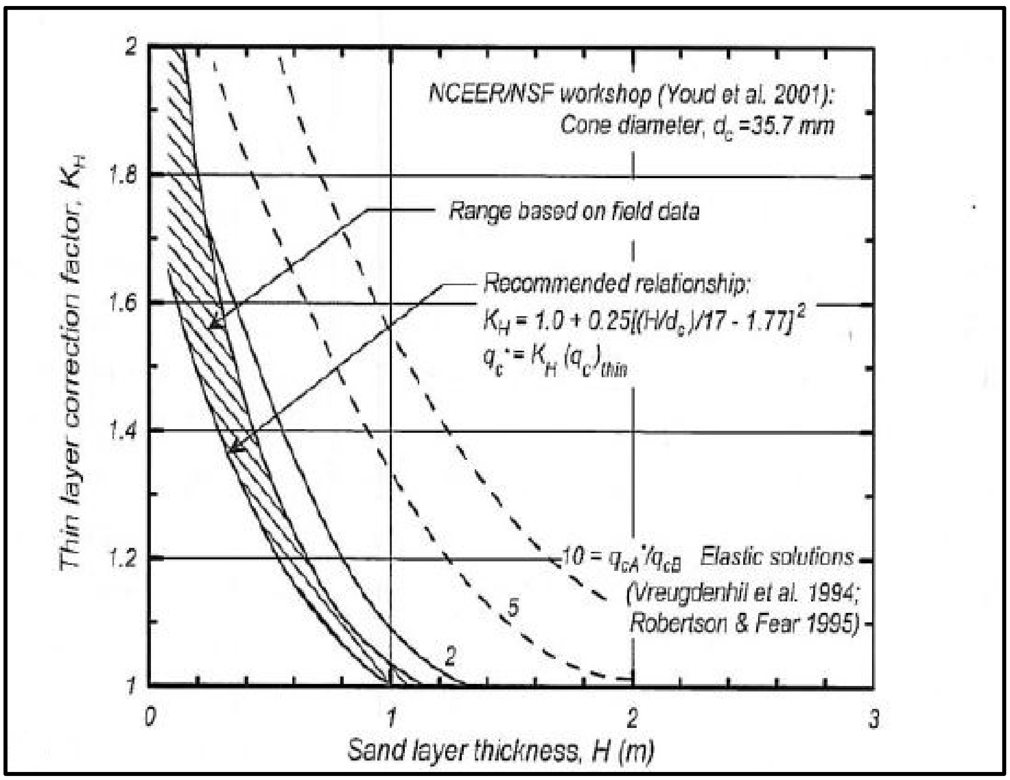

Note: $K_H = C_{Thin}$

Figure 7-2, CPTu Thin Layer Correction (C_{Thin}) (Idriss and Boulanger (2008))

7.7.2.3 Soil Behavior Type and Normalization of CPTu Data

The Soil Behavior Type, I_c, is computed using normalized tip resistance (Q_T) and normalized sleeve friction (F_R). The normalized corrected CPTu tip resistance ($q_{t,1,Thin,N}$) is computed by dividing the corrected CPTu resistance ($q_{t,1,Thin}$) by the atmospheric pressure (P_a = 1 atm = 1 tsf) to eliminate units. The following equations should be used.

$$Q_T = \frac{q_{t,1,Thin} - \sigma_v}{\sigma'_v}$$ **Equation 7-14**

$$F_R = \left(\frac{f_{s,1}}{q_{t,1,Thin} - \sigma_v}\right) * 100$$ **Equation 7-15**

$$B_q = \frac{(u_2 - u_0)}{(q_{t,1,Thin} - \sigma_v)}$$ **Equation 7-16**

$$q_{t,1,Thin,N} = \frac{q_{t,1,Thin}}{P_a}$$ **Equation 7-17**

Where,

$q_{t,1,Thin}$ = Normalized, corrected and thin layer corrected tip resistance, tsf
$f_{s,1}$ = Where f_s is the normalized CPTU cone tip resistance, tsf
σ'_v = Effective overburden pressure, tsf
σ_v = Total overburden pressure, tsf
u_2 = Pore pressure measurement located on the tip shoulder, tsf
u_0 = Hydrostatic water pressure, tsf

The Soil Behavior Type, I_c, is computed using the following equation.

$$I_c = \sqrt{(3.47 - \log Q_T)^2 + (1.22 + \log F_R)^2}$$ **Equation 7-18**

The I_c can be generally correlated to a soil classification as indicated in Chapter 6 and using Figure 7-3 to relate Q_T to B_q. The numbers indicated in each zone correspond to the CPTu soil behavior type indicated in Chapter 6.

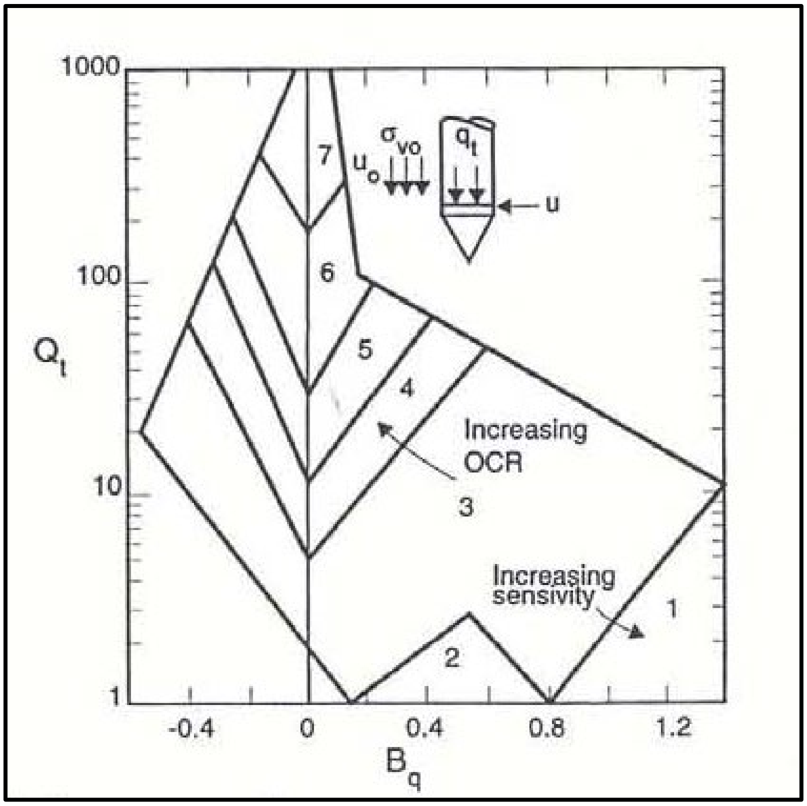

Figure 7-3, Normalized CPT Soil Behavior Chart Using Q_T versus B_q
(Robertson and Cabal (2015))

7.7.3 Correlations for Relative Density From SPT and CPTu

Correlations to compute relative density (D_r) from SPT and CPTu testing may be required for soil SSL analyses. The correlations proposed by Boulanger (2003) to relate SPT N-values ($N^*_{1,60}$) and CPTu tip resistance ($q_{t,1,Thin,N}$) to relative density (D_r) are provided below.

$$D_r = \left[\left(\frac{N^*_{1,60}}{46}\right)^{0.5}\right] * 100\%$$ **Equation 7-19**

Where,

$$N^*_{1,60} \leq 46\ bpf$$

Equation 7-20

$$D_r = \left[0.478 * \left(q_{t,1,Thin,N}\right)^{0.264} - 1.063\right] * 100\%$$

Where,

$$q_{t,1,Thin,N} \leq 254$$

Where,

$N^*_{1,60}$ = Corrected SPT N-value, blows per foot
$q_{t,1,Thin,N}$ = Normalized, corrected and thin layer corrected tip resistance, unitless
D_r = Relative Density in percent

The relative density correlations (Equations 7-19 and 7-20) for SPT and CPTu results can be combined to develop an SPT equivalent correlation for normalized CPTu tip resistance as indicated by the following equation.

$$N^*_{1,60} = 46 * \left[0.478 * \left(q_{t,1,Thin,N}\right)^{0.264} - 1.063\right]^2$$ **Equation 7-21**

Alternatively, Jefferies and Davies (1993) recommend a correlation between q_t and N_{60}. This correlation has modified to the following equation.

$$N_{60} = \left(\frac{q_t}{p_a}\right) \Big/ \left[8.5 - \left(1 - \frac{I_c}{4.6}\right)\right]$$ **Equation 7-22**

Where,

q_t = Corrected CPTu tip resistance, tsf
p_a = Atmospheric Pressure (1 tsf = 1 atm), tsf
I_c = Soil Behavior Type, dimensionless

7.7.4 Dilatometer Correlation Parameters

Using the corrected pressure readings, p_0, p_1 and p_2 (see Chapter 6), the horizontal stress index (K_D), the material index (I_D), the Dilatometer modulus (E_D) and the pore pressure index (U_D) shall be reported for all DMT results. The following equations shall be used.

$$K_D = \frac{(p_0 - u_0)}{\sigma'_{vo}}$$ **Equation 7-23**

$$I_D = \frac{(p_1 - p_0)}{(p_0 - u_o)}$$ **Equation 7-24**

$$E_D = 34.7 * (p_1 - p_0)$$ **Equation 7-25**

$$U_D = \frac{(p_2 - u_0)}{(p_0 - u_0)}$$ **Equation 7-26**

Where,

p_0 = Corrected A-pressure, bars (1 bar ≈ 1 tsf)
p_1 = Corrected B-pressure, bars (1 bar ≈ 1 tsf)
p_2 = Corrected C-pressure, bars (1 bar ≈ 1 tsf)
σ'_{vo} = Effective overburden stress, tsf (1 bar ≈ 1 tsf)
u_0 = Equilibrium pore pressure, bars (1 bar ≈ 1 tsf)

7.8 SOIL LOADING CONDITIONS AND SOIL SHEAR STRENGTH SELECTION

Geotechnical engineering as presented in this Manual has a statistical (LRFD) and performance-base design component that requires selection of appropriate soil properties in order to design within an appropriate margin of safety consistent with Chapter 9 and also to predict as reasonably as possible the geotechnical performance required in Chapter 10. The selection of soil shear strengths by the GEOR requires that the designer have a good understanding of the loading conditions and soil behavior, high quality soil sampling and testing, and local geotechnical experience with the various geologic formations. This Section provides guidance in the selection of shear strengths for Clay-Like soils (i.e., clays and plastic silts) and Sand-like soils (i.e., sands and nonplastic silts) for use in geotechnical design. The selection of shear strength parameters for rock is covered in Section 7.14.

An in-depth review of the topics addressed in this Section is provided in Sabatini, Bachus, Mayne, Schneider and Zettler (2002); Duncan and Wright (2005) and Duncan, Wright and Brandon (2014).

Geotechnical load resisting analyses that are typically performed in the design of transportation facilities are bearing resistance of a shallow foundation, axial (tension and compression) load resistance of deep foundations (drilled shafts and piles), lateral load resistance of deep foundations, stability analyses of hillside slopes and constructed embankments, sliding resistance of ERSs, and passive soil resistance. Each of these analyses can have various loading conditions that are associated with the limit state (Strength, Service, and Extreme Event) under evaluation.

Soil shear strength is not a unique property and must be determined based on the anticipated soil response for the loading condition being evaluated. This requires the following 3-step evaluation process:

1. **Evaluate the Soil Loading**: The soil loading should be investigated based on the soil loading rate, the direction of loading, and the boundary conditions for the limit state (Strength, Service, Extreme Event) being evaluated.
2. **Evaluate Soil Response**: The soil response should be evaluated based on pore pressure build-up (Δu), the soil's state of stress, and volumetric soil changes during shearing, and the anticipated magnitude of soil deformation or strain for the soil loading being applied.
3. **Evaluate Appropriate Soil Strength Determination Method:** This consists of determining the most appropriate soil testing method that best models the loading condition and the soil response for determination of soil shear strength design parameters. Also included in this step is the review of the results for reasonableness based on available correlations and regional experience.

The 3-step evaluation process is discussed in detail in the following Sections.

7.8.1 Soil Loading

The soil loading can be evaluated with respect to loading rate, direction of loading, and boundary conditions. The loading rate primarily affects the soil's response with respect to pore water pressure build-up (Δu). When the loading rate either increases or decreases the pore water pressure ($\Delta u \neq 0$), the loading is referred to as short-term loading. Short-term loading, during or immediately after construction, typically occurs in Clay-Like soils, because these soils drain much slower than Sand-Like soils which allows for an increase or decrease in pore pressures (Δu) during loading. Conversely, if the loading rate does not affect the pore water pressure ($\Delta u = 0$), the loading is referred to as a long-term loading. Sand-Like soils, typically, do not build pore pressures, because drainage is relatively rapid. Therefore, long-term loading conditions would be applicable even immediately after the completion of construction. The next Section discusses the response of the soil in greater detail.

Short-term loadings typically occur during construction such as when earth-moving equipment places large soil loads within a relatively short amount of time. The actual construction equipment (cranes, dump trucks, compaction equipment, etc.) should also be considered during the evaluation of construction loadings. Construction loadings are typically evaluated under the Strength limit state. Earthquakes or impacts (vessel or vehicle collisions) that can apply a significant amount of loading on the soil within a short amount of time are also referred to as short-term loadings; however, because of the relative transient and infrequent nature of earthquake and impact loadings, geotechnical design for these types of loadings are performed under the Extreme Event limit state. It is noted that Sand-Like soils during an Extreme Event loading may experience an increase in pore pressure ($\Delta u > 0$) that may significantly affect the soil response (see Chapter 13).

Long-term loadings are typically the result of static driving loads placed on the soils when performing limit state equilibrium analyses such as those that occur with embankments, retaining walls, or foundations that have been in place for a sufficient length of time that the pore water pressures have dissipated. These types of loadings are typically evaluated under the Strength and Service limit states.

The direction of loading is directly related to the critical failure surface and its angle of incidence with respect to the soil element under evaluation. This becomes important when analyzing the soil shear strength with respect to a base of a retaining wall sliding over the foundation or during the analysis of soil stability where the failure surface intersects the soil at various angles within the soil mass. The shear strength is also affected by plane strain loading condition as is typically observed under structures such as continuous wall footings. Plane strain loading occurs when the strain in the direction of intermediate principal stress is zero.

Soil loading boundary conditions result from the soil-structure interaction between the loads imposed by the structure and the soil. The loadings and soil response are interdependent based on the stress-strain characteristics of the structure and the soil. Boundary conditions also include the frictional interface response between the structure and the soil. These boundary conditions can be very complex and affect the magnitude of the soil loadings, magnitude of the soil resistance, the distribution of the soil loading (rigid or flexible foundation), and the direction of the loading.

7.8.2 Soil Response

The application of load to a soil results in a change in either pore pressures (Δu) and/or a change in soil volume (δ_v). How the soil responds to these changes in part determines whether drained or undrained shear strengths are required. Further how fast the load is applied also affects these changes. The following discussion is based on the assumptions that the soil is completely saturated (S = 100 percent) and that the load is instantaneously placed. If the load is placed incrementally, it is assumed that each increment is placed instantaneously. Guidance will be provided at the end of the Section on how to handle unsaturated soil. The following paragraphs discuss in greater detail the effects of loading on the soil.

The ability of a soil to behave in an undrained ($\Delta u \neq 0$) or a drained ($\Delta u = 0$) condition is controlled by the percentage of fines and the plasticity of the fines. For the purpose of determining soil response, the soil behaviors provided in Table 7-6 shall be used. The use of Sand-Like soils strictly as a frictional material and Clay-Like soils as a strictly cohesive material is only anticipated when using correlations. The results of actual shear strength testing will determine shear strength parameters (i.e., ϕ and c) that are to be used in design. In addition, the Soil Behavior Type, I_c, from CPTu and the material index, I_D, from DMT testing is also included.

Table 7-6, Soil Response Classification

Percent Fines	Soil Behavior	LL	PI	I_c[1,2]	I_D[1]	Loading Condition	Shear Strength	Stress Condition	Settlement	AASHTO (USCS) Classification
≤ 20	Sand-Like	N/A[3]	N/A[3]	≤ 2.05	≥ 1.8	Short-term	Drained	Effective	Elastic	A-1-a, A-1-b, A-3 (SP, SP-SM, SP-SC, SM, SC, SC-SM)[4]
						Long-term	Drained	Effective		
> 20	Sand-Like	≤ 40	≤ 10	≤ 2.05	≥ 1.8	Short-term	Drained	Effective	Elastic	A-1-b, A-2-4, A-4 (SM, SC, SC-SM, ML, CL-ML, CL)
						Long-term	Drained	Effective		
	Clay-Like	> 40	> 10	≥ 2.6	≤ 0.6	Short-term	Undrained	Total	Consolidation	A-2-7, A-7-5, A-7-6 (SM, SC, ML, CL, MH, CH)
						Long-term	Drained	Effective		
	Clay-Like[5,6]	≤ 40	> 10	> 2.05 to < 2.6	> 0.6 to < 1.8	Short-term	Undrained	Total	Consolidation	A-2-6, A-6 (SC, SM, CL, ML)
						Long-term	Drained	Effective		
	Sand-Like[5,6]	> 40	≤ 10	> 2.05 to < 2.6	> 0.6 to < 1.8	Short-term	Drained	Effective	Elastic	A-2-5, A-5 (SM, ML, MH)
						Long-term	Drained	Effective		

[1]These are typical values and may change based on the correlation between CPTu or DMT and soil test boring.
[2]I_c to be correlated with Soil Test Boring to verify soil classification.
[3]Not Applicable – plasticity not expected to affect these soils
[4]Does not include gravels (GW, GP, etc.) and well graded sands (SW, etc.)
[5]Possible Transitional Soil may be either Sand-Like or Clay-Like. Additional laboratory testing may be required and shall be approved by PC/GDS
[6]Pore pressure dissipation test during CPTu testing may be required to determine difference between Sand-Like and Clay-Like

The pore water pressure response (Δu) that allows water to move in or out of the soil over time is dependent on the soil drainage characteristics (i.e., percent fines) and the drainage path length. The time for drainage to occur can be estimated by using Terzaghi's theory of 1-dimensional consolidation where the time required to reach 99% of the equilibrium volume change, t_{99}, is determined by the following equation.

$$t_{99} = 4 * \left(\frac{D^2}{c_v}\right) \qquad \textbf{Equation 7-27}$$

Where,

D = Longest distance that water must travel to flow out of the soil mass, ft
c_v = Coefficient of vertical consolidation, ft^2/sec

Typical drainage times for various types of soil deposits based on Equation 7-27 are provided in Figure 7-4. It can readily be seen that Sand-Like soils (see Table 7-6) drain within minutes to months while Clay-Like soils drain within months to years. Please note that it is assumed that Sand-Like soils will behave cohesionlessly (i.e., in frictional manner) and that Clay-Like soils will behave cohesively. The transitional soils may behave as either Sand-Like or Clay-Like depending on percent fines and plasticity. The behavior of the transitional soils is anticipated to be a combination of cohesionless and cohesive. The determination of the behavior of these soils will be the responsibility of the GEOR. Depending on the percent fines and the plasticity these soils may drain in days to years. Even though a soil formation may behave in an undrained condition at the beginning of the load application with excess pore water pressures ($\Delta u \neq 0$), with sufficient time to allow for pore pressure dissipation, the soils will reach a drained condition where static loads are in equilibrium and there is no excess pore water pressure ($\Delta u = 0$). Because soil layers may have different drainage characteristics and drainage paths within a soil profile, soil layers may be at various stages of drainage with some soil layers responding in an undrained condition while other layers respond in a drained condition.

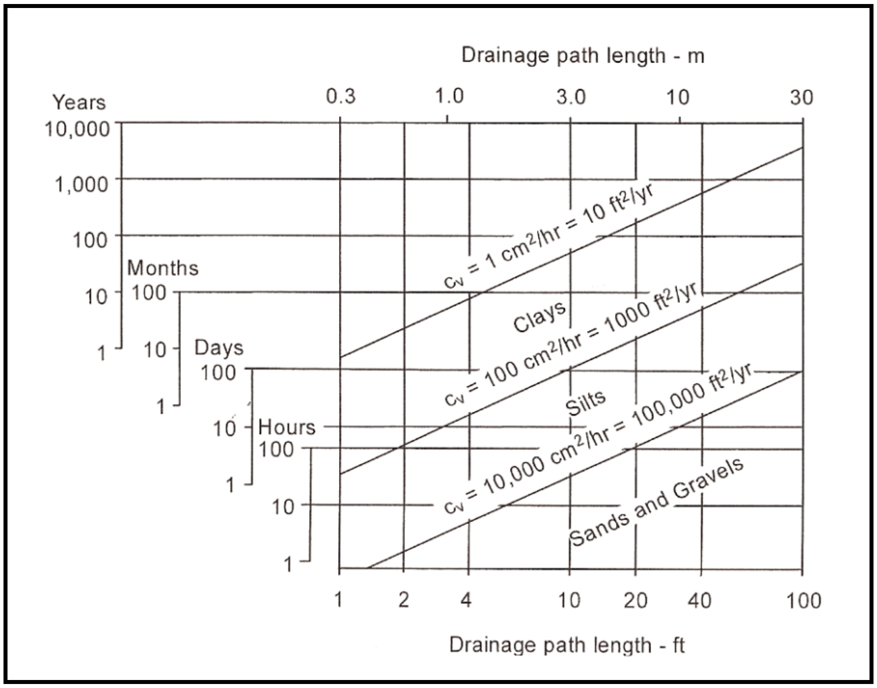

Figure 7-4, Drainage Time Required
(Duncan and Wright (2005))

Volumetric change (δ_v) during shearing can significantly affect the shear strength behavior of the soils. When the soil response is a decrease ($-\delta_v$) in volume during soil shearing the soils are termed to have ***contractive*** behavior. Loose sands and soft clays typically have contractive behavior. When the soil response is an increase ($+\delta_v$) in volume during soil shearing these soils are termed to have ***dilative*** behavior. Overconsolidated clays and medium-dense sands typically have dilative behavior. Soils that do not exhibit volumetric change during shearing ($\delta_v = 0$) are termed to have ***steady state*** behavior.

For typical Sand-Like or Clay-Like soils, it has been observed that the soil shear stress (τ) varies as the soil strains or deforms during soil shearing. Selection of the appropriate soil shear strength to be used in design must be compatible with the deformation or strain that the soil will exhibit under the loading. This is best illustrated in Figure 7-5, where the drained behavior of 2 stress-strain curves is depicted, with each curve representing a different effective consolidation stress (σ'_{v1} and σ'_{v2}) shown. On the left of Figure 7-5 is a shear stress vs. shear strain plot (τ-γ_s plot). Because there is a well-defined peak shear stress (τ_{max}) in the plots this would be indicative of dilative soil behavior of either dense sand or overconsolidated clay. The maximum shear stress (τ_{max}) is termed the ***peak shear strength*** ($\tau_{Peak} = \tau_{max}$). In overconsolidated clay soils, as the maximum shear stress (τ_{max}) is exceeded, post-peak strain softening occurs until a ***fully-softened strength*** (τ_{NC}) is reached. The fully-softened strength is a post-peak strain softening strength that is considered to be the shear strength that is equivalent to peak shear strength of the same soil in the normally consolidated (NC) stress state ($\tau_{Peak} \approx \tau_{NC}$). For very large shearing strains in soils (cohesive or cohesionless), the shear stress value is reduced further to a residual shear strength (τ_r). The Mohr-Coulomb effective shear strength envelopes for peak shear strength ($\tau_{Peak} = \tau_{max}$), fully-softened shear strength ($\tau_{Peak} \approx \tau_{NC}$), and residual shear strength (τ_r) are illustrated on the right side of Figure 7-5.

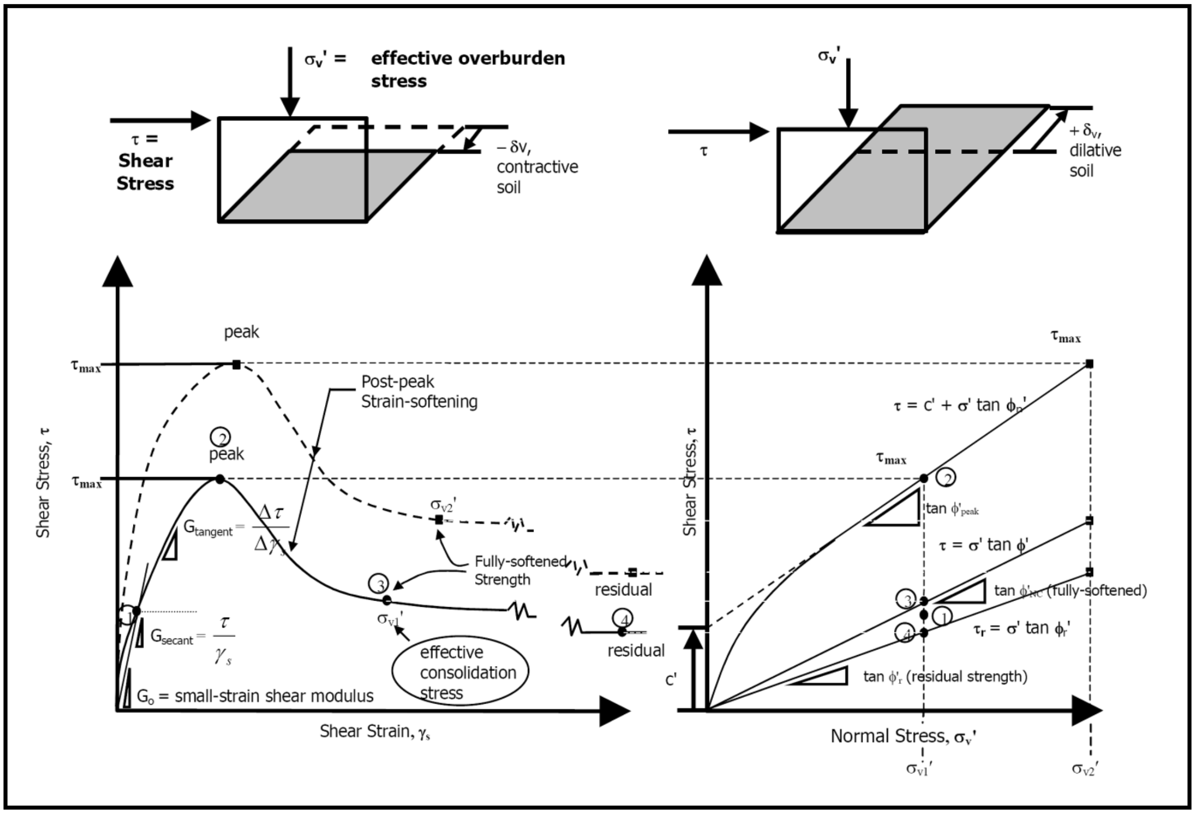

Figure 7-5, Drained Stress-Strain Behavior (Sabatini, et al. (2002))

There are various soil models that are used to characterize soil shear strength. The simplest and most commonly used soil shear strength model is the Mohr-Coulomb soil failure criteria. More sophisticated soil shear strength models such as critical state soil mechanics and numerical models (finite element constitutive soil models) exist and are to be used when simpler models such as the Mohr-Coulomb soil failure criteria cannot accurately predict the soil response.

7.8.2.1 Soil Response – Sand-Like

The soils included in this category are typically clean to dirty sands and inelastic silts (AASHTO classifications A-1-a, A-1-b, A-2-4, A-3 and A-4). Refer to Table 7-6 for the fine contents and plasticity requirements for Sand-Like soils. The fines content and plasticity of these soils is such that the effect on the rate of loading will be minimal. An I_c less than or equal to 2.05 ($I_c \leq 2.05$) from CPTu testing is also indicative of sandy type soil behavior. This is a nominal value from Robertson and Cabal (2015); however, the actual soil behavior shall be determined from the correlation boring obtained adjacent to the CPTu as required in Chapter 4. If the I_c value for sandy type soil behavior is shown to be different, then that I_c shall be used for the entire project site. It is noted that I_c is not a soil classification, but an indication of Soil Behavior Type. In addition, a material index, I_D, of greater than or equal to 1.8 ($I_D \geq 1.8$) is also indicative of sandy behavior from the DMT. These soils will have cohesionless behavior. Because of the relatively rapid drainage anticipated for these soils, less than 100 hours (see Figure 7-4), no excess pore pressures are anticipated ($\Delta u = 0$) (i.e., drained conditions and effective stresses are applicable) and all changes in volume will occur either during loading or immediately after the completion of loading (i.e., all settlement will be elastic).

When drained conditions exist ($\Delta u = 0$), effective stress parameters are used to evaluate soil shear strength. Effective stress is characterized by using effective shear strength parameters (c', ϕ') and effective stress, σ'_{vo}, (use total unit weights above the water table and buoyant (total unit weight minus the unit weight of water) unit weight below the water table). The basic Mohr-Coulomb soil failure criteria for effective stress shear strength (τ') is shown in the following equation.

$$\boldsymbol{\tau' = c' + \sigma'_{vo} \tan \phi'}$$ **Equation 7-28**

Where,

c' = Effective soil cohesion. The effective cohesion for cohesionless soils is typically assumed to equal zero ($c' = 0$), psf.

σ'_{vo} = Effective vertical overburden pressure. Buoyant unit weights ($\gamma_B = \gamma_T - \gamma_w$) are used below the water table and total unit weights (γ_T) are used above the water table, psf.

ϕ' = Effective internal soil friction angle. The effective internal soil friction angle (ϕ') for a cohesionless soil is typically greater than the total internal soil friction angle (ϕ), degrees.

The soil behavior of typical Sand-Like soils can be further illustrated by comparing the stress-strain behavior of granular soils having various densities as shown in Figure 7-6. Medium and dense sands typically reach a peak shear strength ($\tau_{Peak} = \tau_{max}$) value and then decrease to a residual shear strength value at large displacements. The volume of medium and dense sands initially decreases (contractive behavior) and then increases as the soil grains dilate (dilative behavior) with shear displacement until it reaches a point of almost constant volume (steady state behavior). The shear stress in loose sands increases with shear displacement to a maximum value and then remains constant. The volume of loose sands gradually decrease (contractive behavior) until it reaches a point of almost constant volume (steady state behavior).

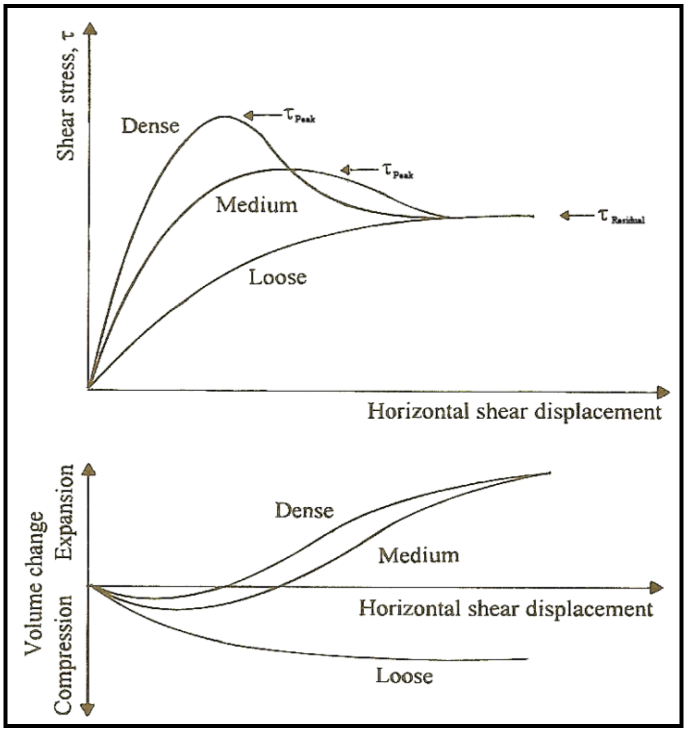

Figure 7-6, Shear Strength Sands (Direct Shear-Test)
(Das (1997))

The soil response is influenced significantly by the soils pore water pressure response (Δu) resulting from the rate of loading as the soils attempt to reach a state of equilibrium. The undrained condition is a soil response that occurs when there is either an increase (+) in pore water pressure ($\Delta u > 0$) or a decrease (-) in pore water pressure ($\Delta u < 0$) within the soil during soil loading. The drained condition is a soil response that occurs when there is no change in pore water pressure ($\Delta u = 0$) as a result of the soil loading.

7.8.2.2 Soil Response – Clay-Like

The soils in this category are typically elastic silts and fat (plastic) clays (AASHTO classifications A-2-7, A-7-5, and A-7-6). Clay-Like soils will have more than 20 percent fines. Refer to Table 7-6 for the plasticity requirements for Clay-Like soils. The rate of loading and plasticity can have a significant impact on how these soils perform. An I_c greater than or equal to 2.6 ($2.6 \leq I_c$) from CPTu testing is also indicative of clayey type soil behavior. This is a nominal value from Robertson and Cabal (2015); however, the actual soil behavior shall be determined from the correlation boring obtained adjacent to the CPTu as required in Chapter 4. If the I_c value for clayey type soil behavior is shown to be different, then that I_c shall be used for the entire project site. It is noted that I_c is not a soil classification, but an indication of Soil Behavior Type. In addition, an I_D of less than or equal to 0.6 ($I_D \leq 0.6$) is also indicative of clayey behavior from the DMT. These soils will have cohesive behavior. Typically, these soils will have drainage times measured in months to years, pore pressures are anticipated to change ($\Delta u \neq 0$) and any changes in volume ($\pm\delta_v$) will occur over time. Undrained shear strengths and total stress conditions are applicable to these types of soils for short-term loading conditions. Under long-term loading conditions, drained shear strengths and effective stress conditions are applicable. See the previous Section for the discussion on the development of drained shear strengths and effective stress conditions.

When undrained conditions exist ($\Delta u \neq 0$), total stress parameters are used to evaluate soil shear strength. The total stress condition is characterized by using total shear strength parameters (c, ϕ) and total stress, σ_{vo}, (total unit weights). The basic Mohr-Coulomb soil failure criteria for total stress shear strength (τ), also referred to as the undrained shear strength (S_u), is shown in the following equation.

$$\boldsymbol{\tau = c + \sigma_{vo} \tan \phi}$$ **Equation 7-29**

Where,

c = Total soil cohesion, psf.

σ_{vo} = Total vertical overburden pressure. Total unit weights (γ_T) are used, psf.

ϕ = Total internal soil friction angle. The total internal soil friction angle for cohesive soils is typically assumed to equal zero (ϕ = 0). Total internal soil friction angle (ϕ) for a cohesionless soil is typically less than the effective internal soil friction angle (ϕ'), degrees.

Another factor that affects soil response of these soils is the in-situ stress state. The stress state is defined by either total (σ_{vo}) or effective (σ'_{vo}) vertical stress, total (σ_{ho}) or effective (σ'_{ho}) horizontal stress, and the effective preconsolidation stress (σ'_p or p'_c). The effective preconsolidation stress is the largest state of stress that the soil has experienced. The state of stress is often quantified by the overconsolidation ratio (OCR) as indicated by the following equation.

$$\boldsymbol{OCR = \frac{\sigma'_p}{\sigma'_{vo}}}$$ **Equation 7-30**

Clay-Like soils are often defined by the in-situ state of stress as indicated in Table 7-7:

Table 7-7, OCR Values

Description	State of Stress	OCR
Underconsolidated, UC	$\sigma'_p < \sigma'_{vo}$	< 1.0
Normally Consolidated, NC	$\sigma'_{vo} = \sigma'_p$	1.0
Overconsolidated, OC	$\sigma'_{vo} < \sigma'_p$	1.1 - 4.0
Heavily Overconsolidated, OC	$\sigma'_{vo} << \sigma'_p$	> 4.0

The soil behavior of typical Clay-Like soils can be further illustrated by comparing the stress-strain behavior of normally consolidated clays (OCR = 1) with the stress-strain behavior of overconsolidated clays (OCR > 1) for consolidated drained and undrained Triaxial tests in Figures, 7-7 and 7-8, respectively. The stress-strain behavior for overconsolidated clays (OCR > 1) indicates that they are subject to strain softening, similar to medium-dense sands shown in Figure 7-6, and that normally consolidated clays (OCR = 1) increase in strength, similar to loose sands also shown in Figure 7-6. Overconsolidated (drained or undrained) clays typically reach peak shear strength ($\tau_{Peak} = \tau_{max}$) and then decrease to a fully-softened strength that is approximately equal to the peak shear strength of a normally consolidated clay ($\tau_{Peak} \approx \tau_{NC}$). The volume change of overconsolidated clays in a drained test is very similar to the volume change in medium-dense sand; the volume initially decreases (contractive behavior) and then increases (dilative behavior). The pore pressures in an undrained test of overconsolidated clays initially increase slightly and then become negative as the soil begins to expand or dilate. The shear stress (drained or undrained test) of a normally consolidated (OCR = 1) clay increases with shear displacement to a maximum value (τ_{Peak} = τ_{NC}). The volume of normally consolidated clays in a drained test gradually decreases (contractive behavior) as it reaches a point of almost constant volume (steady state behavior). The pore pressure in an undrained test of normally consolidated clay increases until failure and remains positive for the entire test.

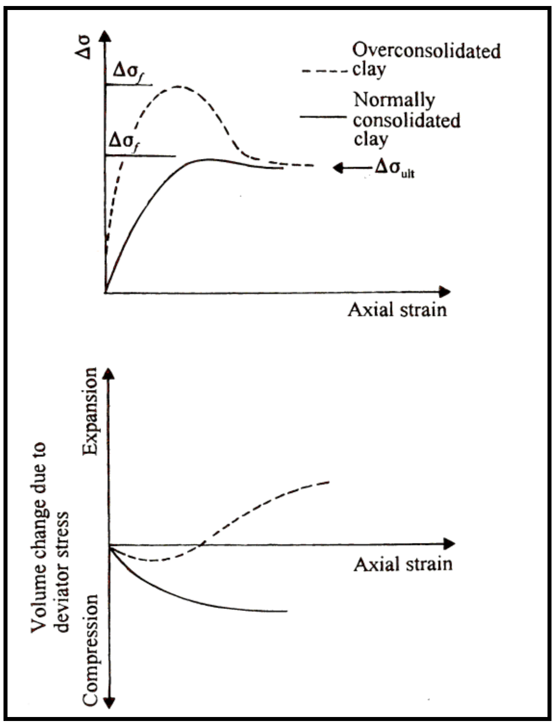

Figure 7-7, Shear Strength of Clay Consolidated Drained Triaxial (Das (1997))

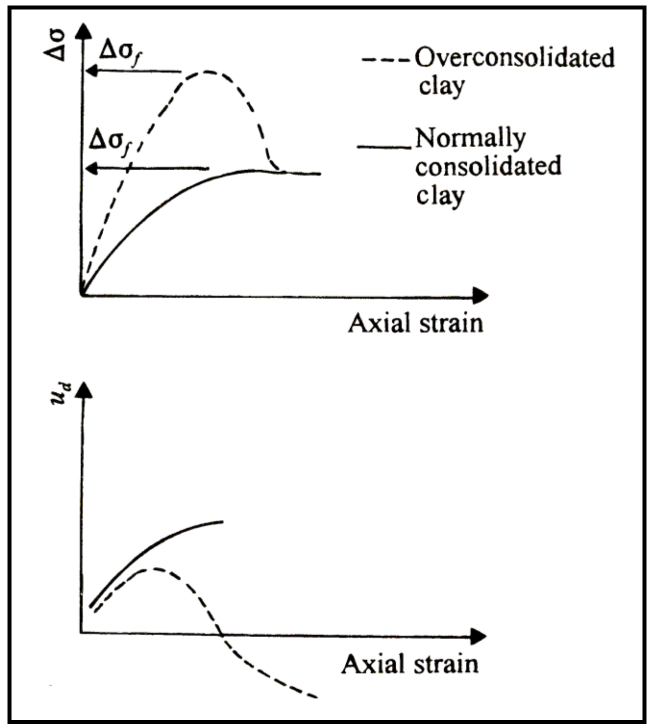

Figure 7-8, Shear Strength of Clay Consolidated Undrained Triaxial (Das (1997))

7.8.2.3 Soil Response – Transitional Soils

As indicated in Table 7-6, these soils can behave either as Sand-Like or Clay-Like depending on the plasticity of the soil. The GEOR will be responsible for determining whether these soils will behave as Sand-Like or Clay-Like and determining whether undrained or drained shear strengths are to be used. These soils will typically have more than 20 percent fines and will classify as sands with fines to elastic silts and clays (AASHTO classification A-2-5, A-2-6, A-5, and A-6). An I_c greater than 2.05 and less than 2.6 ($2.05 < I_c < 2.6$) from CPTu testing is also indicative of soil behavior between cohesionless and cohesive. This is nominal value from Robertson and Cabal (2015); however, the actual soil behavior shall be determined from the correlation boring obtained adjacent to the CPTu as required in Chapter 4. If the I_c value for silty type soil behavior is shown to be different, then that I_c shall be used for the entire project site. It is noted that I_c is not a soil classification, but an indication of Soil Behavior Type. In addition, the I_D will range from greater than 0.6 to less than 1.8 ($0.6 < I_D < 1.8$). See the previous Sections for a discussion of drained and undrained shear strengths.

7.8.2.4 Soil Response – Unsaturated Soils

The preceding Sections assume that the soils are 100 percent saturated. For unsaturated soils (S < 100 percent), the GEOR should be aware of the impacts that unsaturated soils can cause. First, there could be volumetric change ($-\delta_v$) without an associated increase in pore pressure ($+\Delta u$). For Clay-Like soils, the air in the soil voids will eventually be squeezed out and the sample will become fully saturated and should be treated accordingly. The time required for this to occur is not easily determined. Further the determination of when to use undrained or drained shear strengths will not be clear. Therefore, SCDOT recommends that all soils are assumed to 100 percent saturated and that all design analysis be based on this assumption.

7.8.3 Soil Strength Testing

Selection of soil shear strengths should be made based on laboratory testing and soil strain level anticipated from analyses. Table 7-8 provides a summary of published stress-strain behavior from Holtz and Kovacs (1981), Terzaghi, Peck, and Mesri (1996), and Duncan and Wright (2005) for various soils types. This table is provided for "general" guidance in the selection of shear strengths and soil strain level anticipated from equilibrium analyses.

Table 7-8, Soil Shear Strength Selection Based on Strain Level

Sand-Like	**Strain Level [1]**		
	±5% Strains	**15–20% Strains**	**Large Strains >20%**
Med. To Dense Sand	τ_{Peak}	τ_r	τ_r
Non-Liquefying Loose Sands	τ_{Peak}	τ_{Peak}	τ_r
Clay-Like	**Strain Level [1]**		
	±2% Strains	**10–15% Strains**	**Large Strains >15%**
Clay (OCR = 1)	$\tau_{Peak} = \tau_{NC}$	$\tau_{Peak} = \tau_{NC}$	$\tau_{Peak} = \tau_{NC}$
Clay (OCR >1)	τ_{Peak}	$\approx \tau_{NC}$	τ_r

Shear Strength Nomenclature:

τ_{Peak} = Peak Soil Shear Strength

τ_r = Residual Soil Shear Strength

τ_{NC} = Normally Consolidated Soil Shear Strength

[1] Strain levels indicated are generalizations and are dependent on the stress-strain characteristics of the soil and should be verified by laboratory testing.

Once the soil loading and soil response has been evaluated, the next step is to select the method of evaluating the soil shear strength. The shear strength can be evaluated by one of the following methods:

1. Soil shear strength determined by geotechnical laboratory testing.
2. Soil shear strength correlations with in-situ field testing results.
3. Soil shear strength correlations based on index parameters.

The laboratory testing should be selected based on shear strength testing method and the testing parameters best suited to model the loading condition and the soil response. Shear strength laboratory testing methods are described in Chapter 5. A summary of the design parameters that should be used in selection of the appropriate testing method and procedure is provided below:

1. **Total or Effective Stress:** Selection of soil shear strength parameters based on total or effective stress state (drained or undrained). Guidance for typical geotechnical analyses for each limit state (Strength, Service, and Extreme Event) being analyzed is provided for bridge foundations in Table 7-9 and for earth retaining structures and embankments in Table 7-10. Total and effective shear strength determination guidelines for laboratory and in-situ testing are provided in Sections 7.10 and 7.11, respectively.
2. **Soil Shear Strength:** Soil shear strength parameters (τ_{Peak} or τ_r) selection should be based on strain level anticipated from equilibrium analyses. See Table 7-8 for guidance. Seismic soil shear strengths used to design for the Extreme Event I limit state are discussed in Chapter 13.
3. **Loading Direction:** The shearing direction should be compatible with how the soil is being loaded or unloaded and the angle of incidence with respect to soil normal stress. Figure 7-9 illustrates test methods that would be appropriate for shear modes for embankment instability shear surface. Figure 7-10 provides undrained strength (UU Triaxial) of typical clays and shales as a function of stress orientation.

Table 7-9, Bridge Foundation Soil Parameters

Limit State		Strength		Service	Extreme Event			
Load Combinations		Strength I, II, III, IV, V		Service I	Extreme Events I & II[2]			
Seismic Event		N/A			FEE & SEE			
Loading Condition		Static			During Earthquake Shaking		Post-Earthquake	
Soil Shear Strength Stress State		Total	Effective	Effective	Total [1]	Effective	Total (1)	Effective
Shallow Foundation Design	Soil Bearing Resistance	√	√	---	√	√	√	---
	Sliding Frictional Resistance	√	√	---	√	√	√	---
	Sliding Passive Resistance	√	√	---	√	√	√	---
	Structural Capacity	√	√	---	√	√	√	---
	Lateral Displacement	√	√	√	√	√	√	---
	Vertical Settlement	√	√	∇	∇	∇	∇	∇
	Overall Stability	---	---	√	√	√	√	---
Deep Foundation Design	Axial Capacity	√	•	---	---	√	√	---
	Structural Capacity	√	√	---	---	√	√	---
	Lateral Displacements	√	√	√	√	√	√	---
	Vertical Settlement	√	√	∇	∇	∇	∇	∇

[1] Residual soil shear strengths of liquefied soils must include effects of strain softening due to liquefaction.

[2] For Extreme Event II use During Earthquake Shaking – Total.

Soil Stress State Legend:

√ Indicates that soil stress state indicated requires analysis

--- Indicates that soil stress state does not require analysis

• Indicates that soil stress state may need to be evaluated depending on method of analysis

∇ Indicates that soil stress state transitions from undrained to drained (i.e., consolidation)

Table 7-10, Earth Retaining Structures & Embankment Soil Parameters

Limit State		Strength		Service		Extreme Event			
Load Combinations		Strength I, II, III, IV, V		Service I		Extreme Events I & II[2]			
Seismic Event		N/A				FEE & SEE			
Loading Condition		Static				During Earthquake Shaking		Post-Earthquake	
Soil Shear Strength Stress State		Total	Effective	Total	Effective	Total[1]	Effective	Total[(1)]	Effective
Earth Retaining Structure Design	Soil Bearing Resistance	√	√	---	---	√	√	---	√
	Sliding Frictional Resistance	√	√	---	---	√	√	---	√
	Sliding Passive Resistance	√	√	---	---	√	√	---	√
	Structural Capacity	√	√	---	---	√	√	---	√
	Lateral Load Analysis (Lateral Displacements)	√	√	√	√	√	√	---	√
	Settlement	√	√	▽	▽	▽	▽	▽	▽
	Global Stability	√	---	---	√	√	√	---	√
Embankment Design	Soil Bearing Resistance	√	√	---	---	√	√	---	√
	Lateral Spread	√	√	---	---	√	√	---	√
	Lateral Squeeze	√	√	---	---	√	√	---	√
	Lateral Displacements	---	---	√	√	√	√	---	√
	Vertical Settlement	√	√	▽	▽	▽	▽	▽	▽
	Global Stability	√	---	---	√	√	√	---	√

[1] Residual soil shear strengths of liquefied soils must include effects of strain softening due to liquefaction

[2] For Extreme Event II use During Earthquake Shaking – Total.

Soil Stress State Legend:

√ Indicates that soil stress state indicated requires analysis

--- Indicates that soil stress state does not require analysis

• Indicates that soil stress state may need to be evaluated depending on method of analysis

▽ Indicates that soil stress state transitions from undrained to drained (i.e., consolidation)

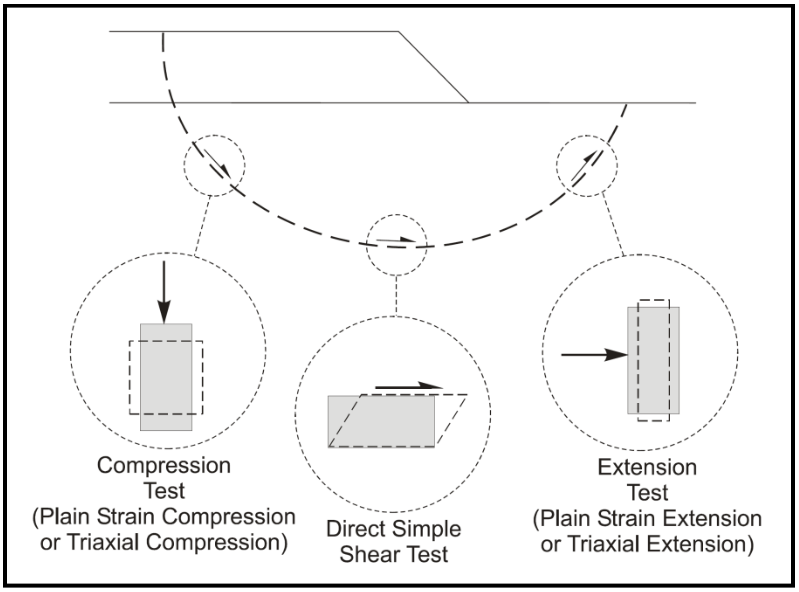

Figure 7-9, Shear Modes for Embankment Stability Shear Failure Surface (Sabatini, et al. (2002))

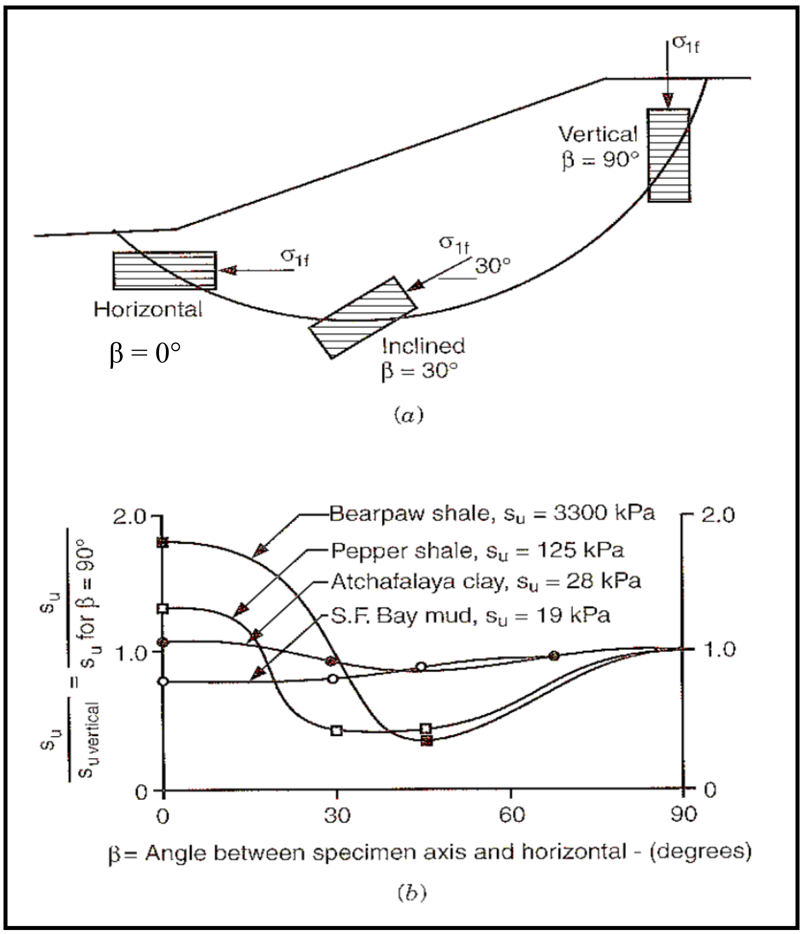

Figure 7-10, τ of Clays and Shales as Function of Failure Orientation (modified from Duncan and Wright (2005))

The undrained and drained shear strengths of soils can be obtained from laboratory testing. The laboratory testing procedures are described in Chapter 5. A summary of laboratory testing methods suitable for determining the undrained and drained shear strengths of cohesive and cohesionless soils is provided in Table 7-11.

Table 7-11, Laboratory Testing Soil Shear Strength Determination

Laboratory Testing Method	Undrained Shear Strength				Drained Shear Strength			
	Cohesive		Cohesionless		Cohesive		Cohesionless	
	τ_{Peak}	τ_r	τ_{Peak}	τ_r	τ'_{Peak}	τ'_r	τ'_{Peak}	τ'_r
Unconfined Compression (UC) Test	√	√	---	---	---	---	---	---
Unconsolidated Undrained (UU) Test[2]	√	√	---	---	---	---	---	---
Direct Simple Shear (DS) Test[2]	---	---	---	---	---	---	√	√
Consolidated Drained (CD) Test[2]	---	---	---	---	√[1]	√[1]	√	√
Consolidated Undrained (CU) Test with Pore Pressure Measurements[2]	√	√	√	√	√	√	√	√

√ - Indicates laboratory method provides indicated shear strength
√[1] – Test not considered practical due to time required to perform test
[2] – Confining stress for triaxial tests and the normal stress for direct shear test shall be determined by GEOR
--- - N/A

Definitions:

τ_{Peak} = Peak Undrained Shear Strength
τ'_{Peak} = Peak Drained Shear Strength
τ_r = Residual Undrained Shear Strength
τ'_r = Residual Drained Shear Strength

In-situ testing methods (Chapter 5), such as the SPT, the CPTu, the DMT, and the FVST, can be used to evaluate soil shear strength parameters by the use of empirical/semi-empirical correlations. Even though the torvane (TV) or the pocket penetrometer (PP) are soil field testing methods, their use is restricted to only qualitative evaluation of relative shear strength during field visual classification of soil stratification. The major drawback to the use of in-situ field testing methods to obtain soil shear strength parameters is that the empirical/semi-empirical correlations are based on a limited soil database that is typically material or soil formation specific and therefore, the reliability of these correlations must be verified for each project site until sufficient substantiated regional experience is available. Poor correlation between in-situ testing results and soil shear strength parameters may also be due to the poor repeatability of the in-situ testing methods. The CPTu, in all versions, has been shown to be more repeatable while the SPT has been shown to be highly variable. Another source of variability is the sensitivity of the test method to different soil types with different soil consistency (very soft to hard cohesive soils) or density (very loose to very dense cohesionless soils). In-situ penetration testing values correspond to the peak of the stress-strain shear strength curve as indicated in Figure 7-11. Since deformations induced from penetration tests are close to the initial stress state, correlations have been developed for the soil modulus.

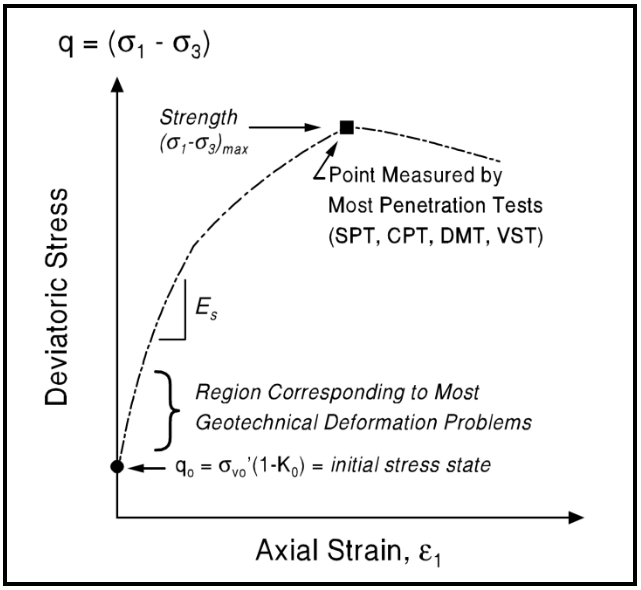

Figure 7-11, Shear Strength Measured by In-Situ Testing (Sabatini, et al. (2002))

A summary of in-situ testing methods suitable for determining the undrained and drained shear strengths of cohesive and cohesionless soils is provided in Table 7-12. The suitability of in-situ testing methods to provide soil shear strength parameters is provided in Table 7-13.

Table 7-12, In-Situ Testing - Soil Shear Strength Determination

In-Situ Testing Method	Undrained Shear Strength				Drained Shear Strength			
	Cohesive		Cohesionless		Cohesive		Cohesionless	
	τ_{Peak}	τ_r	τ_{Peak}	τ_r	τ'_{Peak}	τ'_r	τ'_{Peak}	τ'_r
Standard Penetrometer Test (SPT)	√	---	---	---	---	---	√	---
Piezocone with pore pressure measurements (CPTu)	√	√	---	---	---	---	√	---
Flat Plate Dilatometer Test (DMT)	√	---	---	---	---	---	√	---
Field Vane Shear Test (FVST)	√	√	---	---	---	---	---	---

√ - Indicates in-situ method provides indicated shear strength
--- - N/A
Definitions:
τ_{Peak} = Peak Undrained Shear Strength
τ_r = Residual Undrained Shear Strength
τ'_{Peak} = Peak Drained Shear Strength
τ'_r = Residual Drained Shear Strength

Table 7-13, Soil Suitability of In-Situ Testing Methods (Modified from Canadian Geotechnical Society (2006) and Holtz and Kovacs (1981))

In-Situ Test Method	Suitable Soils [1]	Unsuitable Soils	Correlated Properties	Remarks
Standard Penetrometer Test (SPT)	Sand, Clay, Residual Soils	Gravel	Sand and residual soil effective peak internal friction angle, clay undrained peak shear strength, soil modulus.	SPT repeatability is highly variable. Disturbed samples. Very variable S_u correlations are available for clays.
Piezocone with pore pressure measurements (CPTu)	Sand, Silt, Clay, Residual Soil	Gravel	Sand, silt, and residual soil effective peak internal friction angle, clay and residual soil undrained peak shear strength, soil modulus.	Continuous evaluation of soil properties. CPT is very repeatable. No samples recovered.
Flat Plate Dilatometer Test (DMT)	Sand, Clay, and Residual Soil	Gravel	Sand, silt, and residual soil effective peak internal friction angle, clay and undrained peak shear strength, overconsolidation ratio, at-rest pressure coefficient, soil modulus.	Unreliable results may occur with very dense sand, cemented sand, and gravel. No samples recovered.
Field Vane Shear Test (FVST)	Clay	Sand, Residual Soil, and Gravel	Clay undrained peak shear strength.	May overestimate shear strength. Very soft clays need to be corrected. Unreliable results may occur with fissured clays, varved clays, and highly plastic clays, sand, residual soil, and gravel. FVST repeatability may be variable with rate of rotation. No samples recovered.

[1] The suitability of testing Piedmont residual soils should be based on Mayne et al. (2002). Residual soils frequently have a dual USCS description of SM-ML and behave as both cohesive soils and cohesionless soils because the Piedmont residuum soil is close to the opening size of the U.S. No. 200 Sieve (0.075 mm).

Shear strength of cohesive and cohesionless soils can also be estimated based on effective overburden stress (σ'_{vo}), effective preconsolidation stress (σ'_p or p'_c), the overconsolidation ratio (OCR), and index properties such as grain-size distribution (Fines Content – FC), moisture content (*w*), and Atterberg Limits (LL, PI). Index properties are described in Chapter 6. Unless indicated otherwise, these correlations are used only for preliminary analyses or for evaluating reasonableness of laboratory or in-situ shear strength results.

7.9 TOTAL STRESS

Total stress is the force per unit area carried by both the soil grains and the water located in the pores between the soil grains. The total stress state uses undrained soil shear strengths ($\Delta u \neq 0$) and is typically used to resist short-term loadings (i.e., construction loading, earthquake loadings, etc.). The Mohr-Coulomb undrained shear strength equation ($\tau = S_u$) is defined as follows:

$$\tau = c + \sigma_v \tan \phi$$ **Equation 7-31**

The deviator compression stress at failure ($\Delta\sigma_f$) for unconfined compression tests ($\sigma_3 = 0$) on clays is equal to the unconfined compression strength ($\sigma_1 = q_u = c$). The deviator compression stress at failure ($\Delta\sigma_f$) for undrained triaxial testing (unconsolidated or consolidated) is equal to the total major principal stress (σ_1) minus the total minor principal stress (σ_3) (see Figure 7-12).

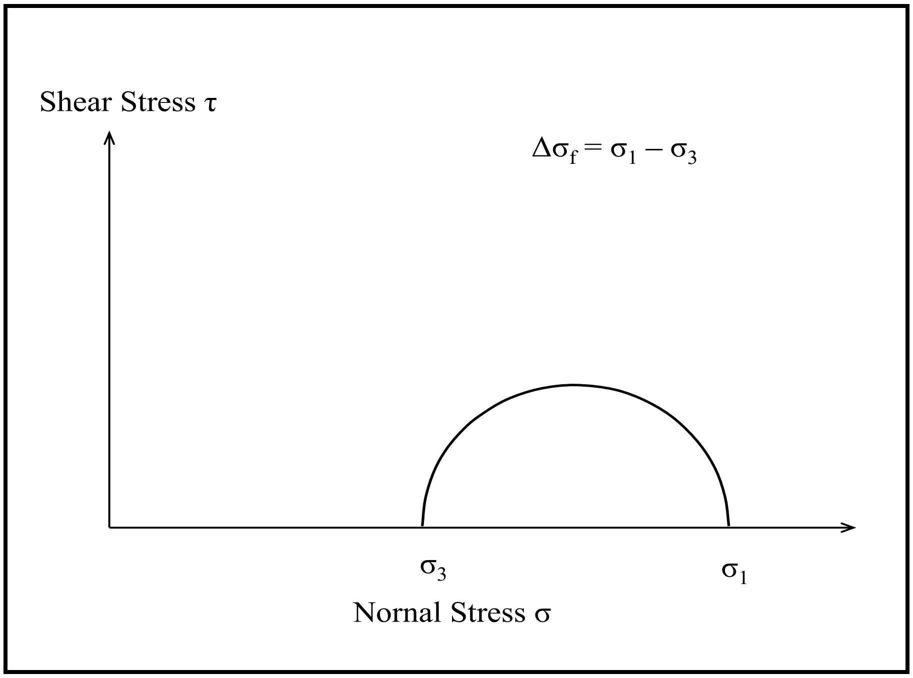

Figure 7-12, Total Principal Stresses

7.9.1 Sand-Like Soils

Undrained shear strengths for Sand-Like soils (cohesionless soils) should be used when the rate of loading is so fast that the soil does not have sufficient time to drain such as in the case of rapid draw-down (specifically not addressed in this Manual), cyclic loadings (typically caused by machine loading and are not anticipated on SCDOT projects), and earthquake loadings. Based on Table 7-6 Sand-Like soils are not anticipated to require undrained shear strengths; therefore, no undrained shear strengths will be used or provided. The only exception is during earthquake loadings; see Chapter 13 for the development of undrained shear strengths for use during seismic events. Undrained residual shear strength ratio of liquefied soils (τ_{rl}/σ'_{vo}) as proposed by Idriss and Boulanger (2008) are presented in Chapter 13.

7.9.2 Clay-Like Soils

The τ for Clay-Like soils should be determined using UC tests, UU triaxial tests, or CU triaxial tests of undisturbed samples. The undrained shear strength for these soils should be compatible with the level of strain anticipated under Service conditions (see Table 7-8). Undrained shear strengths are used for short-term loading conditions, the length of time to reduce pore pressures induced by loading may require months to years, in a total stress analysis. Typically the total internal friction angle is negligible and assumed equal to zero (ϕ = 0) and the Mohr-Coulomb shear strength equation for the τ of cohesive soils can be expressed as indicated by the following equation.

$$\boldsymbol{\tau = c = \frac{\Delta\sigma_f}{2}}$$ **Equation 7-32**

The undrained shear strength of Clay-Like soils may also be determined by in-situ testing such as the SPT, the CPTu, the DMT, or the FVST as described in Chapter 5. As stated previously, in Section 7.9.3, the biggest drawback to the use of in-situ field testing methods to obtain undrained shear strengths of Clay-LIke soils is that the empirical correlations are based on a soil database that is material or soil formation specific and therefore the reliability of these correlations must be verified for each project site by substantiated regional experience or by conducting laboratory testing and calibrating the in-situ testing results.

7.9.2.1 Undrained Shear Strength – SPT Method

The SPT can provide highly variable results in Clay-Like soils as indicated in Table 7-13. However, the following correlations may be used if laboratory undrained shear strengths are correlated to the corrected N_{60} value obtained from the SPT. Peak undrained shear strength (τ = $(S_u)_{SPT}$), in units of ksf, for Clay-Like soils (McGregor and Duncan (1998)) can be computed for low plasticity clays using Equation 7-33 and medium to high plasticity clays using Equation 7-34. Plasticity is defined in Chapter 6.

$$\boldsymbol{\tau = (S_u)_{SPT} = 0.075 * N_{60}}$$ **Equation 7-33**

$$\boldsymbol{\tau = (S_u)_{SPT} = 0.15 * N_{60}}$$ **Equation 7-34**

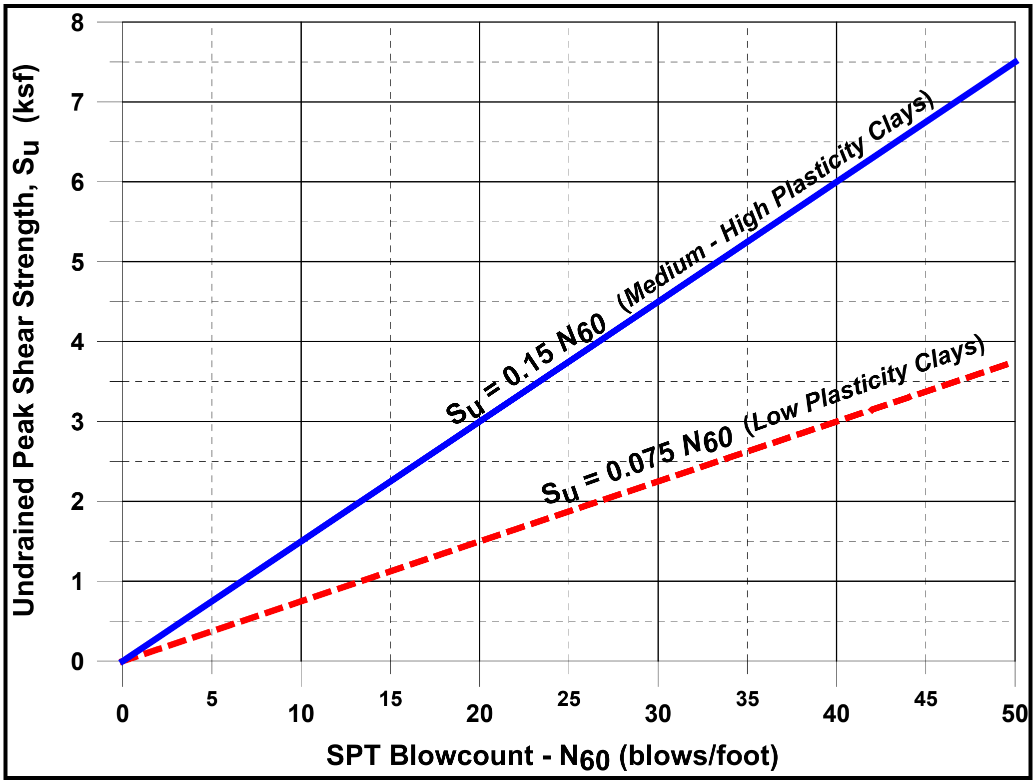

Note: $N_{60} = N^*_{60}$

Figure 7-13, Undrained Shear Strength – SPT Relationship (modified from McGregor and Duncan (1998))

7.9.2.2 Undrained Shear Strength – CPTu Method

The peak undrained shear strength ($\tau = (S_u)_{cpt}$) of cohesive soils can also be obtained from the CPTu (Mayne (2007)) as indicated by the following equation.

$$\tau = (S_u)_{cpt} = \frac{(q_t - \sigma_{vo})}{N_k} \qquad \textbf{Equation 7-35}$$

Where,

q_t = Corrected CPT tip resistance, tsf (see Chapter 5)
σ_{vo} = total overburden pressure at test depth, tsf
N_k = cone factor (see Chapter 6)

According to Robertson and Cabal (2015), N_k can vary between 10 and 18 and is typically set at 14. N_k tends to increase with increasing plasticity and decrease with increasing soil sensitivity. N_k will be determined on a site-specific basis and reported as required in Chapter 6. As the parameter B_q increases N_k decreases such that is very sensitive as B_q approaches 1.0, N_k can be as low as 6. As can be seen from Equation 7-35 an accurate determination of N_k is required, especially in soft fine-grained (Clay-Like) soils. The use of the typical value could under estimate the shear strength.

7.9.2.3 Undrained Shear Strength – DMT Method

The peak undrained shear strength ($\tau = (S_u)_{DMT}$) of Clay-Like soils can also be obtained from the DMT (Marchetti, Monaco, Totani, and Calabrese (2001)) as indicated by the following equation.

$$\tau = (S_u)_{DMT} = 0.22 * \sigma'_{vo} * (0.5 * K_D)^{1.25} \quad \textbf{Equation 7-36}$$

Where,

σ'_{vo} = effective overburden pressure at test depth, psf
K_D = horizontal stress index

7.9.2.4 Undrained Shear Strength – FVST Method

The peak undrained shear strength ($\tau = (S_u)_{FVST}$) and the remolded shear strength $(S_{urem})_{FVST}$ of Clay-Like soils can also be obtained from the FVST (Mayne, Christopher and DeJong (2002)) using Equation 7-37. $(S_{urem})_{FVST}$ is substituted for $(S_u)_{FVST}$ after the 10 revolutions have been completed.

$$\tau = (S_u)_{FVST} = \frac{12T_{net}}{\pi D^2\left(\frac{D}{\cos i_T} + \frac{D}{\cos i_B} + 6*H\right)} \quad \textbf{Equation 7-37}$$

Where,

T_{net} = Net torque, inch-pounds (see Chapter 5)
D = Diameter of the field vane, inches (see Chapter 5)
H = Height of the field vane, inches (see Chapter 5)
i_T and i_B = Taper angle, degrees (see Chapter 5)

Correction of $(S_u)_{FVST}$ is required prior to use in engineering design to account for rate effects in the test. Mayne, et al. (2002) recommends using the following equations to correct the undrained shear strength for testing rate effects based on plasticity (PI > 5):

$$\tau_{mobilized} = \mu_R * (S_u)_{FVST} \quad \textbf{Equation 7-38}$$

$$\mu_R = 1.05 - 0.045 * (PI)^{0.5} \quad \textbf{Equation 7-39}$$

Where,

PI = Plasticity Index

7.9.2.5 Undrained Shear Strength – Empirical Methods

Empirical correlations based on SHANSHEP (Stress History and Normalized Soil Engineering Parameters) laboratory testing results can be used for preliminary designs and to evaluate the peak undrained shear strength (S_u) obtained from laboratory testing or in-situ testing. This method is only applicable to clays without sensitive structure where undrained shear strength increases proportionally with the effective overburden pressure (σ'_{vo}). The SHANSHEP laboratory test results of Ladd, Foot, Ishihara, Schlosser, and Poulos (1977) revealed trends in undrained shear strength ratio (S_u / σ'_v) as a function of overconsolidation ratio as indicated in Figure 7-14.

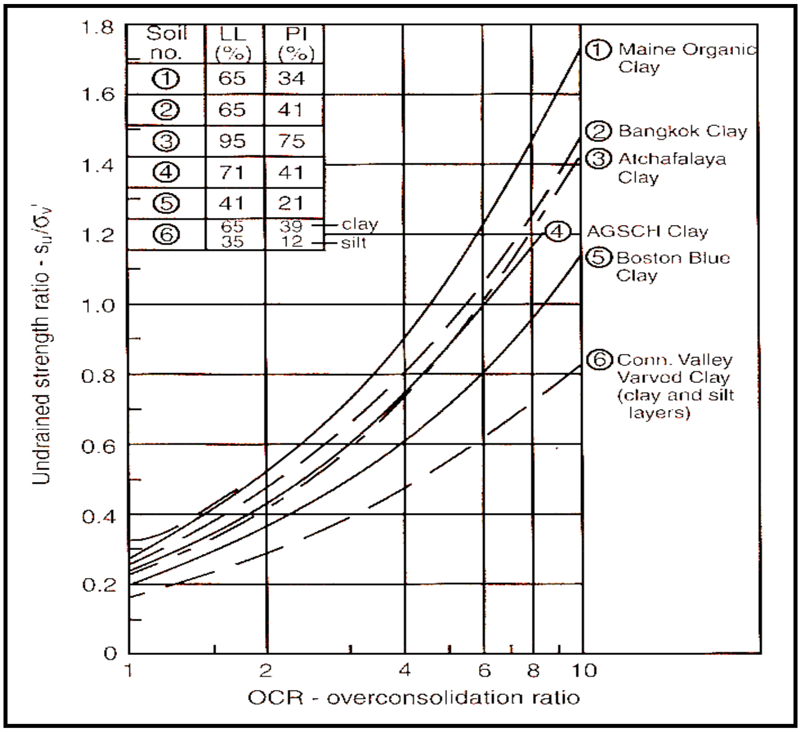

Figure 7-14, Undrained Shear Strength Ratio and OCR Relationship (Ladd, et al. (1977))

The average peak undrained shear strengths (τ) shown in Figure 7-14 can be approximated by an empirical formula developed by Jamiolkowski, Ladd, Germaine, and Lancellotta (1985) as indicated by the following equation.

$$\tau = (0.23 * (OCR)^{0.8}) * \sigma'_{vo}$$ **Equation 7-40**

Where,

τ	=	Undrained shear strength, tsf
OCR	=	Overconsolidation ratio
σ'_{vo}	=	Effective overburden pressure at test depth, tsf

The τ can be compared to the remolded shear strength (τ_{rem}) or τ_r to determine the sensitivity (S_t) of cohesive soils. Sensitivity is the measure of the breakdown and loss of interparticle attractive forces and bonds within Clay-Like soils. Typically in dispersed Clay-Like soils the loss is relatively small, but in highly flocculated structures the loss in strength can be large. Sensitivity is determined using the following equation.

$$S_t = \frac{\tau}{\tau_{rem}} = \frac{\tau}{\tau_r}$$ **Equation 7-41**

Sensitivity may also be estimated directly from CPT results using the following equation,

$$S_t \cong \frac{(q_t - \sigma_{vo})}{f_s * N_k}$$ **Equation 7-42**

The description of sensitivity is defined in the following table.

Table 7-14, Sensitivity of Cohesive Soils (Modified from Spangler and Handy (1982))

Sensitivity	Descriptive Term
< 1	Insensitive
1 - 2	Slightly Sensitive
3 - 4	Medium Sensitive
5 - 8	Sensitive
9 - 16	Very Sensitive
17 - 32	Slightly Quick
33 - 64	Medium Quick
>64	Quick

The τ_{rem} of Clay-Like soils can be determined from remolded triaxial specimens or from in-situ testing methods (CPTu or FVST). Triaxial specimens should have the same moisture content as the undisturbed sample as well as the same degree of saturation and confining pressure. Sensitivity can also be related to the liquidity index using the following figure.

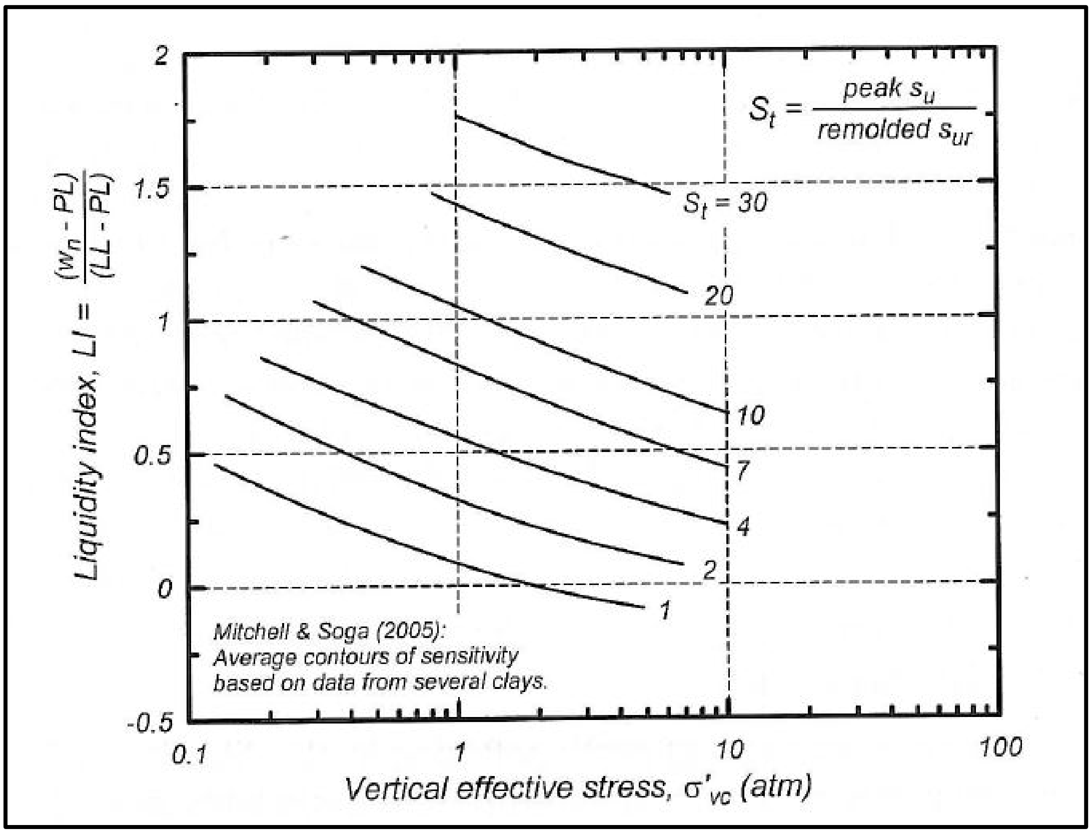

Figure 7-15, Sensitivity based on Liquidity Index and σ'_{vo} (Idriss and Boulanger (2008))

The Liquidity Index (LI) can also be related to remolded shear strength ($\tau_{rem} = c_{urem} = S_{urem}$) as indicated in the following.

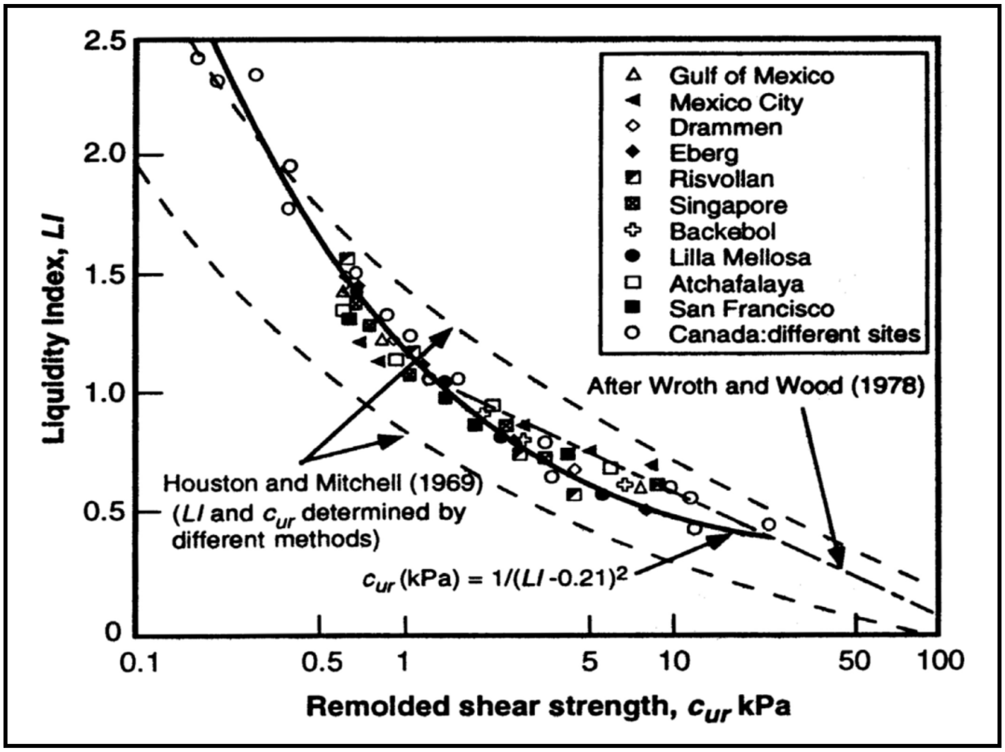

1 kPa = 0.0209 ksf = 20.89 psf

Figure 7-16, Remolded Shear Strength vs Liquidity Index (Mitchell (1993))

The Liquidity Index (LI) is the relationship between *w*, PL, and the LL. The LI is a measure of the relative softness of a Clay-Like soil as indicated by the closeness of the *w* to the LL. The LI can be determined by the following equation.

$$LI = \frac{(w - PL)}{(LL - PL)}$$ **Equation 7-43**

An LI equal to 1 is general indication that a Clay-Like soil is normally consolidated and an LI equal to 0 is a general indication that a Clay-Like soil is overconsolidated.

The undrained residual shear strength of Clay-Like soils (S_t < 2) can be estimated for preliminary design and to evaluate the τ_r (S_{ur}) obtained from laboratory testing or in-situ testing. In addition, the τ_r (S_{ur}) can be estimated by reducing τ_{Peak} by a residual shear strength loss factor (λ_τ) as indicated in the following equation.

$$\tau_r = \lambda_\tau * \tau$$ **Equation 7-44**

The λ_τ factor typically ranges from 0.50 to 0.67 depending on the type of clay soil. The λ_τ factors recommended in Table 7-15 are based on the results of a pile soil set-up factor study prepared by Rausche, Thendean, Abou-matar, Linkins and Goble (1997)

Table 7-15, Residual Shear Strength Loss Factor (λ_τ)

Soil Type		Residual Shear Strength Loss Factor (λ_τ)
USCS	**Description**	
Low Plasticity Clay	CL-ML	0.57
Medium to High Plasticity Clay	CL & CH	0.50

7.9.3 Transitional Soils

The undrained shear strength of transitional materials may have both ϕ and c components which should be determined in the laboratory using the appropriate testing methods. However, if samples for this type of testing have not been obtained (e.g., during the preliminary exploration), then the GEOR should review the percent fines and the plasticity of the soil to determine whether the soil will behave Sand-Like or Clay-Like. If transitional soils are identified in the preliminary exploration, obtaining undisturbed samples of these materials should be attempted during the final exploration. For soils that are difficult to determine the approximate classification, the undrained shear strength parameters for both Sand-Like and Clay-Like soils should be determined and the more conservative design should be used.

7.9.4 Maximum Allowable Total Soil Shear Strengths

SCDOT has established maximum allowable peak (c, ϕ) and residual (c_r, ϕ_r) undrained soil shear strength design parameters for in-situ soils shown in Table 7-16, for use in design. These soil shear strength design parameters may be exceeded with appropriate laboratory testing results (see Table 7-11). Alternately, these shear strengths may be exceeded using correlations with field testing results (see Table 7-12) and the express written permission of the OES/GDS.

Table 7-16, Maximum Allowable Total Soil Shear Strengths

Soil Type		Peak		Residual	
USCS	**Description**	**c (psf)**	**ϕ (degrees)**	**c_r (psf)**	**ϕ_r (degrees)**
ML, MH, SC	Silt, Clayey Sand, Clayey Silt	1,500	15	1,200	6
SM, ML	Residual Soils	900	14	700	6
CL-ML	NC Clay (Low Plasticity)	1,500	0	900	0
CL, CH	NC Clay (Med-High Plasticity)	2,500	0	1250	0
CL-ML	OC Clay (Low Plasticity)	2,500	0	1400	0
CL, CH	OC Clay (Med-High Plasticity)	4,000	0	2000	0

7.10 EFFECTIVE STRESS

Effective stress is the force per unit area carried by the soil grains. The effective stress state uses drained soil shear strengths ($\Delta u = 0$). The Mohr-Coulomb drained shear strength equation is defined as follows.

$$\tau' = c' + \sigma'_v * \tan\phi' \qquad \textbf{Equation 7-45}$$

The deviator compression stress at failure ($\Delta\sigma_f$) for undrained triaxial testing (consolidated) is equal to the total or effective major principal stress (σ_1) minus the total or effective minor principal stress (σ_3) [i.e., the confining or consolidating stress]. The effective major and minor principal stresses are the total major and minor principal stresses minus the pore pressure at failure (u_f) (see Figure 7-17).

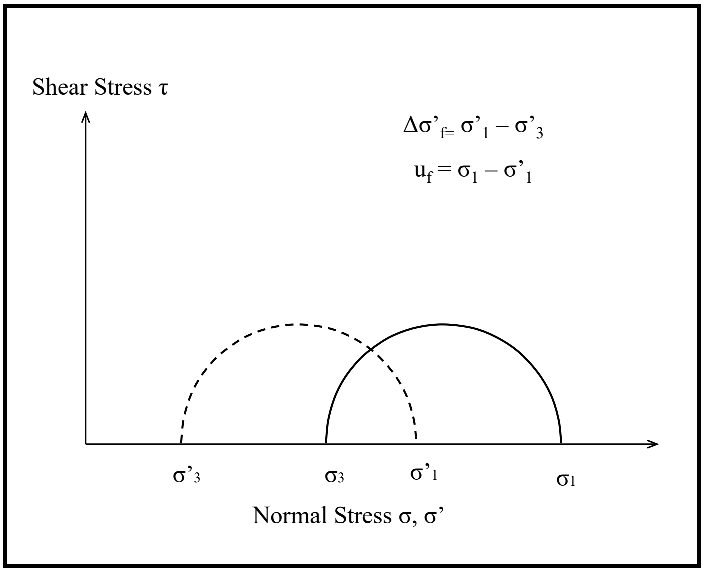

Figure 7-17, Effective Principal Stresses

7.10.1 Sand-Like Soils

Drained shear strengths for Sand-Like soils should be used when there is relatively no change in pore water pressure ($\Delta u \approx 0$) as a result of soil loading. The drained shear strength for these soils should be compatible with the level of strain anticipated under service conditions (see Table 7-8). Sand-Like soils that are subjected to construction loads and static driving loads typically use peak or residual drained shear strengths due to the relatively rapid (minutes to hours) drainage characteristics of granular soils as indicated in Section 7.9.2. The peak or residual drained soil shear strength parameters can be obtained from CD triaxial tests, CU triaxial tests with pore pressure measurements, or DS tests. Typically the effective cohesion (c') is negligible and assumed to be equal to zero (c' = 0) and the Mohr-Coulomb shear strength criteria for drained shear strength of Sand-Like soils can then be expressed as indicated in the following equation.

$$\tau' = \sigma'_v * tan\,\phi' \qquad \textbf{Equation 7-46}$$

The peak drained shear strength of Sand-Like soils may also be determined by in-situ testing methods such as the SPT, the CPTu, or the DMT. As stated previously, in Section 7.9.3, the biggest drawback to the use of in-situ field testing methods to obtain drained shear strengths of Sand-Like soils is that the empirical correlations are based on a soil database that is material or soil formation specific and therefore the reliability of these correlations must be verified for each project site by either using substantiated regional experience or conducting laboratory testing and calibrating the in-situ testing results.

7.10.1.1 Effective Peak Friction Angle – SPT Method

The effective peak friction angle, ϕ', of Sand-Like soils can be obtained from the SPT. Most SPT correlations were developed for clean sands and their use for micaceous sands/silts, silty soils, and gravelly soils may be may be unreliable as indicated below:

- SPT blow counts in micaceous sands or silts may be significantly reduced producing very conservative correlations.
- SPT blow counts in silty soils may produce highly variable results and may require verification by laboratory triaxial testing depending on a sensitivity analysis of the impact of the variability of results on the analyses and consequently the impact on the project.
- SPT blow counts in gravelly soils may overestimate the penetration resistance. Conservative selection of shear strength parameter or substantiated local experience should be used in lieu of laboratory testing.

The effective peak friction angle, ϕ', of Sand-Like soils can be estimated using the relationship of Hatanaka and Uchida (1996) for corrected N-values ($N^*_{1,60}$) as indicated below or using Figure 7-18:

$$\boldsymbol{\phi' = \left(15.4 * N^*_{1,60}\right)^{0.5} + 20^\circ} \qquad \textbf{Equation 7-47}$$

Where,

4 blows per foot ≤ $N^*_{1,60}$ ≤ 50 blows per foot

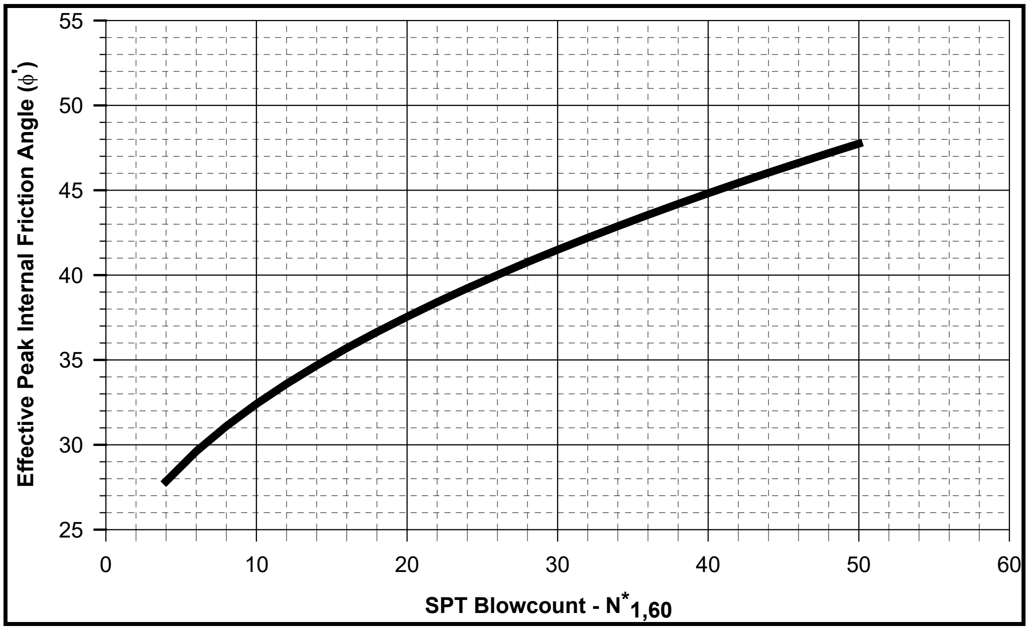

Figure 7-18, Effective Peak Friction Angle and SPT ($N^*_{1,60}$) Relationship (Based on Hatanaka and Uchida (1996))

7.10.1.2 Effective Peak Friction Angle – CPTu Method

The effective friction angle, ϕ′, of Sand-Like soils can also be estimated by the CPTu based on Robertson and Campanella (1983). This method requires the estimation of the effective overburden pressure (σ'_{vo}) and the corrected tip resistance (q_t) using the relationship in Figure 7-19. This relationship may be approximated by the following equation.

$$\boldsymbol{\phi' = \tan^{-1}\left[0.1 + 0.38 * \log\left(\frac{q_t}{\sigma'_{vo}}\right)\right]}$$ **Equation 7-48**

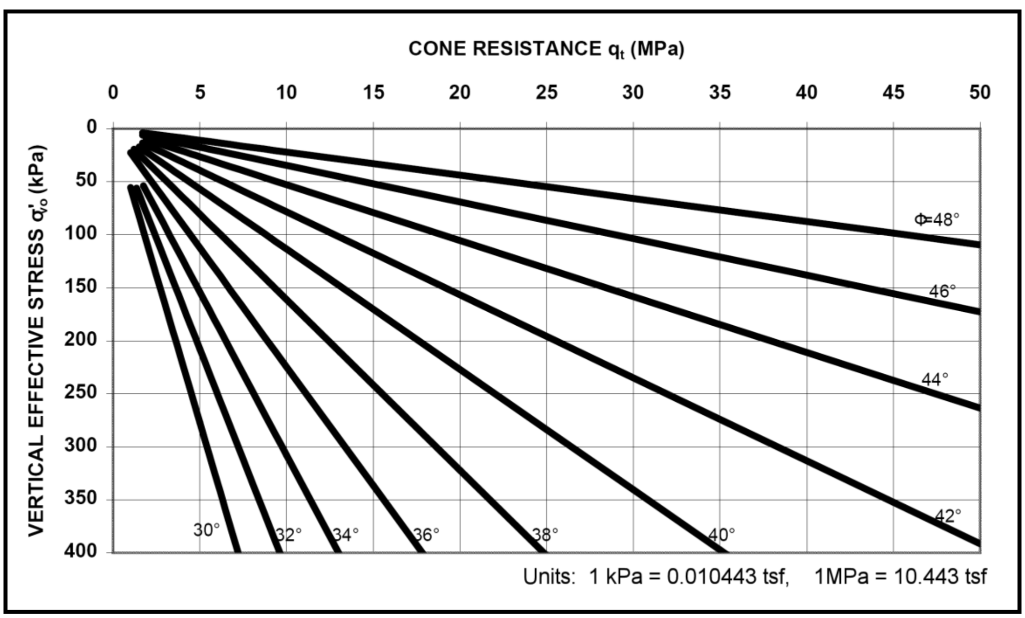

Figure 7-19, Effective Peak Friction Angle and CPT (q_t) Relationship (Robertson and Campanella (1983))

7.10.1.3 Effective Peak Friction Angle – DMT Method

The effective friction angle, ϕ', of Sand-Like soils can also be estimated by the DMT using the Marchetti (1997) relationship shown in Figure 7-20. The Marchetti (1997) relationship may be approximated by the following equation.

$$\boldsymbol{\phi' = 28^\circ + 14.6^\circ * \log K_D - 2.1^\circ \log^2 K_D}$$ **Equation 7-49**

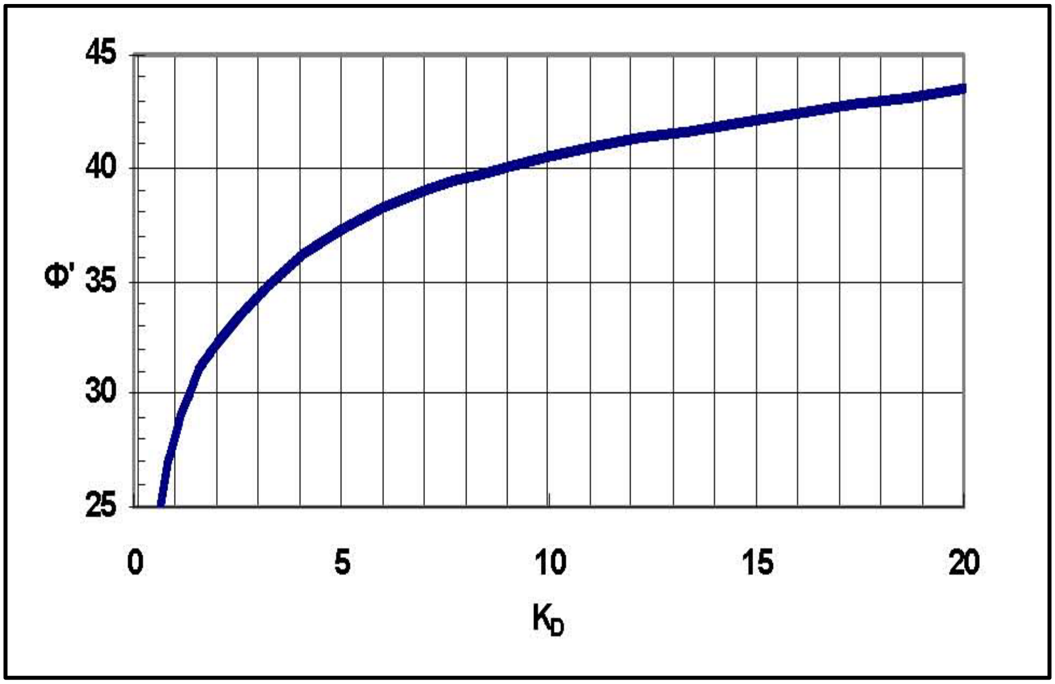

Figure 7-20, Effective Peak Friction Angle and DMT (K_D) Relationship (Sabatini, et al. (2002))

7.10.2 <u>Clay-Like Soils</u>

Drained shear strengths for Clay-Like soils should be used when there is relatively no change in pore water pressure ($\Delta u \approx 0$) as a result of soil loading such as static driving loads. The drained shear strength for these soils should be compatible with the level of strain anticipated under service conditions (see Table 7-8). Drained shear strengths are used for long-term loading conditions, geotechnical analyses for these types of loadings are based on effective stress analyses. The peak or residual drained soil shear strength parameters can be obtained from CD triaxial testing (this test is normally not performed because of the time requirements for testing), or CU triaxial testing with pore pressure measurements. It is noted that use of the following methods should only be used if the appropriate laboratory testing for shear strength has not been performed and that preference is that the testing should be performed. Typically for normally consolidated (OCR = 1; see Table 7-7) Clay-Like soils the effective cohesion (c') is negligible and is assumed to be equal to zero (c' = 0) and the Mohr-Coulomb shear strength equation for drained shear strength for Clay-Like soils can be expressed as indicated in the following equation.

$$\boldsymbol{\tau' = \sigma'_v * \tan \phi'_{NC}}$$ **Equation 7-50**

Typically for overconsolidated Clay-Like soils the effective cohesion is greater than zero with the effective friction angle less than that determined for normally consolidated Clay-Like soils. When the preconsolidation pressure (σ'_p or p'_c) is exceeded the overconsolidated Clay-Like soil becomes normally consolidated (see Figure 7 -21).

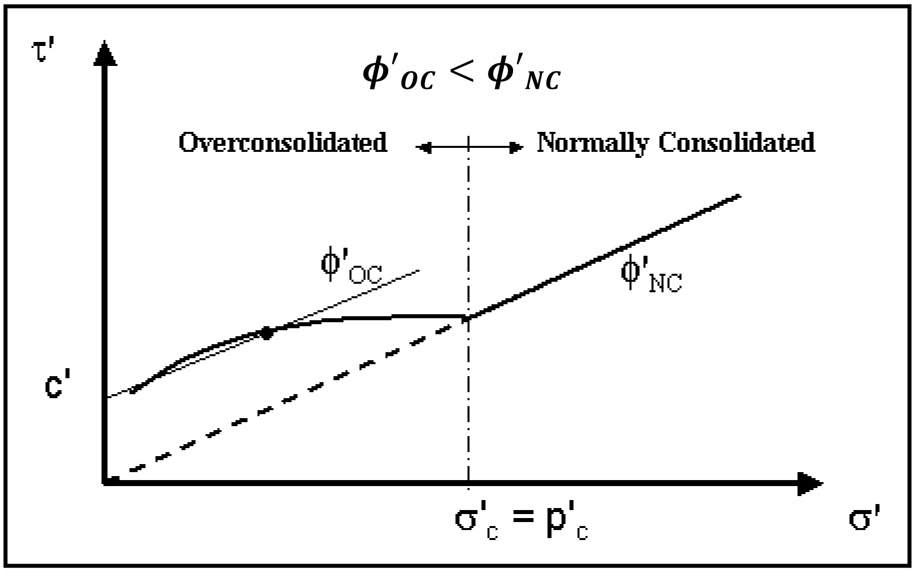

Figure 7-21, Overconsolidated Clay Failure Envelope (CUw/pp Triaxial Test)

The effective peak and residual drained shear strength of Clay-Like soils should not be evaluated using in-situ testing methods. Drained shear strengths should be developed using appropriate laboratory testing. However, SCDOT recognizes the fact that this type of testing may not be practicable; therefore, the correlations provided in the following paragraphs may be used.

Correlations have been developed between drained shear strengths of Clay-Like soils and index parameters such as plasticity index (PI or I_P), LL, clay fraction (CF) and effective overburden pressure (σ'_{vo} = effective normal stress). Similarly to relationships developed for in-situ testing methods, these relationships for drained shear strengths of Clay-Like soils were developed based on a soil database that is typically material or soil formation specific and may require verification by laboratory triaxial testing depending on a sensitivity analysis of the impact of the variability of results on the analyses and consequently the impact on the project. These relationships should be used to evaluate the validity of laboratory testing results and to improve the relationship database for regional soil deposits by SCDOT.

In normally consolidated Clay-Like soils (OCR = 1.0) the shear strength test will result in a peak effective friction angle (ϕ'). Terzaghi, et al. (1996) proposed the relationship in Figure 7-22 between peak effective friction angle (ϕ') for normally consolidated clays and the plasticity index (I_P or PI). For plasticity indices above 60 percent, the peak effective friction angle (ϕ') should be determined from laboratory testing. The Terzaghi, et al. (1996) relationship between peak effective friction angle (ϕ') for normally consolidated clays and the plasticity index (I_P or PI) may be estimated by the following equation.

$$\boldsymbol{\phi'_{NC} = 35.7^\circ - [0.28^\circ * (PI)] + [0.00145^\circ * (PI)^2] \pm 4^\circ} \qquad \textbf{Equation 7-51}$$

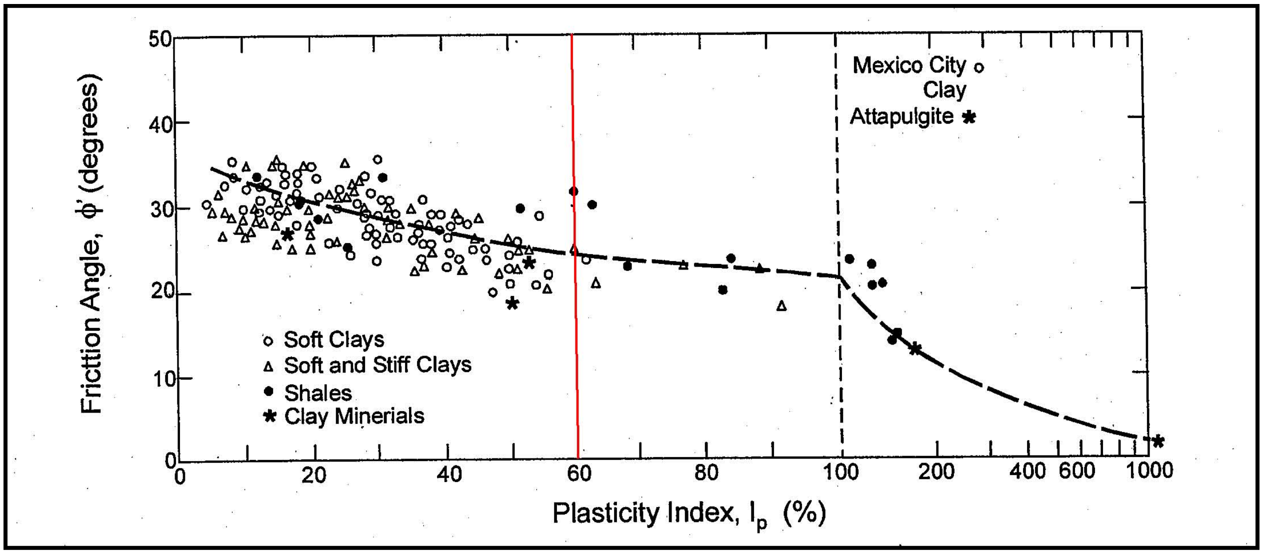

Figure 7-22, Plasticity Index versus Drained Friction Angle for NC Clays (Terzaghi, et al. (1996))

As an alternate to Terzaghi, et al. (1996), Sorensen and Okkels (2013) may be used. Sorensen and Okkels (2013) have developed 2 equations for obtaining the drained friction angle for normally consolidated Clay-Like soils (ϕ'_{NC}) using PI and CF. These equations apply for CF less than 90 percent (CF < 90%) because the available data from which this equation is based did not have any samples with CFs greater than about 90 percent. However, it is noted that PI has a greater influence on ϕ'_{NC} then does CF. Figure 7-23 depicts the data set used by Sorensen and Okkels (2013) to develop these equations. As can be seen in Figure 7-23, a mean equation and a lower bound equation have been developed. The lower bound equation should have no more than 5 percent of the data points below the lower bound line. SCDOT recommends that the lower bound curve be used first to develop the normally consolidated drained shear strength for use in design. The mean equation should be used if the lower bound equation does not achieve the required resistances.

Lower Bound Equation

$$\phi'_{NC} = 39^{\circ} - 11^{\circ} * \log PI \qquad \textbf{Equation 7-52}$$

Mean Equation

$$\phi'_{NC} = 43^{\circ} - 10^{\circ} * \log PI \qquad \textbf{Equation 7-53}$$

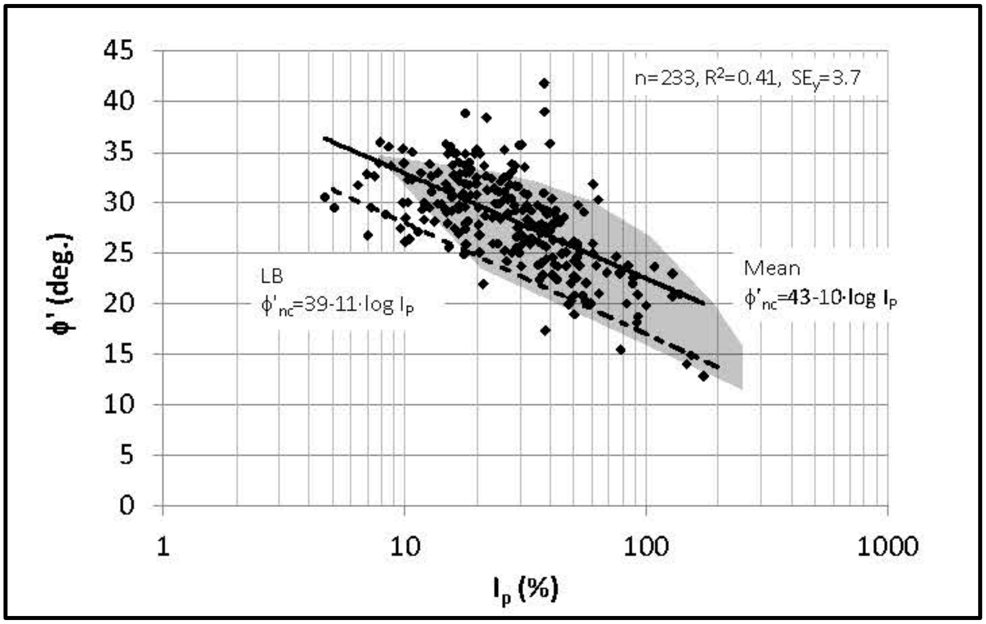

Note: I_P = PI

Figure 7-23, Plasticity Index versus Drained Shear Resistance for NC Clays (Sorensen and Okkels (2013))

Sorensen and Okkels (2013) have also developed procedures for determining the drained shear strength (c'_{OC} and ϕ'_{OC}) for overconsolidated Clay-Like soils (OCR $\geq$ 1.1). For overconsolidated Clay-Like soils the Mohr-Coulomb shear strength equation for drained shear strength can be expressed as indicated in the following equation.

$$\tau' = c'_{OC} + \sigma'_v * \tan \phi'_{OC}$$ **Equation 7-54**

Sorensen and Okkels (2013) have demonstrated that drained shear strength of overconsolidated Clay-Like soils are related not only to PI but also the CF of the material. Similarly to the development of drained shear strength for normally consolidated Clay-Like soils, Sorensen and Okkels have developed 2 equations based on both best fit of the drained shear strength data for overconsolidated Clay-Like soils as well as a lower bound equation for which approximately 95 percent of the available data points are above the lower bound line (see Figure 7-24). SCDOT recommends that the lower bound curve be used first to develop the overconsolidated drained shear strength for use in design. The best fit equation should be used if the lower bound equation does not achieve the required resistances.

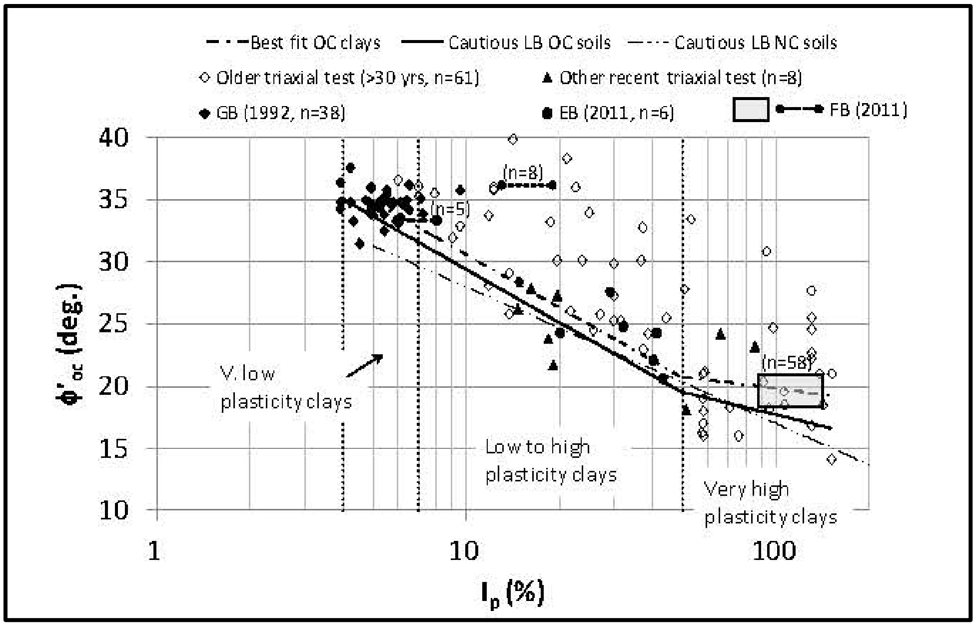

Note: I_P = PI

Figure 7-24, Plasticity Index versus Drained Shear Resistance for OC Clays (Sorensen and Okkels (2013))

As can be seen from the lower bound curve in Figure 7-24, both the lower bound and best fit curves kink at a PI of approximately 50 percent (50% < PI); therefore 2 equations will be required to describe each curve based on PI.

Lower Bound Equations

$$4 < PI < 50 \qquad \phi'_{OC} = 44^{\circ} - 14^{\circ} * \log PI$$ **Equation 7-55**

$$50 \leq PI < 150 \qquad \phi'_{OC} = 30^{\circ} - 6^{\circ} * \log PI$$ **Equation 7-56**

Bet Fit Equations

$$4 < PI < 50 \qquad \phi'_{OC} = 45^{\circ} - 14^{\circ} * \log PI$$ **Equation 7-57**

$$50 \leq PI < 150 \qquad \phi'_{OC} = 26^{\circ} - 3^{\circ} * \log PI$$ **Equation 7-58**

These equations are for soils that CFs less than 80 percent (CF < 80%). These equations may be used for soils with CFs greater 80 percent (CF $\geq$ 80%); however, extreme caution should be exercised in the use of these equations at greater CFs. Soils with greater CFs were not part of the data set used to develop these equations.

As indicated previously, overconsolidated Clay-Like soils can have a drained cohesion (c'_{OC}). Sorensen and Okkels (2013) have developed equations relating c'_{OC} to PI; however, since c'_{OC} is more related to soil structure than ϕ'_{OC} the use of their equations may not be appropriate. Considering the fact that ϕ'_{OC} is based on soil mineralogy, which is partially based on PI, while c'_{OC} is more based soil structure which is lost during the sample preparation for PI determination. Therefore, Sorensen and Okkels (2013) recommends using a relationship between c'_{OC} and S_u

(see Figure 7-25). This relationship is applicable for clays having PIs greater than or equal to 7 (PI $\geq$ 7). For clays with PI less than 7 (PI < 7), Sorensen and Okkels (2013) recommend c'_{OC} be assumed to be 0 psf.

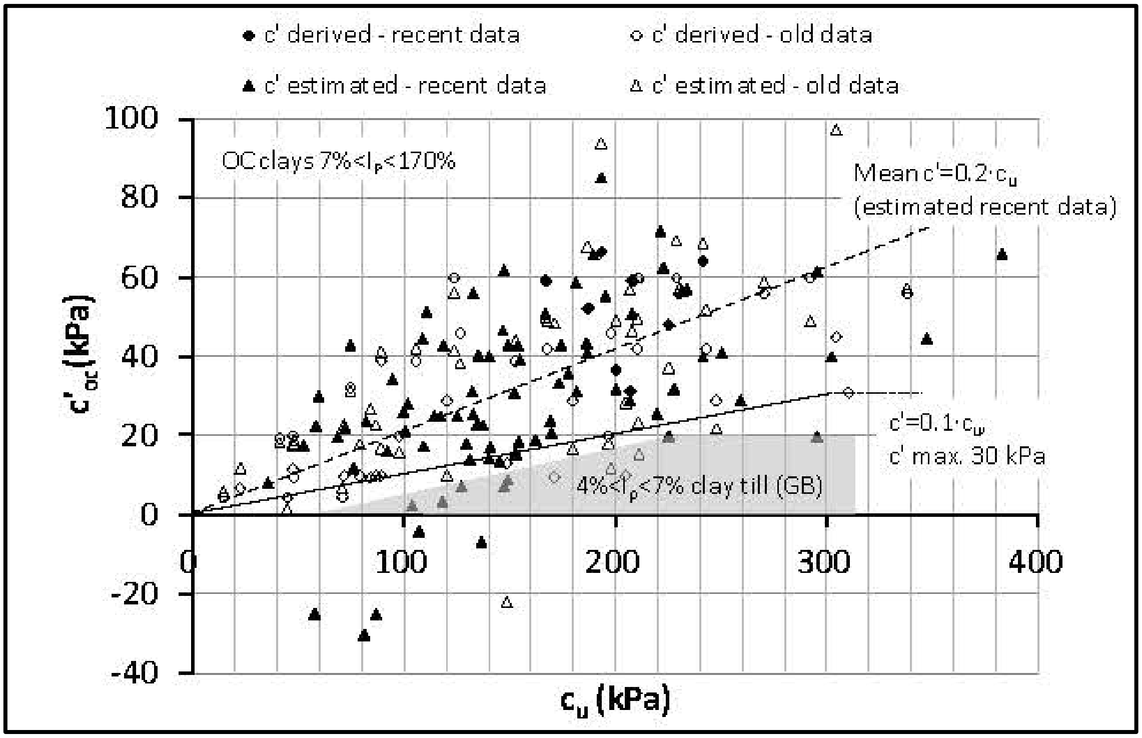

Note: $c_u = S_u$

Figure 7-25, Undrained Shear Strength versus Drained Shear Resistance for OC Clays (Sorensen and Okkels (2013))

$$PI < 7 \qquad c'_{OC} = 0\,psf \qquad \textbf{Equation 7-59}$$

$$7 \leq PI < 150 \qquad c'_{OC} = 0.1 * S_u \leq 630\,psf \qquad \textbf{Equation 7-60}$$

It is noted that the c'_{OC} has a maximum value of 630 psf.

The preceding paragraphs discussed the development of the peak drained shear strength for normally (ϕ'_{NC}) and overconsolidated (ϕ'_{OC} and c'_{OC}) Clay-Like soils. The following paragraphs discuss the development of drained residual shear strength. Stark and Eid (1994 and 1997) developed a graphical relationship between PI, CF and σ'_{vo} (effective normal stress) to obtain the drained shear strength of Clay-Like soils (see Figure 7-26). This graph was used for heavily overconsolidated (OCR > 4) Clay-Like soils. This method for determining drained residual shear strength has been updated by Stark and Hussain (2013) (see Figure 7-27). The Stark and Hussain (2013) procedure shall be used to determine the drained residual shear strength (ϕ'_r). Stark and Hussain (2013) have developed 3 sets of equations based on CF with individual equations based on LL (surrogate for PI) and σ'_{vo}.

- CF $\leq$ 20%
- 25% $\leq$ CF $\leq$ 45%
- CF $\geq$ 50%

Each set of equations also has a range of LL over which the equations apply. The limitations imposed by the LL are a result of the testing results used to develop the equations.

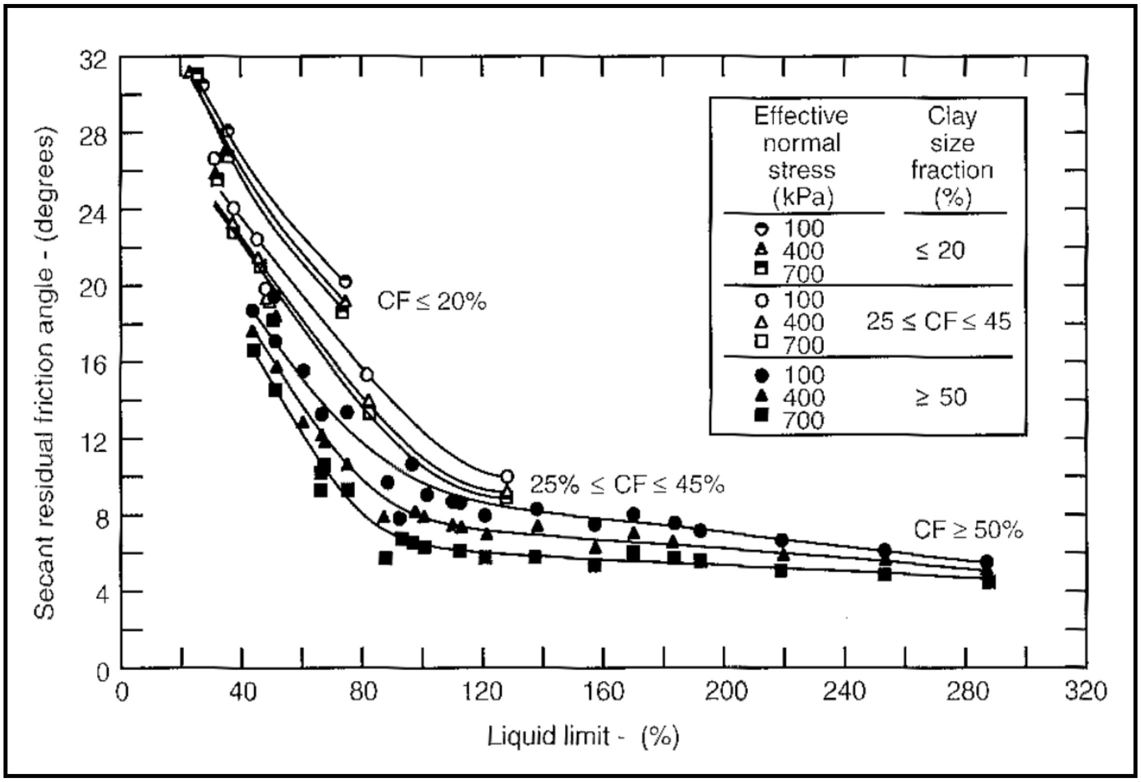

Figure 7-26, Drained Residual Friction Angle and Liquid Limit Relationship (Stark and Eid (1994) with permission from ASCE)

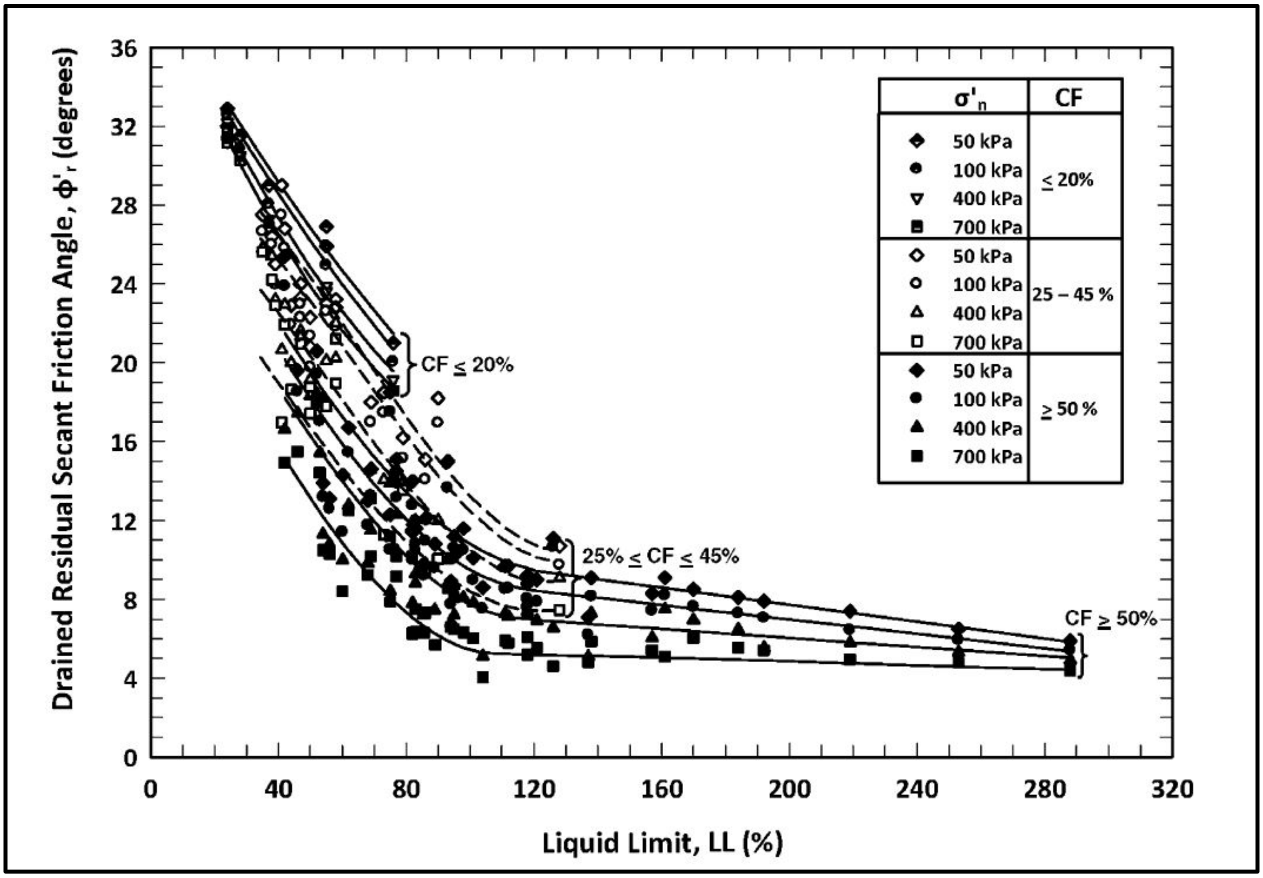

Figure 7-27, Updated Drained Residual Friction Angle and Liquid Limit Relationship (Stark and Hussain (2013) with permission from ASCE)

The first set of equations (CF $\leq$ 20%) for determining the drained residual shear strength are presented below. These equations should be used for soils that have 30% $\leq$ LL < 80%; however, these equations may be used with extreme caution on soils having LLs outside of this range.

$$(\phi'_r)_{\sigma'_{vo}=50kPa} = 39.71 - 0.29 * (LL) + [6.63 * 10^{-4} * (LL)^2]$$ **Equation 7-61**

Equation 7-62

$$(\phi'_r)_{\sigma'_{vo}=100\ kPa} = 39.41 - 0.298 * (LL) + [6.81 * 10^{-4} * (LL)^2]$$

$$(\phi'_r)_{\sigma'_{vo}=400kPa} = 40.24 - 0.375 * (LL) + [1.36 * 10^{-3} * (LL)^2]$$ **Equation 7-63**

Equation 7-64

$$(\phi'_r)_{\sigma'_{vo}=700\ kPa} = 40.34 - 0.412 * (LL) + [1.683 * 10^{-3} * (LL)^2]$$

Note 1 kPa is equal to approximately 20.89 psf.

The second set of equations (25% $\leq$ CF $\leq$ 45%) for determining the drained residual shear strength are presented below. These equations should be used for soils that have 30% $\leq$ LL < 130%; however, these equations may be used with extreme caution on soils having LLs outside of this range.

Equation 7-65

$$(\phi'_r)_{\sigma'_{vo}=50kPa} = 31.4 - 6.79 * 10^{-3} * (LL) - 3.616 * 10^{-3}(LL)^2 + 1.864 * 10^{-5} * (LL)^3$$

Equation 7-66

$$(\phi'_r)_{\sigma'_{vo}=100kPa} = 29.8 - 3.627 * 10^{-4} * (LL) - 3.584 * 10^{-3}(LL)^2 + 1.854 * 10^{-5} * (LL)^3$$

Equation 7-67

$$(\phi'_r)_{\sigma'_{vo}=400kPa} = 28.4 - 5.622 * 10^{-2} * (LL) - 2.952 * 10^{-3}(LL)^2 + 1.721 * 10^{-5} * (LL)^3$$

Equation 7-68

$$(\phi'_r)_{\sigma'_{vo}=700kPa} = 28.05 - 0.2083 * (LL) - 8.183 * 10^{-4}(LL)^2 + 9.372 * 10^{-6} * (LL)^3$$

The third set of equations (CF ≥ 50%) for determining the drained residual shear strength are presented below; however, a review of Figure 7-27 indicates that the 2 equations for each curve will be required. For soils that have 30% ≤ LL < 120% a third-degree polynomial will be required to describe this portion of the curve, while for soils having 120% ≤ LL < 300% a linear equation may be used. For each effective overburden pressure, the third-degree polynomial is provided first followed by the linear equation. Extreme caution should be used when applying these to soils having LLs outside of this range.

30% ≤ LL < 120%

Equation 7-69

$$(\phi'_r)_{\sigma'_{vo}=50kPa} = 33.5 - 0.31 * (LL) + 3.9 * 10^{-4}(LL)^2 + 4.4 * 10^{-6} * (LL)^3$$

120% ≤ LL < 300%

$$(\phi'_r)_{\sigma'_{vo}=50kPa} = 12.03 - 0.0215 * (LL)$$ **Equation 7-70**

30% ≤ LL < 120%

Equation 7-71

$$(\phi'_r)_{\sigma'_{vo}=100kPa} = 30.7 - 0.2504 * (LL) - 34.2053 * 10^{-4}(LL)^2 + 8.0479 * 10^{-6} * (LL)^3$$

120% ≤ LL < 300%

$$(\phi'_r)_{\sigma'_{vo}=100kPa} = 10.64 - 0.0183 * (LL) \qquad \textbf{Equation 7-72}$$

30% ≤ LL < 120%

Equation 7-73

$$(\phi'_r)_{\sigma'_{vo}=400kPa} = 29.42 - 0.2621 * (LL) - 4.011 * 10^{-4}(LL)^2 + 8.718 * 10^{-6} * (LL)^3$$

120% ≤ LL < 300%

$$(\phi'_r)_{\sigma'_{vo}=400kPa} = 8.32 - 0.0114 * (LL) \qquad \textbf{Equation 7-74}$$

30% ≤ LL < 120%

Equation 7-75

$$(\phi'_r)_{\sigma'_{vo}=700kPa} = 27.7 - 0.3233 * (LL) + 2.896 * 10^{-4}(LL)^2 + 7.1131 * 10^{-6} * (LL)^3$$

120% ≤ LL < 300%

$$(\phi'_r)_{\sigma'_{vo}=700kPa} = 5.84 - 0.0049 * (LL) \qquad \textbf{Equation 7-76}$$

As indicated previously the above approach for developing drained residual shear strength is for heavily overconsolidated Clay-Like soils. Typically most heavily overconsolidated Clay-Like soils are indurated (hard) and aggregated (i.e., the clay particles stick together) additional processing of the samples is required to get accurate CFs and LLs. Using the appropriate ASTM procedures, the samples will be processed using a mortar and pestle with the sample being passed through a No. 40 sieve. The CF and LL for the material passing the No. 40 sieve is then determined ($CF_{No.\ 40}$ and $LL_{No.\ 40}$). The equations presented above are typically based on some of the samples being processed using ball milling to completely disaggregate the sample and then pass the sample through the No. 200 sieve. The material passing the No. 200 sieve is then tested for CF and LL ($CF_{No.\ 200}$ and $LL_{No.\ 200}$) using the appropriate ASTM testing method. Typically, the $CF_{No.\ 200}$ and $LL_{No.\ 200}$ are greater than the $CF_{No.\ 40}$ and $LL_{No.\ 40}$. The use of ball milling is not a typical testing preparation method. Stark and Hussain (2013) have developed based on the available data correlations between $CF_{No.\ 40}$ and $CF_{No.\ 200}$; and $LL_{No.\ 40}$ and $LL_{No.\ 200}$. These correlations shall only be used with this procedure.

$$LL_{No.200} = 0.003 * (LL_{No.40})^2 + 1.23 * LL_{No.40} \qquad \textbf{Equation 7-77}$$

Equation 7-78

$$CF_{No.200} = 0.0002 * (CF_{No.40})^3 - 0.0278 * (CF_{No.40})^2 + 2.15 * (CF_{No.40})$$

Please note that these equations have been slightly rearranged from the way Stark and Hussain (2013) presented.

7.10.3 Transitional Soils

The drained shear strength of transitional soils may have both ϕ' and c' components; these components should be determined in the laboratory using the appropriate testing methods. However, if samples for this type of testing have not been obtained (e.g., during the preliminary exploration), then the GEOR should review the percent fines and the plasticity of the soil to determine whether the soil will behave Sand-Like or Clay-Like. If transitional soils are identified in the preliminary exploration, obtaining undisturbed samples of these materials should be attempted during the final exploration. For soils that are difficult to determine the approximate classification, the undrained shear strength parameters for both Sand-Like and Clay-Like soils should be determined and the more conservative design should be used.

7.10.4 Maximum Allowable Effective Soil Shear Strength

SCDOT has established maximum allowable peak (c, ϕ) and residual (c_r, ϕ_r) undrained soil shear strength design parameters for in-situ soils shown in Table 7-17, for use in design. These soil shear strength design parameters may be exceeded with appropriate laboratory testing results (see Table 7-11). Alternately, these shear strengths may be exceeded using correlations with field testing results (see Table 7-12) and the express written permission of the OES/GDS.

Table 7-17, Maximum Allowable Effective Soil Shear Strengths

Soil Description		Peak [1]		Residual	
USCS	Description	c' (psf)	ϕ' (degrees)	c' (psf)	ϕ' (degrees)
GW, GP, GM, GC	Stone and Gravel	0	40	0	34
SW	Coarse-grained Sand	0	38	0	32
SM, SP	Fine-grained Sand	0	36	0	30
SP	Uniform Rounded Sand	0	32	0	32
ML, MH, SC	Silt, Clayey Sand, Clayey Silt	0	30	0	27
SM, ML	Residual Soils	0	27	0	22
CL-ML	NC Clay (Low Plasticity)	0	35	0	31
CL, CH	NC Clay (Med-High Plasticity)	0	26	0	16
CL-ML	OC Clay (Low Plasticity)	0	34	0	31
CL, CH	OC Clay (Med-High Plasticity)	0	28	0	16

[1] The same maximum peak effective shear strength parameters shall be used for peak effective internal friction angle of normally consolidated cohesive soils and to the fully-softened internal friction angle of overconsolidated cohesive soils.

7.11 BORROW MATERIALS SOIL SHEAR STRENGTH SELECTION

This Section pertains to the selection of soil shear strength design parameters for borrow materials used in embankments or behind retaining walls (other than MSE walls or Reinforced Soil Slopes (RSSs)). Soil shear strength selection shall be based on the soil loading and soil response considerations presented in Section 7.9. The soil shear strength design parameters selected must be locally available, cost effective, and be achievable during construction. The selection of soil shear strength design parameters that require the importation of materials from outside of the general project area should be avoided. To this end, bulk samples will be obtained from existing fill embankments or from proposed cut areas and tested as indicated in Chapter 4. The purpose of sampling and testing the existing fill is the assumption that similar fill materials will be available locally. The purpose of sampling and testing proposed cut areas is to determine the suitability of the material for use as fill. The selection of design soil shear strengths required for borrow sources should take into consideration the construction borrow specifications as indicated in Section 7.12.1.

The procedure for selecting soil shear strength design parameters varies depending on the type of project as indicated below:

1. **Traditional Design-Bid-Build W/Existing Embankments:** This type of project can occur when existing roads are being improved by widening the existing embankment. An investigation of locally available materials should be made to confirm that the existing embankment soils are still locally available. If the existing embankment soils are available, the selection of soil shear strength design parameters for these types of projects will be based on using laboratory testing from composite bulk sample obtained from the existing embankment as required in Chapter 4 and appropriately selecting the drained and undrained soil shear strength design parameters for the borrow material. The plans and contract documents may specify the minimum required soil shear strength parameters for the borrow sources based on the existing embankment soils, if necessary. If the existing embankment soils are not locally available, borrow material shear strength parameters will be determined as if the project were on a new alignment.
2. **Traditional Design-Bid-Build On New Alignment:** This type of project requires the pre-selection of soil shear strength design parameters without performing any laboratory testing. The preliminary subsurface investigation may need to identify locally available soils (or borrow sources) and appropriately select soil shear strength design parameters for the borrow materials. Locally available soils can be investigated by using USDA Soil Survey maps as indicated in Section 7.12.2. The plans and contract documents may specify the minimum required soil shear strength parameters for the borrow sources, if necessary.

7.11.1 SCDOT Borrow Specifications

The SCDOT Standard Specifications for Highway Construction (latest edition), Section 203, provides the requirements for borrow material. Embankment material must not have optimum moisture content greater than 25.0% as defined in accordance with SC-T-29. Acceptable soils for use in embankments and as subgrade vary by county indicated by the following 2 Groups.

Group A: Includes the following counties: Abbeville, Anderson, Cherokee, Chester, Edgefield, Fairfield, Greenville, Greenwood, Lancaster, Laurens, McCormick, Newberry, Oconee, Pickens, Saluda, Spartanburg, Union, and York. Below the upper 5 feet of embankment, any soil that does not meet the description of muck may be used provided it is stable when compacted to the required density.

Group B: Aiken, Allendale, Bamberg, Barnwell, Beaufort, Berkeley, Calhoun, Charleston, Chesterfield, Clarendon, Colleton, Darlington, Dillon, Dorchester, Florence, Georgetown, Hampton, Horry, Jasper, Kershaw, Lee, Lexington, Marion, Marlboro, Orangeburg, Richland, Sumter, and Williamsburg. The soil material below the upper 5 feet of embankment is soil that classifies as A-1, A-2, A-3, A-4, A-5, and A-6.

Groups A and B are shown graphically on a South Carolina map in Figure 7-28.

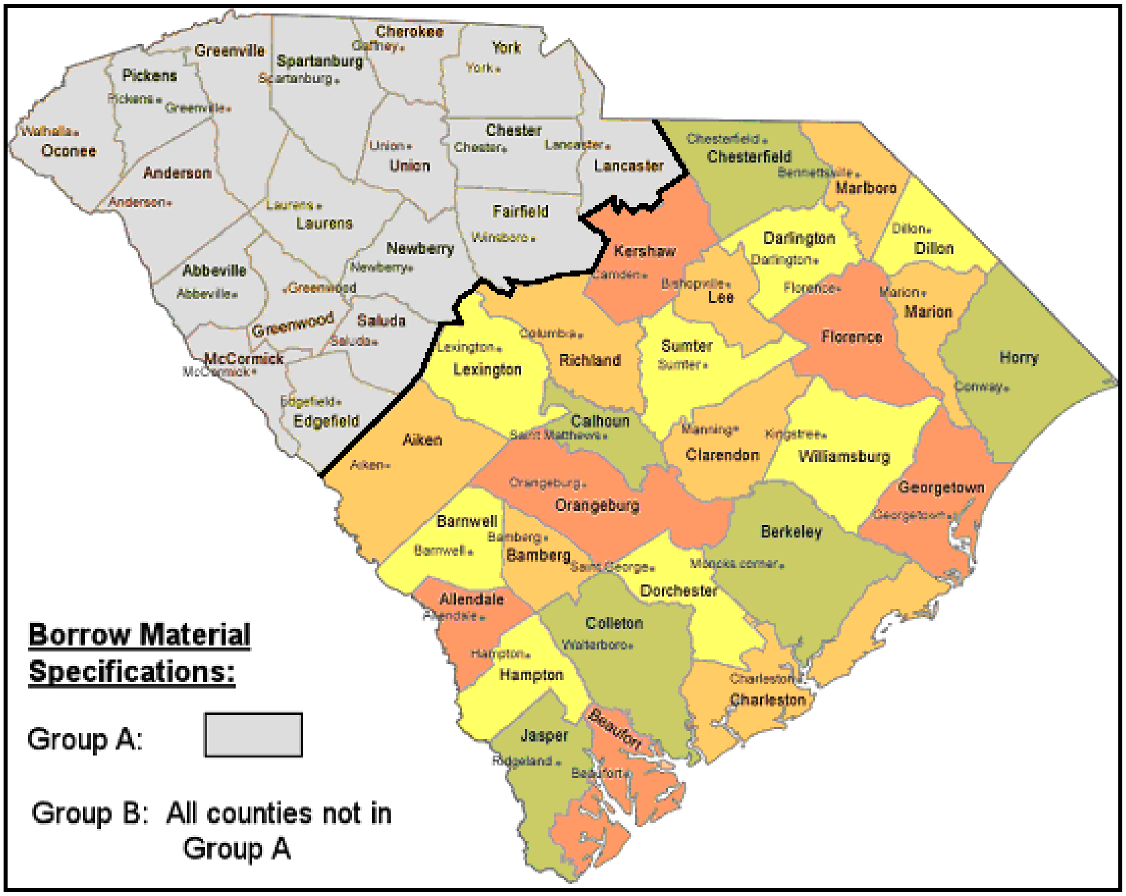

Figure 7-28, Borrow Material Specifications By County

A brief geologic description of the surface soils in Groups A and B are provided below and for more detail see Chapter 11.

<u>Group A</u>: This group is located northwest of the “Fall Line” in the Blue Ridge and Piedmont physiographic geologic units. The Blue Ridge unit surface soils typically consist of residual soil profile consisting of clayey soils near the surface where weathering is more advanced, underlain by sandy silts and silty sands. There may be colluvial (old land-slide) material on the slopes. The Piedmont unit has a residual soil profile that typically consists of clayey soils near the surface, where soil weathering is more advanced, underlain by sandy silts and silty sands. The residual soil profile exists in areas not disturbed by erosion or the activities of man.

<u>Group B:</u> This group is located south and east of the “Fall Line” in the Coastal Plain physiographic geologic unit. Sedimentary soils are found at the surface consisting of unconsolidated sand, clay, gravel, marl, cemented sands, and limestone.

7.11.2 USDA Soil Survey Maps

Locally available borrow sources can be researched by using the United States Department of Agriculture (USDA) Soil Survey Maps. A listing of USDA Soil Surveys that are available can be obtained by selecting "South Carolina" at http://soils.usda.gov/survey/printed_surveys/ and reviewing results by county. Soil surveys can be obtained as either printed documents, CD-ROM, downloading online .pdf documents, or generated using USDA Web Soil Survey (WSS) Internet application.

The USDA Soil Surveys typically indicate Soil Map Units that are described based on USDA textural classification system. Recent USDA Soil Survey manuscripts contain tables with equivalent material descriptions for the AASHTO and the USCS soil classification systems. When only the USDA textural classification is indicated in the maps, the GEOR will need to correlate the USDA textural classifications to the AASHTO and the USCS soil classification systems.

The USDA WSS Internet application can be accessed at: http://websoilsurvey.nrcs.usda.gov/app/. The USDA WSS is an online web application that can provide soil data and natural resource information produced by the National Cooperative Soil Survey. The web site is under constant development and being updated with new information. Soil survey maps and maps of Roadfill sources for project specific locations can be generated as shown in Figure 7-29 and Figures 7-30, respectively.

Figure 7-29, USDA Soil Map – Newberry County, South Carolina (USDA Web Soil Survey)

Figure 7-30, USDA Roadfill Source Map - Newberry County, South Carolina (USDA Web Soil Survey)

7.11.3 Compacted Soils Shear Strength Selection

Compacted soils are used to construct roadway embankments, bridge approaches, and backfill behind retaining walls. This Section does not govern the selection of backfill soil properties for MSE walls or RSSs. The method of selecting soil shear strength parameters for compacted soils will be either:

- Measured using appropriate laboratory shear strength tests or
- Conservatively selected based on drained soil shear strength parameters typically encountered in South Carolina soils.

The method to be used for selection will be dependent on the type of project as discussed previously.

SCDOT experience with borrow materials typically found in Group A are Piedmont residual soils. These borrow materials are typically classified as micaceous clayey silts and micaceous sandy silts, clays, and silty soils in partially drained conditions. These soils may have USCS classifications of either ML or MH and typically have LL greater than 30. Published laboratory shear strength testing results for Piedmont residual soils (Sabatini, et al. (2002), Appendix A, page A-40) indicate an average effective friction angle of 35.2^{o} with a ± 1 standard deviation range of $29.9^{o} < \phi' < 40.5^{o}$. A conservative lower bound of 27.3^{o} is also indicated.

SCDOT experience with borrow materials typically found in Group B are Coastal Plain soils that are typically uniform fine sands that are sometimes difficult to compact and behave similar to silts. When these soils are encountered, caution should be used in selecting effective soil shear strength friction angles since values typically range from $28^{o} < \phi' < 32^{o}$.

7.11.4 Allowable Soil Shear Strengths of Compacted Soils

SCDOT has determined, through a research project, the effective and total soil strength parameters (i.e., c' and ϕ' or c and ϕ) that are typically available for each South Carolina County. The results of this research and the allowable parameters are available on the SCDOT website (http://www.scdot.org/doing/geoTech_Design.aspx). If the results of the on-site soil testing or the selected shear strength parameters are less than the shear strength parameters provided on the SCDOT website then shear strength verification testing during construction should not be required during compaction. However, the GEOR may select a project-specific soil classification (i.e., AASHTO and USCS Classifications (see Chapter 6)) in order to assure that the borrow materials meet the shear strength requirements. This project-specific soil classification shall be provided on the project plans. The required testing for this verification, is not anticipated to be different than the classification testing already currently being performed during construction. If the on-site soil has a shear strength greater than the allowed for the county, the GEOR may elect to use this higher shear strength without the requirement for shear strength verification testing during construction. However, a project-specific classification (i.e., AASHTO and USCS Classifications) shall be required to be indicated on the project plans. If the GEOR's design needs to exceed the on-site shear strength parameters and the county shear strength values, the GEOR shall use the proposed plan notes (see Chapter 22) to convey the required soil strength properties to the Contractor. The following testing shall be required to confirm the anticipated revised shear strength parameters:

- Moisture-density Relationship (Standard Proctor)
- Grain-size Distribution with wash No. 200 Sieve
- Moisture-Plasticity Relationship Determination (Atterberg Limits)
  - Performed only on samples with more than 20 percent passing #200 sieve
- Natural Moisture Content
- Direct Simple Shear Test
  - Performed only on samples with less than or equal to 20 percent passing #200 sieve
  - Sample remolded to 95 percent of Standard Proctor value
  - Sample moisture content shall be between -1 percent to +2 percent of optimum moisture content
- Consolidated-Undrained Triaxial Shear Test with pore pressure measurements
  - Performed only on samples with more than 20 percent passing #200 sieve
  - Sample remolded to 95 percent of Standard Proctor value
  - Sample moisture content shall be between -1 percent to +2 percent of optimum moisture content

Once a borrow source achieving the required shear strength parameters has been located, additional shear strength testing during construction will be required every approximate 50,000 CY. Classification testing performed at the intervals required by the SCDOT Standard Specifications for Highway Construction, latest edition, will be required to assure that the borrow materials continue to be similar to the materials used in the shear strength testing. The GEOR shall determine when and if additional shear strength testing is required if the classification testing indicates a change in classification.

If stone (e.g., Nos. 57, 67, 789 or No. 4 ballast) is selected as the borrow material, large scale direct shear (minimum size of direct shear box of 12 inches square by 8 inches deep) should be required. However, to avoid the cost and time for testing these materials a maximum ϕ' of 46° shall be assumed for all of the stones. If a ϕ' greater than this value is required, then testing will be required. However, prior to testing the GEOR shall obtain approval from the OES/GDS for the increased ϕ' and will provide the name of the laboratory performing the tests. It is noted that this ϕ' does not apply to MSE wall design. See Supplemental Technical Specification (STS) *Mechanically Stabilized Earth (MSE) Walls*, SC-M-713, for the ϕ' that applies to MSE wall design.

7.12 SOIL SETTLEMENT PARAMETERS

Settlements are caused by the introduction of loads (stresses, $+\Delta\sigma$) on to the subsurface soils located beneath a site. These settlements can be divided into 2 primary categories, elastic and time-dependent settlements (consolidation). Settlements (strains) are a function of the load (stress) placed on the subsurface soils. Elastic settlements typically predominate in Sand-Like soils or soils with 0 to 20 percent fines regardless of the plasticity of the fines. Time-dependent settlements predominate in Clay-Like soils or soils with more than 20 percent fines and with LL greater than 40 ($LL > 40$) and PI greater than 10 ($PI > 10$). The GEOR should evaluate soils with either LL less than 40 ($LL < 40$) or PI less than 10 ($PI < 10$) as to whether the soils will behave elastically or have time-dependent settlement characteristics. The GEOR is responsible for making this determination for these soils (see Table 7-6 for guidance).

Settlement parameters can be developed from high quality laboratory testing (triaxial shear for elastic parameters and consolidation testing for time-dependent parameters). However, for cohesionless soils, obtaining high quality samples for testing can be extremely difficult. Therefore, in-direct methods (correlations) for measuring the elastic parameters are used. Time-dependent settlement parameter correlations for cohesive soils also exist. These correlations should be used for either preliminary analyses or for evaluating the reasonableness of laboratory consolidation testing.

7.12.1 <u>Elastic Parameters</u>

Elastic settlements are instantaneous and are considered recoverable. These settlements are calculated using elastic theory. The determination of elastic settlements is provided in Chapter 17. In the determination of the elastic settlements the elastic modulus, E, (tangent or secant) and the Poisson's ratio, ν, are used. Since E and ν are both dependent on the laboratory testing method (unconfined, confined, undrained, drained), the overconsolidation ratio, water content, strain rate and sample disturbance, considerable engineering judgment is required to obtain reasonable values for use in design. Provided in Table 7-18 are elastic modulus correlations with $N^*_{1,60}$ values. Table 7-19 provides typical values of soil elastic modulus and Poisson's ratio for various soil types.

Table 7-18, Elastic Modulus Correlations for Soil Using SPT N-values (AASHTO LRFD Specifications (2020))

Soil Type	Elastic Modulus, E_s (psi)
Silts, sandy silts, slightly cohesive mixtures	56*($N^*_{1,60}$)
Clean fine to medium sands and slightly silty sands	97*($N^*_{1,60}$)
Coarse sands	139*($N^*_{1,60}$)
Sandy gravels and gravels	167*($N^*_{1,60}$)

The elastic modulus of soil may also be correlated to corrected tip resistance (q_t) and the soil behavior type (I_c) according to Robertson and Cabal (2015), using the following equations:

$$E_s = \alpha_E * (q_t - \sigma_{vo})$$ **Equation 7-79**

$$\alpha_E = 0.015 * \left[10^{(0.55*I_c+1.68)}\right]$$ **Equation 7-80**

Where,

q_t = Corrected tip resistance (see Chapter 5)
σ_{vo} = Total overburden stress at depth of q_t (see Chapter 5)
I_c = Soil behavior type (see Chapter 5)
E_s = Elastic modulus, same units as q_t and σ_{vo}

According to Marchetti, et al. (2001), the elastic modulus of soil, E_s, may be correlated from the DMT using the constrained modulus, M_{DMT}.

$$E_s = \left[\frac{(1+\nu)*(1-2\nu)}{(1-\nu)}\right] * M_{DMT}$$ **Equation 7-81**

Where,

ν = Poisson's ratio
M_{DMT} = constrained modulus (bars) (1 bar ≈ 1 tsf)

$$M_{DMT} = R_M * E_D$$ **Equation 7-82**

Where,

E_D = Dilatometer modulus (bars) (1 bar ≈ 1 tsf)

The term R_M is a function of the Material Index and the Horizontal Stress Index (f(I_D,K_D)). R_M is determined using the following equations when K_D is less than or equal to 10 ($K_D \leq 10$).

$$I_D \leq 0.6 \qquad R_M = 0.14 + 2.36 * log\, K_D$$ **Equation 7-83**

$$0.6 < I_D < 3 \quad R_M = R_{M,0} + \left(2.5 - R_{M,0}\right) * log\, K_D$$ **Equation 7-84**

$$R_{M,0} = 0.14 + 0.15 * [I_D - 0.6]$$ **Equation 7-85**

$$I_D \geq 3 \qquad R_M = 0.5 + 2 * \log K_D$$ **Equation 7-86**

If K_D is greater than 10 (K_D > 10), then use the following equation:

$$R_M = 0.32 + 2.18 * \log K_D$$ **Equation 7-87**

If R_M determined using the above equations is less than 0.85, set R_M equal to 0.85.

For soils with a Poisson's ratio, ν, ranging from 0.25 to 0.30, the following equation may be used. A Poisson's ratio in this range is typical of coarse-grained soils (see Table 7-19).

$$E_s \approx 0.8 M_{DMT}$$ **Equation 7-88**

Table 7-19, Typical Elastic Modulus and Poisson Ratio Values for Soil (AASHTO LRFD Specifications (2020))

Soil Type	Typical Elastic Modulus Values, E (ksi)	Poisson's Ratio, ν
Clay:		0.4 – 0.5 (Undrained)
Soft sensitive	0.347 – 2.08	
Medium stiff to stiff	2.08 – 6.94	
Very stiff	6.94 – 13.89	
Silt	0.278 – 2.78	0.3 – 0.35
Fine Sand:		0.25
Loose	1.11 – 1.67	
Medium dense	1.67 – 2.78	
Dense	2.78 – 4.17	
Sand:		
Loose	1.39 – 4.17	0.20 – 0.36
Medium dense	4.17 – 6.94	0.25 – 0.40
Dense	6.94 – 11.11	0.30 – 0.40
Gravel:		
Loose	4.17 – 11.11	0.20 – 0.35
Medium dense	11.11 – 13.89	0.25 – 0.40
Dense	13.89 – 27.78	0.30 – 0.40

7.12.2 Consolidation Parameters

Consolidation settlement involves the removal of water from the interstitial spaces (pores) between soil grains and the rearrangement of the soil grains. Typically, Clay-Like soils are considered to undergo consolidation settlements. However, soils with either LL greater than 40 (LL > 40) or PI greater than 10 (PI > 10) also undergo consolidation settlements depending on the moisture-plasticity relationship. Clay-Like soils are typically more impervious and therefore will require more time to settle. Further these soil types may also undergo more settlement than Sand-Like soils because of the volume of water within these soils. To determine the amount of consolidation settlement that a soil will undergo, the following soil parameters are required: compression (C_c or $C_{\varepsilon c}$), recompression (C_r or $C_{\varepsilon r}$), and secondary (C_α or $C_{\varepsilon\alpha}$) compression indices, coefficient of consolidation (c_v) and the effective preconsolidation pressure (σ'_p or p'_c). These parameters are normally determined from consolidation testing (see Chapter 5).

Prior to obtaining the parameters indicated previously, the curves obtained from the consolidation test require correction by the GEOR. Curve correction is applied to the test results presented as e-log p and ε-log p curves. Duncan and Buchignani (1976) provide methods for correcting both e-log p and ε-log p for both normally consolidated and overconsolidated soils. The procedures for correcting the e-log p curves (normally consolidated and overconsolidated) are presented in Table 7-20 and for the ε-log p curves (normally consolidated and overconsolidated) are presented in Table 7-21.

Table 7-20, Correction of the e-log p Curve for Disturbance (modified from Duncan and Buchignani (1976))

Step	Description
Normally Consolidated Soil ($\sigma'_{vo} = \sigma'_p$) (Figure 7-31)	
1	Locate point A at the intersection of e_o and σ'_p (P_p)
2	Locate point B on the virgin curve or extension where e = 0.4e_o
3	Connect points A and B with a straight line – this is the corrected virgin curve
Overconsolidated Soil ($\sigma'_{vo} < \sigma'_p$) (Figure 7-32)	
1	Locate point A at the intersection of e_o and σ'_{vo} (P_o')
2	Draw a line from point A parallel to the rebound curve and locate point B where this line intersects σ'_p (P_p)
3	Locate point C on the virgin curve or extension where e = 0.4e_o
4	Connect points B and C with a straight line – this is the corrected virgin curve

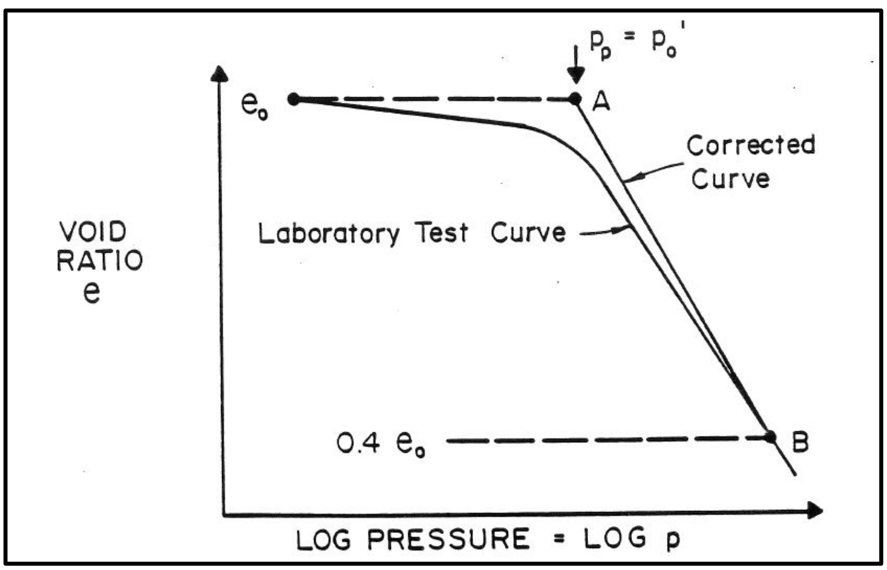

Figure 7-31, Corrected e-log p Normally Consolidated Curve (Duncan and Buchignani (1976))

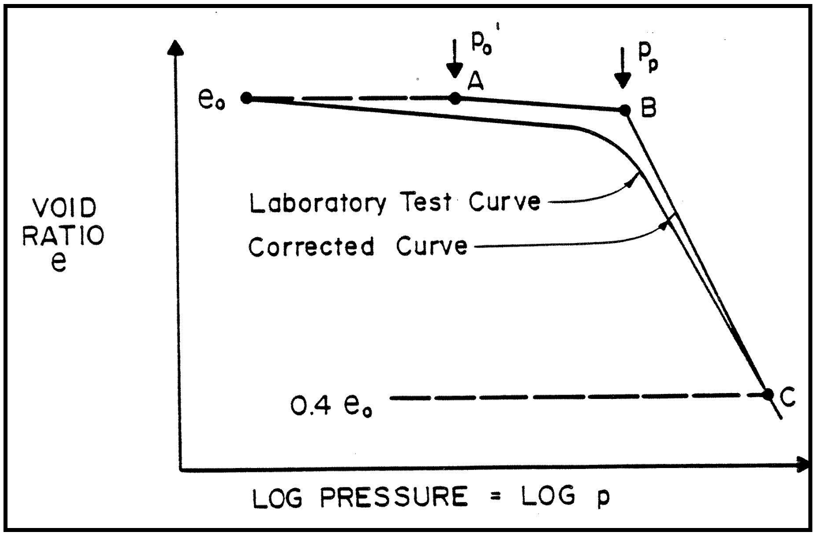

Figure 7-32, Corrected e-log p Overconsolidated Curve (Duncan and Buchignani (1976))

Table 7-21, Correction of the ε-log p Curve for Disturbance (modified from Duncan and Buchignani (1976))

Step	Description
Normally Consolidated Soil ($\sigma'_{vo} = \sigma'_p$) (Figure 7-33)	
1	Locate point A at the intersection of $\varepsilon = 0$ and σ'_p (P_p)
2	Locate point B on the virgin curve or extension where $\varepsilon = 0.4$
3	Contact points A and B with a straight line – this is the corrected virgin curve
Overconsolidated Soil ($\sigma'_{vo} < \sigma'_p$) (Figure 7-34)	
1	Locate point A at the intersection of $\varepsilon = 0$ and σ'_{vo} (P_o')
2	Draw a line from point A parallel to the rebound curve and locate point B where this line intersects σ'_p (P_p)
3	Locate point C on the virgin curve or extension where $\varepsilon = 0.4$
4	Contact points B and C with a straight line – this is the corrected virgin curve

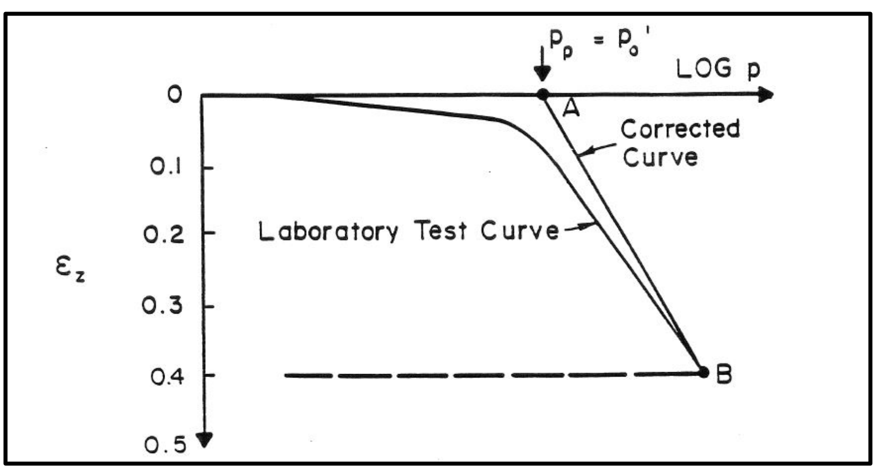

Figure 7-33, Corrected ε-log p Normally Consolidated Curve (Duncan and Buchignani (1976))

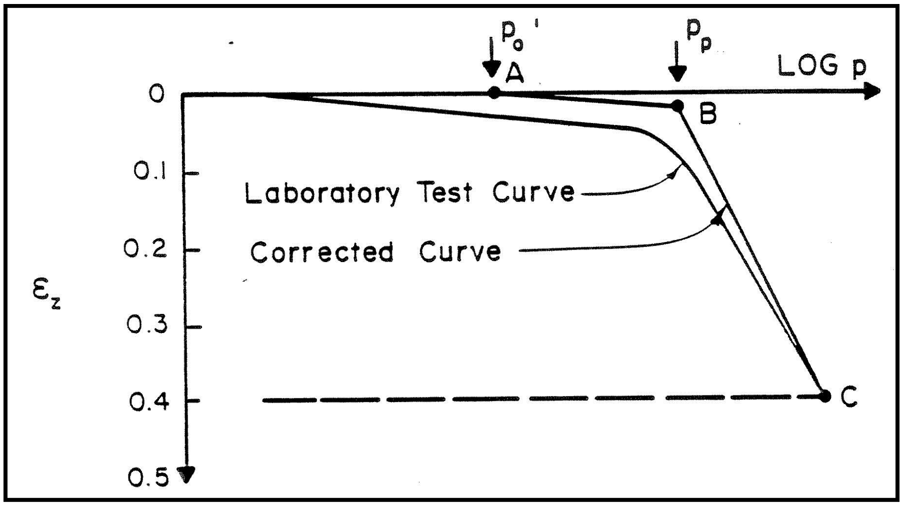

Figure 7-34, Corrected ε-log p Overconsolidated Curve (Duncan and Buchignani (1976))

The compression (C_c or $C_{\varepsilon c}$) and recompression (C_r or $C_{\varepsilon r}$) indices are determined from the corrected curves. The compression (C_c or $C_{\varepsilon c}$) index is the slope of the virgin portion of the corrected curve, either e-log p (C_c) or ε-log p ($C_{\varepsilon c}$), over a full logarithmic cycle. The recompression index is the slope of the recompression portion of the corrected curve, either e-log p (C_r) or ε-log p ($C_{\varepsilon r}$) over a full logarithmic cycle. If the slope of either portion of the curve does not extend over a full logarithmic cycle extend the line in both directions to cover a full logarithmic cycle.

For preliminary estimates and to verify the results of the consolidation testing the correlations listed in the following Sections may be used. These correlations should not be used for final design, except where the GEOR considers the results of the consolidation testing to be questionable. The GEOR shall document the reason for the use of the correlations. In addition, all of the consolidation parameters shall be clearly provided in the geotechnical report.

7.12.2.1 Compression Index

Similarly to the other consolidation parameters, the C_c is best determined from consolidation testing. The Compression Index (C_c) has been related to the Atterberg Limits by Tiwari and Ajmera (2012); however, this correlation should only be used for either preliminary analyses (first order estimates) or for evaluating the reasonableness of laboratory consolidation testing.

$$C_c = 0.014 * (PI) \qquad \textbf{Equation 7-89}$$

Where,

PI = Plasticity Index (%)

The Compression Index may also be related to strain as indicated below.

$$C_{\varepsilon c} = \frac{C_c}{(1+e_o)} \qquad \textbf{Equation 7-90}$$

Where,

e_o = Initial void ratio

C_c = Compression Index

7.12.2.2 Recompression Index

The Recompression Index (C_r) can be correlated to the C_c values. Ladd (1973) indicates the C_r value is approximately 10 to 20 percent of the C_c value. The Recompression Index may also be related to strain as indicated by the following equation.

$$C_{\varepsilon r} = \frac{C_r}{(1+e_o)} \quad \textbf{Equation 7-91}$$

Where,

e_o = Initial void ratio

C_r = Recompression Index

7.12.2.3 Secondary Compression Index

Secondary compression occurs after the completion of elastic and primary consolidation settlements. The amount of secondary compression settlement should be determined and included in the estimate of total settlement for a given project. The Secondary Compression Index (C_α) like the other consolidation settlement parameters is best determined from consolidation testing; however, correlations exist that may be used to provide a preliminary estimate of secondary compression settlement. In addition, these correlations may be used to verify the results of the consolidation testing. Provided in Figure 7-35 is a chart of C_α versus the natural moisture content of soil.

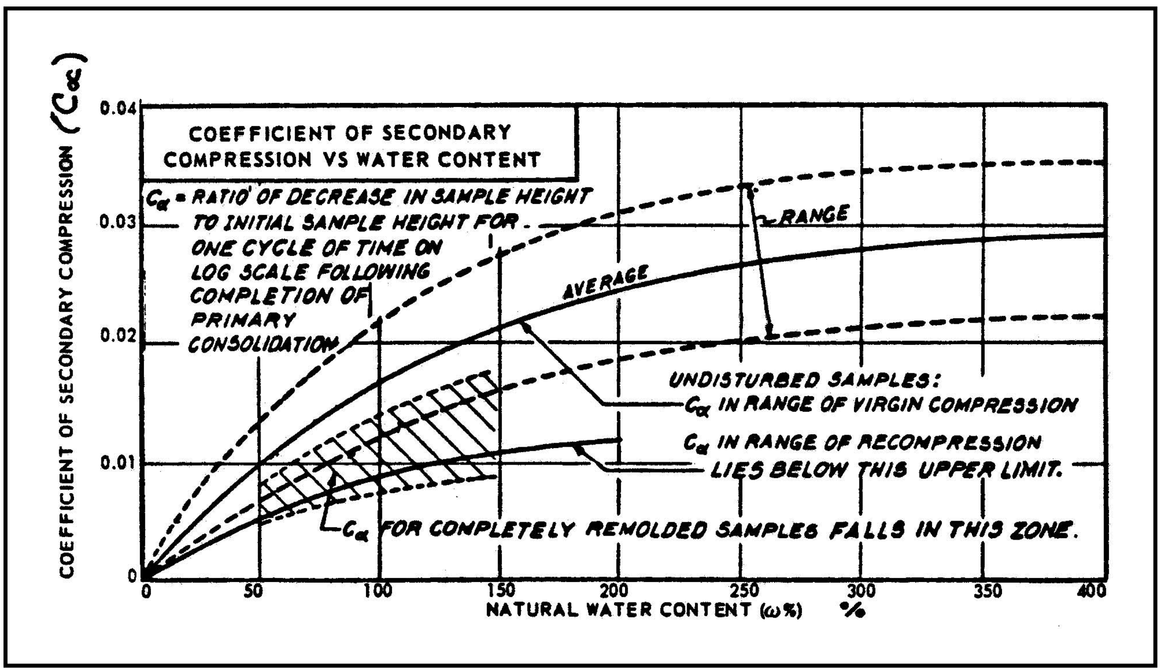

Figure 7-35, Secondary Compression Index Chart (NAVFAC DM-7.1 (1982))

The Secondary Compression Index may also be related to strain as indicated below.

$$C_{\varepsilon\alpha} = \frac{C_\alpha}{(1+e_o)}$$ **Equation 7-92**

Where,

e_o = Initial void ratio

C_α = Secondary Compression Index

For normally consolidated soils, the ratio of the coefficient of secondary compression to the compression index ($C_\alpha/C_c = C_{\varepsilon\alpha}/C_{\varepsilon c}$) is relatively constant for a given soil. On average, the value of C_α/C_c is 0.04±0.01 for inorganic clays and silts. For organic clays and silts the value averages 0.05±0.01. For peats, the value averages 0.06±0.01. These values may be used to assess actual values from laboratory tests or for preliminary analyses. If the final effective stress in the ground is less than the preconsolidation stress, the C_r should be used instead of C_c to estimate the coefficient of secondary compression.

7.12.2.4 Consolidation Coefficient

The preceding Sections dealt with the parameters required to determine the amount of settlement that could be anticipated at a project location; while this Section provides a means to estimate the time for consolidation settlement. As indicated previously, elastic settlements are anticipated to occur relatively instantaneously (i.e., during construction) while consolidation settlements are anticipated to occur at some time after the structure has been completed. The rate of consolidation is directly related to the permeability of the soil. As with the consolidation parameters, the coefficient of consolidation (c_v) should be determined from the results of consolidation testing. Correlations exist that may be used to provide a preliminary estimate of c_v. In addition, these correlations may be used to verify the results of the consolidation testing. Provided in Figure 7-36 is a chart of c_v versus the LL of soil.

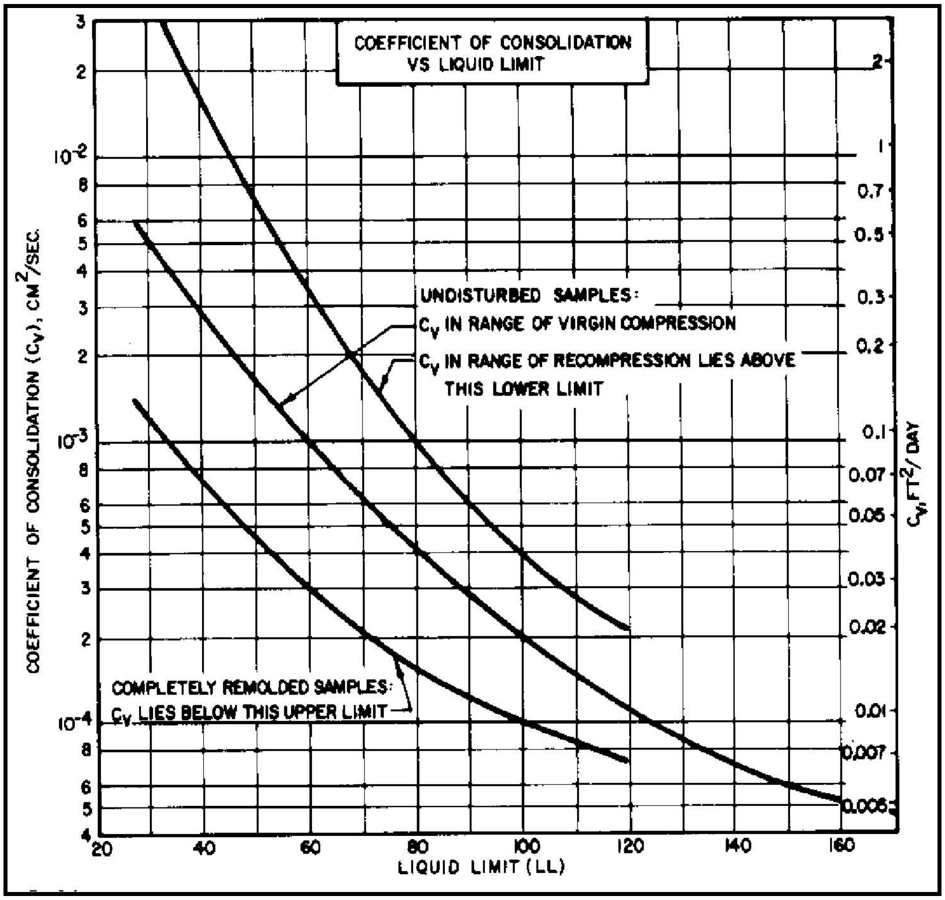

Figure 7-36, Consolidation Coefficient and Liquid Limit Relationship (NAVFAC DM-7.1 (1982))

7.12.2.5 Effective Preconsolidation Stress

The effective preconsolidation stress (σ'_p or p'_c) in soils is used to determine whether to use the Compression or Recompression Index. The effective preconsolidation stress (σ'_p) is the maximum past pressure that a soil has been exposed to since deposition. Similarly to the other consolidation parameters the σ'_p is best determined from consolidation testing. Correlations also exist; however, these correlations should only be used for either preliminary analyses (first order estimates) or for evaluating the reasonableness of laboratory consolidation testing. The effective preconsolidation stress (σ'_p or p'_c) can be correlated to total cohesion, c (NAVFAC DM-7.1 (1982)). As with the other consolidation parameters the correlated σ'_p should be used for preliminary estimates only.

$$\sigma'_p = \frac{c}{(0.11+0.0037*PI)}$$ **Equation 7-93**

The σ'_p can also be estimated from the CPTu using the following equations (Sabatini, et al. (2002)).

$$\sigma'_p = 0.33*(q_t - \sigma_{vo})$$ **Equation 7-94**

CPT Piezocone (shoulder element):

$$\sigma'_p = 0.53 * (u_2 - u_0) \qquad \text{Equation 7-95}$$

$$\sigma'_p = 0.60 * (q_t - u_2) \qquad \text{Equation 7-96}$$

7.13 ROCK PARAMETER DETERMINATION

While the shear strength of individual rock cores is obtained from unconfined axial compression testing, the shear strength of the entire rock mass should be used for design. Therefore, the shear strength and consolidation parameters for the rock mass shall be developed using both the GSI and the RMR methods as defined in Chapter 6. In addition, the GEOR should consider the time rate of rock coring, since typically harder rock masses will take longer to core through than weaker rock masses. There are many factors besides the strength of the rock that will affect the time rate of rock coring including condition of the core barrel, the condition of the drill rig, experience of the driller rig operator in rock operations, etc. The GEOR should be aware of all of these conditions when developing a profile of the rock encountered at a site.

7.13.1 <u>Shear Strength Parameters</u>

7.13.1.1 GSI

The rock mass shear strength from the GSI should be evaluated using the Hoek-Brown failure criterion (Hoek, Carranza-Torres, and Corkum (2002)) as presented in AASHTO LRFD Specifications. The shear strength of the rock mass is represented by a curved envelope that is a function of the unconfined (uniaxial) compressive strength of the intact rock, q_u, and 2 dimensionless factors. The rock mass compressive shear strength, τ is defined as indicated below. This rock mass compressive shear strength is used in design, provided there is no structural defect in the rock mass that would predominate over the rock mass compressive shear strength.

$$\tau = q_u * s^a \qquad \text{Equation 7-97}$$

$$s = e^{\left(\frac{GSI-100}{9-3D}\right)} \qquad \text{Equation 7-98}$$

$$a = \frac{1}{2} + \frac{1}{6} * \left(e^{\left(-\frac{GSI}{15}\right)} - e^{\left(-\frac{20}{3}\right)}\right) \qquad \text{Equation 7-99}$$

Where,

q_u = Unconfined compressive strength of intact rock specimen
GSI = Geological Strength Index (see Chapter 6)
D = Disturbance factor (see Chapter 6)
e = Mathematical constant (i.e., Euler's number)

7.13.1.2 RMR

The rock mass shear strength should be evaluated using the Hoek and Brown criterion as presented in Sabatini, et al. (2002). The shear strength of the rock mass is represented by a curved envelope that is a function of the unconfined (uniaxial) compressive strength of the intact rock, q_u, and 2 dimensionless factors. The rock mass shear strength, τ, (in ksf) is defined as indicated below.

$$\tau = (\cot \phi'_i - \cos \phi'_i) * m * \frac{q_u}{8}$$ **Equation 7-100**

$$\phi'_i = \tan^{-1}\left\{4h * cos^2\left[30 + 0.33 * \sin^{-1}\left(h^{\left(\frac{-3}{2}\right)}\right)\right] - 1\right\}^{\left(\frac{-1}{2}\right)}$$ **Equation 7-101**

$$h = 1 + \frac{[16*(m*\sigma'_n + s*q_u)]}{3*m^2*q_u}$$ **Equation 7-102**

Where,

ϕ'_i = instantaneous friction angle of the rock mass (degrees)
q_u = average unconfined rock core compressive strength (ksf)
σ'_n = effective normal stress (ksf)
m and s = Constants, from Table 7-22

Table 7-22, Constants m and s based on RMR (Sabatini, et al. (2002)

Rock Quality	Constants	**Rock Type:** **A** = Carbonate rocks with well-developed crystal cleavage – dolomite, limestone and marble **B** = Lithified argillaceous rocks – mudstone, siltstone, shale and slate (normal to cleavage) **C** = Arenaceous rocks with strong crystals and poorly developed crystal cleavage – sandstone and quartzite **D** = Fine-grained polymineralic igneous crystalline rocks – andesite, dolerite, diabase and rhyolite **E** = Coarse-grained polymineralic igneous and metamorphic crystalline rocks – amphibolite, gabbro, gneiss, granite, norite, and quartz-diorite				
		A	**B**	**C**	**D**	**E**
Intact rock samples RMR = 100	m s	7.00 1.00	10.00 1.00	15.00 1.00	17.00 1.00	25.00 1.00
Very good quality rock mass RMR = 85	m s	2.40 0.082	3.43 0.082	5.14 0.082	5.82 0.082	8.567 0.082
Good quality rock mass RMR = 65	m s	0.575 0.00293	0.821 0.00293	1.231 0.00293	1.395 0.00293	2.052 0.00293
Fair quality rock mass RMR = 44	m s	0.128 0.00009	0.183 0.00009	0.275 0.00009	0.311 0.00009	0.458 0.00009
Poor quality rock mass RMR = 23	m s	0.029 $3*10^{-6}$	0.041 $3*10^{-6}$	0.061 $3*10^{-6}$	0.069 $3*10^{-6}$	0.102 $3*10^{-6}$
Very poor quality rock mass RMR = 3	m s	0.007 $1*10^{-7}$	0.010 $1*10^{-7}$	0.015 $1*10^{-7}$	0.017 $1*10^{-7}$	0.025 $1*10^{-7}$

7.13.2 Settlement Parameters

Rocks will primarily undergo elastic settlements. The elastic settlements will be instantaneous and considered recoverable. These settlements are calculated using elastic theory. The determination of elastic settlements is provided in Chapter 17. In the determination of the elastic settlements, the elastic modulus of the rock mass, E_m, is required.

7.13.2.1 GSI

The elastic modulus of a rock mass, E_m, is the lesser of modulus determined from intact rock core testing, E_R, or from the equations below (Turner (2006)).

$$q_u \leq 100MPa \quad E_m = \left[\left(\sqrt{\frac{q_u}{100}}\right) * 10^{\left(\frac{GSI-10}{40}\right)}\right] \quad \text{Equation 7-103}$$

$$q_u > 100MPa \quad E_m = 10^{\left(\frac{GSI-10}{40}\right)} \quad \text{Equation 7-104}$$

$$E_m = \frac{E_R}{100} * \left(e^{\left(\frac{GSI}{21.7}\right)}\right) \quad \text{Equation 7-105}$$

Where,

q_u = unconfined (uniaxial) compressive strength of the intact rock, MPa
E_m = elastic modulus of rock mass, GPa
E_R = elastic modulus of intact rock, GPa
1MPa = 10.44 tsf = 20.88 ksf
1GPa = 145 ksi

7.13.2.2 RMR

The elastic modulus of a rock mass is the lesser of modulus determined from intact rock core testing or from the equations below.

RMR $\leq$ 85

$$E_m = 145 * \left(10^{\left(\frac{RMR-10}{40}\right)}\right) \quad \text{Equation 7-106}$$

60 $<$ RMR $<$ 85

$$E_m = (290 * RMR) - 14,500 \quad \text{Equation 7-107}$$

Where,

E_m = Elastic modulus of rock mass, ksi
RMR = Adjusted Rock Mass Rating from Chapter 6

For RMR greater than or equal to 85 (RMR ≥ 85), use either the modulus determined from intact rock core testing or 10,150 ksi whichever is less.

7.14 SCOUR

This Section of the GDM is concerned with the soil and rock properties that are provided to the HEOR for use in scour analysis and design. According to the AASHTO Transportation Glossary (2009) scour is defined as:

> The washing away of streambed material by water channel flow. General (*contraction*) scour occurs as a result of a constriction in the water channel openings; local scour occurs as a result of local flow changes in a channel due to constrictions caused by the presence of bridge piers or abutments.

Scour is typically determined during 2 different hydraulic events; typically the 100-year flow (design flood) event and the 500-year flow (check flood) event. The scour caused by the design flood is used in the Strength and Service limit state checks; while the check flood is part of the Extreme Event II limit state check (see Chapter 8 for more discussion on limit states). Regardless of the flow event used to determine scour, certain soil and rock properties are required to be provided to the HEOR for use in analysis and design. According to the SCDOT Requirements for Hydraulic Design Studies (HDS) (2009), "Scour analysis will be performed for all bridge type *(bridge, wall and culverts)* structures *that are exposed to storm event waters*, utilizing USGS envelope curves and methods found in HEC-18."

7.14.1 Soil

As required in Chapter 4, grain-size analyses including hydrometers are to be conducted on samples within the potential scour zone both at the interior bents of the bridge as well as at the end bents of the bridge. For each grain-size test performed, the D_{50} shall be reported in millimeters to the HEOR.

7.14.2 Rock

In addition to classifying rock using the RMR and GSI systems, rock should also be classified in regards to the erosion potential of the rock to flowing water. Fortunately, most of the information previously used to describe the rock using the RMR and GSI systems is used to describe the erodibility of the rock. Arneson, Zevenbergen, Lagasse, and Clooper (2012) use the Erodibility Index to describe this erodibility of rock. The Erodibility Index, K, is determined using the following equation. The GEOR shall coordinate with the HEOR to determine when K is required and how K will be communicated between the GEOR and HEOR.

$$\boldsymbol{K = (M_s) * (K_b) * (K_d) * (J_s)} \qquad \textbf{Equation 7-108}$$

Where,

M_s = Intact rock mass strength parameter
K_b = Block size parameter
K_d = Shear strength parameter
J_s = Relative orientation parameter

The intact rock mass strength parameter, M_s, is related to the unconfined compressive strength as indicated in Table 7-23.

According to Arneson, et al. (2012):

> Joint spacing and the number of joint sets within a rock mass determines the value of K_b for rock. Joint spacing is estimated from borehole data by means of the rock quality designation (RQD) and the number of joint sets is represented by the joint set number (J_n). The values of the joint set numbers (J_n) are found in Table *7-24*. As seen in the table, J_n is a function of the number of joint sets, ranging from rock with no or few joints (essentially intact rock), to rock formations consisting of one to more than *4* joint sets. The classification accounts for rock that displays random discontinuities in addition to regular joint sets. Random joint discontinuities are discontinuities that do not form regular patterns. For example, rock with two joint sets and random discontinuities is classified as having *2* joint sets plus random. Having determined the values of RQD and J_n, K_b is calculated as:
>
> $$K_b = \frac{RQD}{J_n}$$ **Equation 7-109**
>
> The discontinuity or shear strength number (K_d) is the parameter that represents the relative strength of discontinuities in rock. In rock, it is determined as the ratio between joint wall roughness (J_r) and joint wall alteration (J_a), where J_r represents the degree of roughness of opposing faces of a rock discontinuity, and J_a represents the degree of alteration of the materials that form the faces of the discontinuity. Alteration relates to amendments of the rock surfaces, for example weathering or the presence of cohesive material between the opposing faces of a joint. Values of J_r and J_a can be found in Tables *7-25* and *7-26*. The values of K_d calculated with the information in these tables change with the relative degree of resistance offered by the joints. Increases in resistance are characterized by increases in the value of K_d. The shear strength of a discontinuity is directly proportional to the degree of roughness of opposing joint faces and inversely proportional to the degree of alteration.
>
> $$K_d = \frac{J_r}{J_a}$$ **Equation 7-110**

Table 7-23, Values of Rock Mass Strength Parameter, M_s (Arneson, et al. (2012))

Strength/Hardness		Recognition	Unconfined Compressive Strength (psi)	Mass Strength Number, M_s
Extremely Weak Rock	Very Soft Rock	Material crumbles under firm (moderate) blows from sharp end of geological pick	< 250	0.87
Very Weak Rock	Very Soft Rock	Can be peeled with knife	250 – 480	1.86
Weak Rock	Soft Rock	Can just be scraped and peeled with a knife	480 – 950	3.95
Medium Strong Rock	Soft Rock	Indentations up to 3/16-inch in specimen with firm (moderate) blows of pick point	950 – 1,915	8.39
Strong Rock	Hard Rock	Cannot be scraped or peeled with knife; specimen can be broken with hammer end of geological pick with a single firm (moderate) blow	1,915 – 3,825	17.70
Very Strong Rock	Very Hard Rock	Specimen breaks with hammer end of pick under more than 1 blow	3,825 – 7,685 7,685 – 15,300	35.0 70.0
Extremely Strong Rock	Extremely Hard Rock	Many blows with geological pick to break through intact material	> 30,750	280.0

Table 7-24, Rock Joint Set Number J_n (Arneson, et al. (2012))

Number of Joint Sets	Joint Set Number, J_n
Intact, no or few joint/fissures	1.00
One joint/fissure set	1.22
One joint/fissure set plus random	1.50
Two joint/fissure sets	1.83
Two joint/fissure sets plus random	2.24
Three joint/fissure sets	2.73
Three joint/fissure sets plus random	3.34
Four joint/fissure sets	4.09
Multiple joint/fissure sets	5.00

Table 7-25, Joint Roughness Number, J_r (Arneson, et al. (2012))

Condition of Joint	Joint Roughness Number, J_r
Stepped Joints/fissures	4.0
Rough or irregular, undulating	3.0
Smooth undulating	2.0
Slickensided undulating	1.5
Rough or irregular, planar	1.5
Smooth planar	1.0
Slickensided planar	0.5
Joints/fissures either open or containing relatively soft gouge of sufficient thickness to prevent joint/fissure wall contact upon excavation	1.0
Shattered or micro-shattered clays	1.0

Table 7-26, Joint Alteration Number, J_a (Arneson, et al. (2012))

Description of Gouge	Joint Alteration Number, J_a for Joint Separation (mm)		
	1.00[1]	1.01 – 5.00[2]	> 5.01[3]
Tightly healed, hard, non-softening impermeable filling	0.75	-	-
Unaltered joint walls, surface staining only	1.0	-	-
Slightly altered, non-softening, non-cohesive rock mineral or crushed rock filling	2.0	2.0	4.0
Non-softening, slightly clayey non-cohesive filling	3.0	6.0	10.0
Non-softening, strongly over-consolidated clay mineral filling, with or without crushed rock	3.0	6.0**	10.0
Softening or low friction clay mineral coatings and small quantities of swelling clays	4.0	8.0	13.0
Softening moderately over-consolidated clay mineral filling, with or without crushed rock	4.0	8.0**	13.0
Shattered or micro-shattered (swelling) clay gouge, with or without crushed rock	5.0	10.00**	18.0

[1]Joint walls effectively in contact.
[2]Joint walls come into contact after approximately 100 mm shear.
[3]Joint walls do not come into contact at all upon shear.
**Also applies when crushed rock occurs in clay gouge without rock wall contact.

Relative orientation, in the case of rock, is a function of the relative shape of the rock and its dip and dip direction relative to the direction of flow. The relative orientation parameter J_s represents the relative ability of earth material to resist erosion due to the structure of the ground. This parameter is a function of the dip and dip direction of the least favorable discontinuity (most easily eroded) in the rock with respect to the direction of flow, and the shape of the material units. These *2* variables (orientation and shape) affect the ease by which the stream can penetrate the ground and dislodge individual material units.

Conceptually, the function of the relative orientation parameter J_s incorporating shape and orientation is as follows. If rock is dipped against the direction flow, it will be more difficult to scour the rock than when it is dipped in the direction of flow. When it is dipped in the direction of flow, it is easier for the flow to lift the rock, penetrate underneath and remove it. Rock that is dipped against the direction of flow will be more difficult to dislodge. The shape of the rock, represented by the length to width ratio r, impacts the erodibility of rock in the following manner. Elongated rock will be more difficult to remove than equi-sided blocks of rock. Therefore, large ratios of r represent rock that is more difficult to remove because it represents elongated rock shapes. Values of the relative orientation parameter J_s are provided in Table *7-27*.

Table 7-27, Relative Orientation Parameter, J_s (Arneson, et al. (2012))

Dip Direction of Closer Spaced Joint Set	Dip Angle of Closer Spaced Joint Set (degrees)	Ratio of Joint Spacing, r			
Dip Direction	**Dip Angle**	**Ratio 1:1**	**Ratio 1:2**	**Ratio 1:4**	**Ratio 1:8**
180/0	90	1.14	1.20	1.24	1.26
In direction of stream flow	89	0.78	0.71	0.65	0.61
In direction of stream flow	85	0.73	0.66	0.61	0.57
In direction of stream flow	80	0.67	0.60	0.55	0.52
In direction of stream flow	70	0.56	0.50	0.46	0.43
In direction of stream flow	60	.050	0.46	0.42	0.40
In direction of stream flow	50	0.49	0.46	0.43	0.41
In direction of stream flow	40	0.53	0.49	0.46	0.45
In direction of stream flow	3	0.63	0.59	0.55	0.53
In direction of stream flow	20	0.84	0.77	0.71	0.67
In direction of stream flow	10	1.25	1.10	0.98	0.90
In direction of stream flow	5	1.39	1.23	1.09	1.01
In direction of stream flow	1	1.50	1.33	1.19	1.10
0/180	0	1.14	1.09	1.05	1.02
Against direction of stream flow	-1	0.78	0.85	0.90	0.94
Against direction of stream flow	-5	0.73	0.79	0.84	0.88
Against direction of stream flow	-10	0.67	0.72	0.78	0.81
Against direction of stream flow	-20	0.56	0.62	0.66	0.69
Against direction of stream flow	-30	0.50	0.55	0.58	0.60
Against direction of stream flow	-40	0.49	0.52	0.55	0.57
Against direction of stream flow	-50	0.53	0.56	0.59	0.61
Against direction of stream flow	-60	0.63	0.68	0.71	0.73
Against direction of stream flow	-70	0.84	0.91	0.97	1.01
Against direction of stream flow	-80	1.26	1.41	1.53	1.61
Against direction of stream flow	-85	1.39	1.55	1.69	1.77
Against direction of stream flow	-89	1.50	1.68	1.82	1.91
180/0	-90	1.14	1.20	1.24	1.26

Notes:
1. For intact material take J_s = 1.00
2. For values of r greater than 8 take J_s as for r = 8
3. If the flow direction, FD, is not in the direction of the true dip, TD, the effective dip, ED, is determined by adding the ground slope, GS, to the apparent dip AD: ED = AD + GS

7.15 DYNAMIC PROPERTIES – GENERAL

Soil and rock dynamic properties are required in developing the site characterization model. The site characterization model is used in the development of the site response analysis under the EE I limit state. Chapter 12 provides details on conducting a site response analysis. The static site characterization model (i.e., subsurface profile) has been developed in Section 7.4. This static model forms the basis for the dynamic site characterization model. The dynamic site characterization model consists of the following soil parameters:

- Initial (small strain) dynamic shear modulus.
- The small strain viscous damping ratio.
- Shear modulus reduction and strain-dependent hysteretic damping characteristics.
- Dynamic shear strength.
- Liquefaction (SSL) resistance parameters.
- Post-liquefaction (post-SSL) residual shear strength.

These parameters may be developed using the standard geotechnical exploration as indicated in Chapter 4. Further these parameters may be developed using more advanced in-situ testing techniques or from geophysical surveys. The CPTu is beneficial in the development of the dynamic site characterization because the CPTu can identify thin (~3-inch thick) layers that might be missed in the standard soil test boring. However, it is possible to discover these thin layers in standard soil test borings using continuous sampling techniques and careful logging of each sample obtained. These thin layers, if continuous, could consist of weak or potentially liquefiable soils that could lead to slope instability issues.

The ideal dynamic site characterization profile should extend to competent bedrock. Competent bedrock is defined as having a shear wave velocity of at least 2,500 feet per sec (ft/s), which is indicative, of the B-C Boundary (see Chapter 12). The physical properties (static and dynamic) of the soil should be known over the entire interval from the ground surface to the top of the competent rock. However, in most of the South Carolina, this will not be possible because of the depth of the B-C Boundary. Therefore, the physical properties (static and dynamic) shall be developed for the deepest testing location within the project limits. Because the B-C Boundary is typically found at deeper depths in the Coastal Plain (see Chapter 11), the profile from beneath the deepest boring to the top of the B-C Boundary may be established using previously obtained data. This data is now available on the SCDOT Website at: https://www.scdot.org/business/geotech.aspx look for the GIS Map button on this Webpage.

7.16 SOIL DYNAMIC PROPERTIES

The same parameters used to describe soil properties used in static analyses are the same for seismic analyses. During a geotechnical subsurface investigation conducted in accordance with this Manual, the following information should be obtained for each soil layer of interest:

- Soil classification.
- Index parameters (LL, PL, PI, *w*, etc.).
- Unit weight of the soil (γ_d, γ_{max}, etc.).
- Compressibility parameters (C_c, C_r, σ'_p, etc.).
- Shear strength parameters (ϕ, c, ϕ', c', etc.).

For a site response analysis the following seismic parameters will be required:

1. Consistency of the soil (e.g., relative density, D_r, or overconsolidation ratio, OCR).
2. Shear wave velocity, V_s, or initial (small strain) shear modulus, G_{max}.
3. Cyclic stress-strain behavior.
4. Residual shear strength, τ_r.

7.16.1 Soil Consistency

The consistency of the soil is composed of 2 indicators, relative density, D_r, for Sand-Like soils and the overconsolidation ratio, OCR, for Clay-Like soils. The D_r can be determined from the following equation,

$$D_r = \frac{e_{max}-e_o}{e_{max}-e_{min}} = \left(\frac{1-\frac{\gamma_{dmin}}{\gamma_{do}}}{1-\frac{\gamma_{dmin}}{\gamma_{dmax}}}\right) * 100\% \qquad \textbf{Equation 7-111}$$

Where,

e_{max} = Maximum void ratio
e_{min} = Minimum void ratio
e_o = In-situ void ratio
γ_{dmax} = Maximum dry unit weight
γ_{dmin} = Minimum dry unit weight
γ_{do} = In-situ dry unit weight

The information required to develop the D_r using Equation 7-111 must be obtained through relative density testing and consolidation testing (see Chapter 5); therefore, the D_r is normally correlated to the SPT N-value or the CPTu tip resistance (see 7.8.3). The D_r is normally used on cohesionless (coarse-grained) soils.

As discussed previously, the OCR is the ratio of the past effective overburden to the existing overburden and is typically used for Clay-Like (fine-grained) soils. Table 7-7 indicates that soils with OCRs greater than 1 are overconsolidated; however, in addition to the OCR, the sensitivity, S_t, is also required. S_t and OCR are used in Chapter 13 in the selection of the residual shear strength to be used in design. Soils with a S_t less than 5 use a cyclic residual shear strength, while soils with a S_t greater than or equal to 5 use the remolded shear strength.

7.16.2 Shear Wave Velocity/Initial Shear Modulus

One of the required soil properties needed to perform a soil response analysis is the soil stiffness. Soil stiffness is characterized by either small-strain shear-wave velocity, V_s, or small-strain shear modulus, G_{max}. The measurement of V_s is required in Chapter 4 and is measured in the field as indicated in Chapter 5 and reported as indicated in Chapter 6. The small-strain shear wave velocity, V_s, is related to small-strain shear modulus, G_{max}, by the following equation.

$$G_{max} = \rho * V_s^2 \qquad \textbf{Equation 7-112}$$

$$\rho = \frac{\gamma_t}{g}$$ **Equation 7-113**

Where,

V_s = Shear wave velocity of the soil, feet per sec (ft/s)
ρ = Mass density of the soil, (pound*second squared) per square foot ((lb*s^2)/ft^2)
γ_t = Total unit weight, pounds per cubic foot (lb/ft^3)
g = Acceleration due to gravity, 32.174 feet per second squared (ft/s^2)

The Theory of Elasticity relates G_{max} to the small strain Young's modulus, E_{max}, as a function of the Poisson's ratio, ν, using the following equation:

$$E_{max} = 2 * (1 + \nu) * G_{max}$$ **Equation 7-114**

Poisson's ratio for uncemented Sand-Like materials may be assumed to be approximately 0.35 and for Clay-Like materials Poisson's ratio may be assumed to be approximately 0.48. For transitional materials, review the PI as indicated in Table 7-6 and determine whether the soil will behave as either a Sand-Like material or a Clay-Like material. Alternately, the Poisson's ratio may be determined from the results of geophysical testing using the following equation:

$$\nu = 1 - \left\{ \frac{1}{2 * \left[1 - \left(\frac{V_s}{V_p} \right)^2 \right]} \right\}$$ **Equation 7-115**

Where,

V_s = Shear wave velocity, ft/sec
V_p = Compression wave velocity, ft/sec

Typical values of small-strain shear wave velocity, V_s, and small-strain shear modulus, G_{max}, for various soil types are shown in Table 7-28.

Table 7-28, Typical Small-Strain Shear Wave Velocity and Initial Shear Modulus (Based on Hunt (2005) and Kavazanjian, Matasovic, Hadj-Hamou, and Wang (1998))

Soil Type	Mass Density, ρ	Total Unit Weight, γ_t	Small-strain Shear Wave Velocity, V_S		Initial Shear Modulus, G_{max}	
	kg/m^3	pcf	m/s	ft/s	kPa	psi
Soft Clay	1,600	100	40 – 90	130 – 300	2,600 – 13,000	400 – 2,000
Stiff Clay	1,680	105	65 – 140	210 – 500	7,000 – 33,000	1000 – 5,700
Loose Sand	1,680	105	130 – 280	420 – 920	28,400 – 131,700	4,000 – 19,200
Dense Sand and Gravel	1,760	110	200 - 410	650 – 1,350	70,400 – 300,000	10,000 – 43,300
Residual Soil (IGM)	2,000	125	300 - 600	1,000 – 2,000	180,000 – 720,000	27,000 – 108,000
Piedmont Metamorphic and Igneous Rock (Highly – Moderately Weathered)	2,500	155	760 – 3,000	2,500 – 10,000	1,400,00 – 22,500,000	209,000 – 3,400,000
0 <RQD < 50 RQD = 65 (1) RQD = 80 (1) RQD = 90 (1) RQD = 100 (1)			600 760 1,500 2,500 3,400	2,000 2,500 5,000 8,000 11,000		
Basement Rock (Moderately Weathered to Intact)	2,600	165	> 3,400	> 11,000	> 30,000	> 4,300,000

(1) Typical Values, Linear interpolate between RQD values

When site-specific shear wave velocities, V_s, are not available or need to be supplemented, an estimation of the shear wave velocity, V_s, can be made by the use of correlations with in-situ testing such as the SPT or the CPTu. Procedures for estimating dynamic properties of soils have been developed by Andrus, Hayati, and Mohanan (2009). The procedures for correlating SPT and CPTu results with shear wave velocity, V_s, have been summarized in Sections 7.17.2.1 and 7.17.2.2, respectively. These correlated V_s are for Holocene age clean sands. In addition, V_s is also normalized to 1.0 tsf overburden (V_{s1}). Therefore, $(V_s)_{meas}$ requires correction for fines content and normalization for overburden using the following equations.

$$\left(V_{s,1,CS}\right)_{meas} = C_{Nvs} * K_{cvs} * (V_s)_{meas}$$ **Equation 7-116**

$$C_{Nvs} = \left(\frac{1}{\sigma'_v}\right)^{0.25} \leq 1.4$$ **Equation 7-117**

$$\left(V_{s,1}\right)_{meas} = C_{Nvs} * (V_s)_{meas}$$ **Equation 7-118**

K_{cvs} should only be applied to V_s less than or equal to 1,300 ft/sec. For V_s greater than 1,300 ft/sec, set K_{cvs} equal to 1.0.

Where,

σ'_{vo} = Effective normal stress, tsf

$$FC \leq 5\%$$

$$K_{cvs} = 1.0 \qquad \textbf{Equation 7-119}$$

$$5\% < FC < 35\%$$

$$K_{cvs} = 1 + (FC - 5) * T \qquad \textbf{Equation 7-120}$$

$$35\% \leq FC$$

$$K_{cvs} = 1 + 30 * T \qquad \textbf{Equation 7-121}$$

Where,

$$T = 0.009 - 0.0109 * \left[\frac{(V_{s,1})_{meas}}{328}\right] + 0.0038\left[\frac{(V_{s,1})_{meas}}{328}\right]^2 \qquad \textbf{Equation 7-122}$$

7.16.2.1 SPT - Shear Wave Velocity, V_s, Estimation

Andrus, et al. (2009) have developed a correlation for determining $V_{s,1,CS}$ from $N_{1,60,CS}$, where $N_{1,60,CS}$ is the standard penetration resistance normalized for overburden pressure and corrected for energy and fines content. $N_{1,60}$ is obtained from Equation 7-6. $N_{1,60,CS}$ is obtained from the following equation.

$$N_{1,60,CS} = \alpha + \beta * (N_{1,60}) \qquad \textbf{Equation 7-123}$$

Where,

$$FC \leq 5\%$$

$$\alpha = 0.0 \qquad \beta = 1.0 \qquad \textbf{Equation 7-124}$$

$$5\% \leq FC \leq 35\%$$

$$\alpha = e^{\left(1.76 - \frac{190}{FC^2}\right)} \qquad \beta = 0.99 + \frac{FC^{1.5}}{1000} \qquad \textbf{Equation 7-125}$$

$$35\% \leq FC$$

$$\alpha = 5.0 \qquad \beta = 1.2 \qquad \textbf{Equation 7-126}$$

Where,

$$(V_{s,1,CS})_{SPT} = 288 * (N_{1,60,CS})^{0.253} \qquad \textbf{Equation 7-127}$$

Where,

$(V_{s,1,CS})_{SPT}$ = Corrected and normalized shear wave velocity based on SPT N-values for uncemented, Holocene age sands, ft/sec

7.16.2.2 CPTu - Shear Wave Velocity, V_s, Estimation

Similarly to the N-value correlation presented previously for V_s, Andrus, et al. (2009) have developed a correlation between V_s and $q_{t,1,N,CS}$. Use Equation 7-9 to develop $q_{t,1}$. Normalization of $q_{t,1}$ is required and determined using the following equation.

$$q_{t,1,N} = \frac{q_{t,1}}{P_a}$$ **Equation 7-128**

Where,

$q_{t,1}$ = Corrected tip resistance, tsf

P_a = Atmospheric pressure, assumed to be 1.0 tsf

Therefore, $q_{t,1,N,CS}$ is determined using the following equation.

$$q_{t,1,N,CS} = K_c * q_{t,1,N}$$ **Equation 7-129**

Where,

$$I_c \leq 1.64$$

$$K_c = 1.0$$ **Equation 7-130**

$$I_c > 1.64$$ **Equation 7-131**

$$K_c = -0.403 * (I_c)^4 + 5.581 * (I_c)^3 - 21.631 * (I_c)^2 + 33.75 * (I_c) - 17.88$$

Where,

I_c = Soil Behavior Type (see Equation 7-17)

Once $q_{t,1,N,CS}$ is determined the $(V_{s,1,CS})_{CPT}$ may be determined using the following equation.

$$\left(V_{s,1,CS}\right)_{CPT} = 205 * \left(q_{t,1,N,CS}\right)^{0.231}$$ **Equation 7-132**

Where,

$(V_{s,1,CS})_{CPT}$ = Corrected and normalized shear wave velocity based on CPT tip resistances for uncemented, Holocene age sands, ft/sec

7.16.3 <u>Cyclic Stress-strain Behavior</u>

An additional requirement of the site response analysis is an understanding of how the cyclic loading of the design seismic event (EE I limit state) affects the stress-strain behavior of the soil.

This stress-strain behavior of soil is complex due to the cyclic ground motions induced by the design seismic event (i.e., strong motion). Figure 7-37 provides a schematic of this complexity. In Step 1, the soil element is sheared toward the right, while in Step 2, the soil element is sheared toward the left. While the soil element is sheared right and left, the shear wave that causes this shearing is considered to be vertically propagating and is considered to be normal to the ground surface.

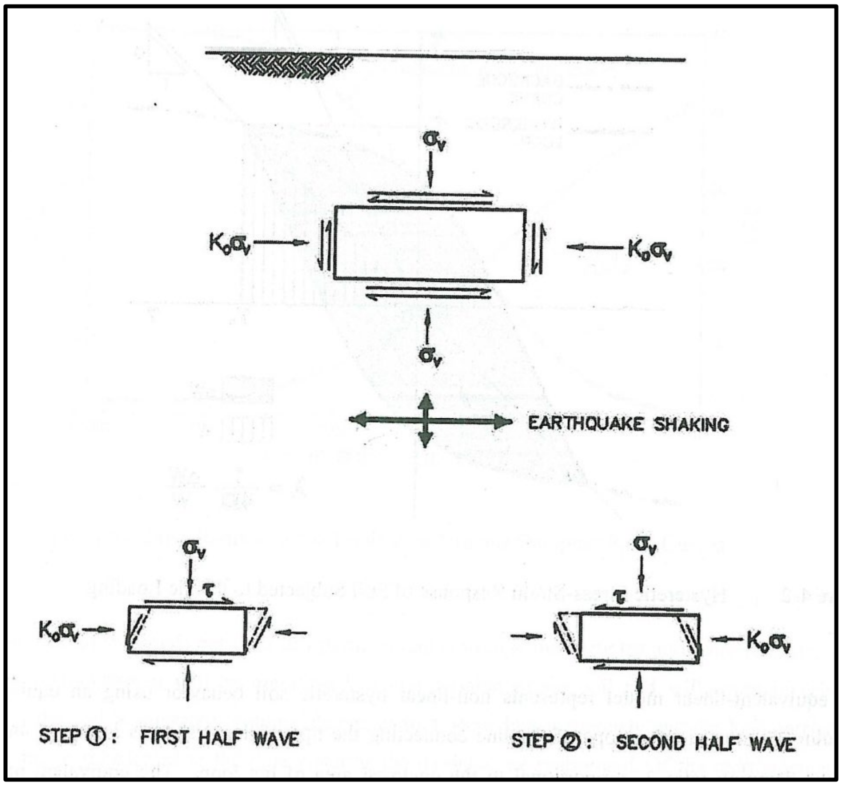

Figure 7-37, Stresses Induced in a Soil Element by Vertical Shear Wave (Kavazanjian, et al. (2011))

The cyclic shearing stress and strain, τ_c and γ_c, is generally considered to be the source of most of the damage caused by a seismic event. The response of the soil to cyclic shear stress and strain is commonly characterized by hysteresis. Figure 7-38 shows a hysterical loop for uniform cyclic loading. This hysteretic loop would apply to soil that is perfectly elastic, but soils are not perfectly elastic and will deform (strain) under the induced shear loading. Therefore, the hysteretic loop "leans" toward increasing shear strain, both positive and negative. A line drawn through the tips of each hysteretic loop is called a "backbone curve" (see Figure 7-38). This "backbone curve" further indicates that under cyclic loading soils will behave non-linearly (i.e., inelastically), but for easier understanding and modeling of the soil in these loading conditions an equivalent linear model is used. The following equation shows that the shear modulus, G, of the soil is related directly to the cyclic shear stress and strain:

$$G = \frac{\tau_c}{\gamma_c}$$ **Equation 7-133**

Where,

τ_c = Cyclic shear stress
γ_c = Cyclic shear strain

As can be seen in Figure 7-38, G_{max} occurs at zero shear strain (γ_c = 0) at least theoretically. However, in reviewing Equation 7-133 at γ_c = 0, G_{max} has no solution; therefore, G_{max} is normally determined at very small shear strains, $\gamma_c = 10^{-4}$ or smaller.

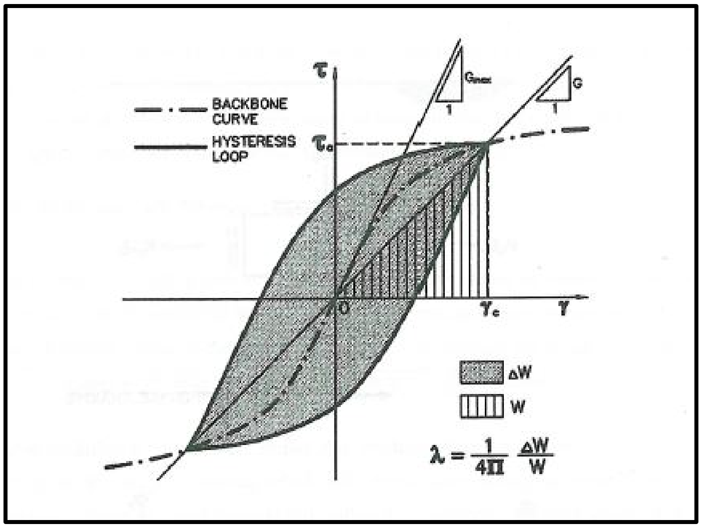

Figure 7-38, Hysteretic Stress-Strain Loop for Uniform Cyclic Loading (Kavazanjian, et al. (2011))

According to Kavazanjian, et al. (2011):

> The equivalent-linear model represents non-linear hysteretic soil behavior using an equivalent shear modulus, G, equal to the slope of the line connecting the tips of the hysteresis loop and an equivalent viscous damping ratio, λ, proportional to the enclosed areas of the loop. … The shear strain dependence of the equivalent modulus and damping ratio are described by the *modulus reduction* and *damping curves* shown *in Figure 7-39*.

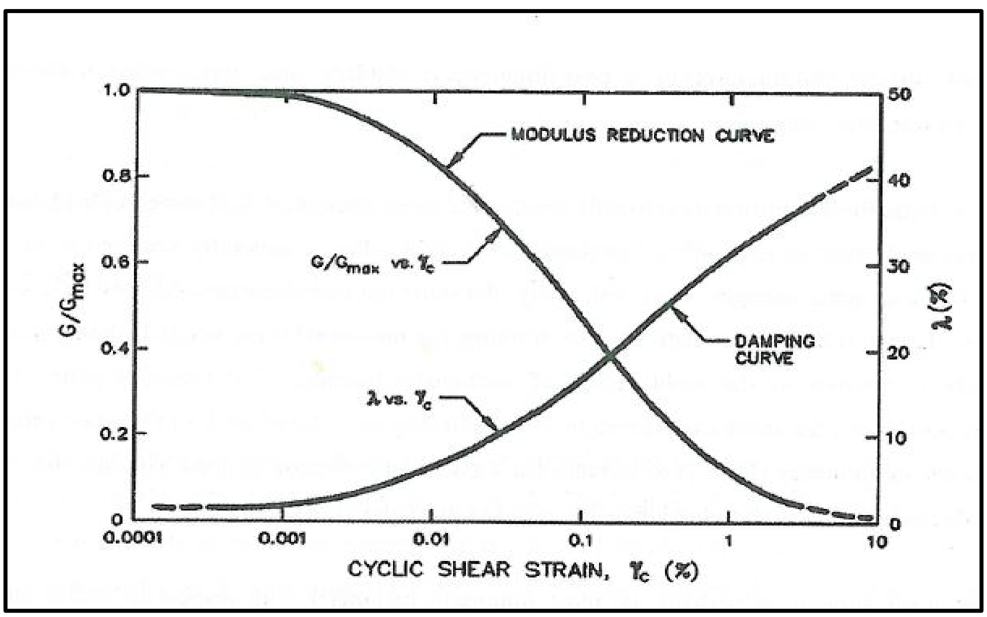

Figure 7-39, Example Shear Modulus Reduction and Damping Ratio Curve (Kavazanjian, et al. (2011))

7.16.3.1 Shear Modulus Reduction Curves

Shear modulus reduction curves are typically presented as normalized shear modulus, G/G_{max} versus cyclic shear strain (γ_c). These curves are used for performing site-specific response analyses. These shear modulus reduction curves are primarily influenced by the strain amplitude, confining pressure, soil type, and plasticity. The shear modulus reduction curve is typically obtained by using a hyperbolic model. A modified hyperbolic model by Stokoe, Darendeli, Andrus and Brown (1999) has been used by Andrus, et al. (2003) to develop shear modulus reduction curves for South Carolina soils. The hyperbolic model by Stokoe, et al. (1999) is shown in the following equation.

$$G/G_{max} = \frac{1}{1+\left(\frac{\gamma_c}{\gamma_{cr}}\right)^{\alpha}} \qquad \textbf{Equation 7-134}$$

Where,

α = Curvature coefficient

γ_c = Cyclic shear strain

γ_{cr} = Cyclic reference shear strain

The curvature coefficient, α, and cyclic reference shear strain, γ_{cr}, have been estimated by Andrus, et al. (2003) to provide the most accurate values for South Carolina Soils. Because it was found that the cyclic reference shear strain, γ_{cr}, varied based on effective confining pressure, γ_{cr} values are computed using cyclic reference shear strain at 1 tsf (100 kPa, 1 atm), γ_{cr1}, as shown in the following equation.

$$\gamma_{cr} = \gamma_{cr1} * \left(\frac{\sigma'_m}{P_a}\right)^{k} \qquad \textbf{Equation 7-135}$$

The mean confining pressure, σ'_m, at depth (Z) is computed as shown in Equation 7-136 in units of kPa, where P_a is the reference pressure of 100 kPa, and k is an exponent that varies based on the geologic formation and PI. Laboratory studies by Stokoe, Hwang, Darendeli, and Lee (1995) indicate that the mean confining pressure, σ'_m, values of each layer within a geologic unit should be within ±50 percent of the range of σ'_m for the major geologic unit.

$$\sigma'_m = \sigma'_v * \left(\frac{1+2*K_o}{3}\right) \qquad \textbf{Equation 7-136}$$

Where,

σ'_v = Vertical effective pressure, kPa

K_o = At-rest earth pressure coefficient

The K_o is defined as the ratio of horizontal effective pressure, σ'_h, to vertical effective pressure, σ'_v and is discussed in greater detail in Chapter 18. Values for the reference strain at 1 tsf (100 kPa, 1 atm), γ_{cr1}, curvature coefficient, α, and k exponent are provided for South Carolina soils based on Andrus, et al. (2003) in Table 7-29.

Table 7-29, Recommended Values γ_{cr1}, α, and k for SC Soils (Andrus, et al. (2003))

Geologic Age and Location of Deposits [(1)]	Variable	Soil Plasticity Index, PI (%)					
		0	15	30	50	100	150
Holocene	γ_{cr1} (%)	0.073	0.114	0.156	0.211	0.350	0.488
	α	0.95	0.96	0.97	0.98	1.01	1.04 [(2)]
	k	0.385	0.202	0.106	0.045	0.005	0.001 [(2)]
Pleistocene (Wando)	γ_{cr1} (%)	0.018	0.032	0.047	0.067	0.117	0.166
	α	1.00	1.02	1.04	1.06	1.13	1.19
	k	0.454	0.402	0.355	0.301	0.199	0.132
Tertiary Ashley Formation (Cooper Marl)	γ_{cr1} (%)	---	---	0.030 [(2)]	0.049	0.096 [(2)]	---
	α	---	---	1.10 [(2)]	1.15	1.28	---
	k	---	---	0.497 [(2)]	0.455	0.362 [(2)]	---
Tertiary (Stiff Upland Soils)	γ_{cr1} (%)	---	---	0.023	0.041 [(2)]	---	---
	α	---	---	1.00	1.00 [(2)]	---	---
	k	---	---	0.102	0.045 [(2)]	---	---
Tertiary (All soils at SRS except Stiff Upland Soils)	γ_{cr1} (%)	0.038	0.058	0.079	0.106	0.174 [(2)]	---
	α	1.00	1.00	1.00	1.00	1.00 [(2)]	---
	k	0.277	0.240	0.208	0.172	0.106 [(2)]	---
Tertiary (Tobacco Road, Snapp)	γ_{cr1} (%)	0.029	0.056	0.082	0.117	0.205 [(1)]	---
	α	1.00	1.00	1.00	1.00	1.00 [(1)]	---
	k	0.220	0.185	0.156	0.124	0.070 [(1)]	---
Tertiary (Soft Upland Soils, Dry Branch, Santee, Warley Hill, Congaree)	γ_{cr1} (%)	0.047	0.059	0.071	0.086	0.125 [(1)]	---
	α	1.00	1.00	1.00	1.00	1.00 [(1)]	---
	k	0.313	0.299	0.285	0.268	0.229 [(1)]	---
Residual Soil and Saprolite	γ_{cr1} (%)	0.040	0.066	0.093 [(1)]	0.129 [(1)]	---	---
	α	0.72	0.80	0.89	1.01 [(1)]	---	---
	k	0.202	0.141	0.099	0.061 [(2)]	---	---

[(1)] SRS = Savannah River Site
[(2)] Tentative Values – Andrus et al. (2003)

The procedure for computing the G/G_{max} correlation using Equation 7-134 is provided in Table 7-30.

Table 7-30, Procedure for Computing G/G_{max}

Step	Procedure Description
1	Perform a geotechnical subsurface exploration and identify subsurface soil geologic units, approximate age, and formation.
2	Develop soil profiles based on geologic units, soil types, average PI, and soil density. Subdivide major geologic units to reflect significant changes in PI and soil density. Identify design ground water table based on seasonal fluctuations and artesian pressures.
3	Calculate the average σ'_m and determine the corresponding ±50% range of σ'_m for each major geologic unit using Equation 7-136.
4	Calculate σ'_m for each layer within each major geologic unit. If the values for σ'_m of each layer are within a geologic unit's ±50% range of σ'_m (Step 3) then assign the average σ'_m for the major geologic unit (Step 3) to all layers within it. If the σ'_m of each layer within a geologic unit is not within the ±50% range of σ'_m for the major geologic unit, then the geologic unit needs to be "subdivided" and more than one average σ'_m needs to be used, provided the σ'_m remain within the ±50% range of σ'_m for the "subdivided" geologic unit.
5	Select the appropriate values for each layer of cyclic reference strain, γ_{cr1}, at 1 tsf (1 atm), curvature coefficient, α, and k exponent from Table 7-29. These values may be selected by rounding to the nearest PI value in the table or by interpolating between listed PI values in the table.
6	Compute the cyclic reference strain, γ_{cr}, based on Equation 7-135 for each geologic unit (or "subdivided" geologic unit) that has a corresponding average σ'_m.
7	Compute the design shear modulus reduction curves (G/G_{max}) for each layer by substituting cyclic reference strain, γ_{cr}, and curvature coefficient, α, for each layer using Equation 7-134. Tabulate values of normalized shear modulus, G/G_{max} with corresponding cyclic shear strain, γ_c, for use in a site-specific response analysis.

7.16.3.2 Equivalent Viscous Damping Ratio Curves

Equivalent Viscous Damping Ratio curves are presented in the form of a Soil Damping Ratio, λ[1] vs. Shear Strain, γ. The Soil Damping Ratio represents the energy dissipated by the soil and is related to the stress-strain hysteresis loops generated during cyclic loading. Energy dissipation or damping is due to friction between soil particles, strain rate effects, and nonlinear behavior of soils. The damping ratio is never zero, even when soils are straining within the linear elastic range of the cyclic loading. The damping ratio, λ, is constant during the linear elastic range of the cyclic loading and is referred to as the small-strain material damping, λ_{min}. The small-strain material damping, λ_{min}, can be computed using the equations developed by Stokoe, et al. (1995).

$$\boldsymbol{\lambda_{min} = \lambda_{min1} * \left(\frac{\sigma'_m}{P_a}\right)^{-0.5*k}} \qquad \textbf{Equation 7-137}$$

Where λ_{min1} is the small-strain damping at σ'_m of 1 tsf (1 atm). The mean confining pressure, σ'_m, at depth (Z) is computed as shown in Equation 7-136 in units of kPa. The k exponent is provided for South Carolina soils based on Andrus, et al. (2003) in Table 7-29. A relationship for λ_{min1}

[1]Editor's Note: In the previous versions of this Manual, the Soil Damping Ratio was identified using "D", as indicated in Andrus, et al. (2003). The Soil Damping Ratio has also been identified using "ξ" in Kramer (1996) and "λ" in Kavazanjian, et al. (2011). To be consistent with current NHI standards "λ" will be used to identify Soil Damping Ratio in this version of the GDM.

based on soil plasticity index, PI, and fitting parameters "a" and "b" for specific geologic units has been developed by Darendeli (2001) as indicated in Figure 7-40. Values for λ_{min1}, small-strain damping @ σ'_m = 1 atm are provided for South Carolina soils based on Andrus, et al. (2003) in Table 7-33.

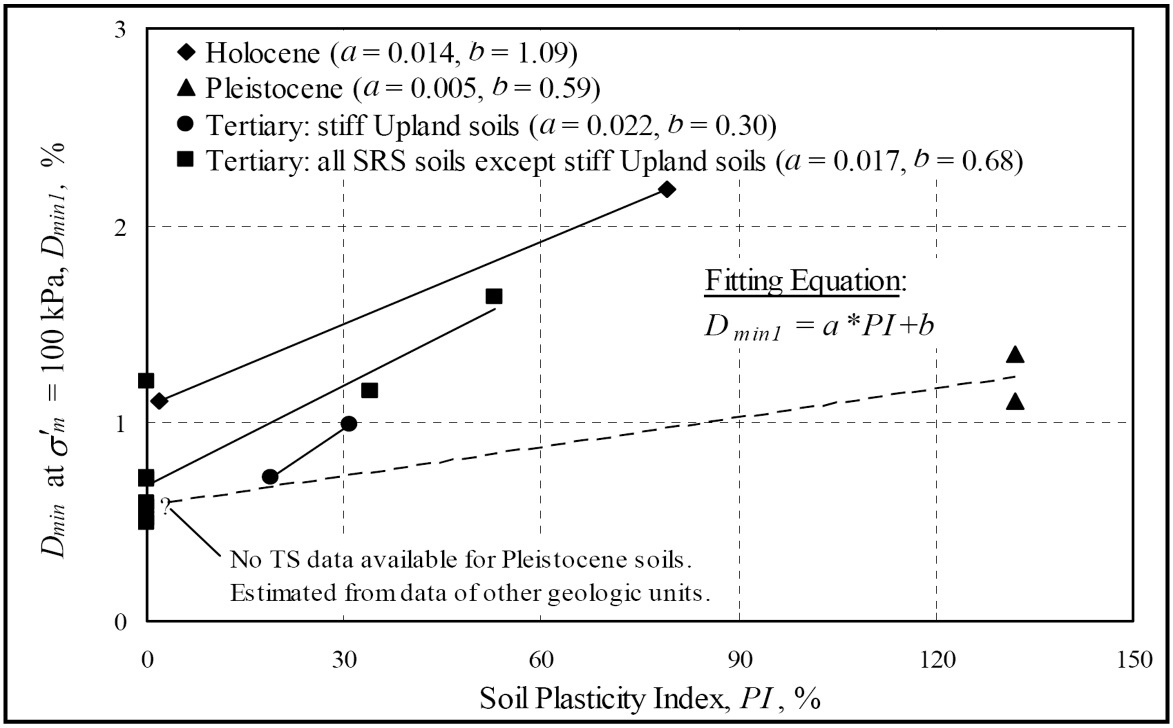

Note: $D_{min1} = \lambda_{min1}$

Figure 7-40, λ_{min1}, Small-Strain Damping @ σ'_m = 1 atm (Andrus, et al. (2003))

Table 7-31, Recommended Value λ_{min1} (%) for SC Soils (Andrus, et al. (2003))

Geologic Age and Location of Deposits	Soil Plasticity Index, PI (%)					
	0	15	30	50	100	150
Holocene	1.09	1.29	1.50	1.78	2.48	3.18 (1)
Pleistocene (Wando)	0.59	0.66	0.73	0.83	1.08	1.32
Tertiary Ashley Formation (Cooper Marl)	---	---	1.14 (1)	1.52 (1)	2.49 (1)	---
Tertiary (Stiff Upland Soils)	---	---	0.98	1.42 (1)	---	---
Tertiary (All soils at SRS except Stiff Upland Soils)	0.68	0.94	1.19	1.53	2.37 (1)	---
Tertiary (Tobacco Road, Snapp)	0.68	0.94	1.19	1.53	2.37 (1)	---
Tertiary (Soft Upland Soils, Dry Branch, Santee, Warley Hill, Congaree)	0.68	0.94	1.19	1.53	2.37 (1)	---
Residual Soil and Saprolite	0.56 (1)	0.85 (1)	1.14 (1)	1.52 (1)	---	---

(1) Tentative Values – Andrus, et al. (2003)

Data compiled by the University of Texas at Austin (UTA) for ($\lambda - \lambda_{min}$) vs. (G/G_{max}) is plotted in Figure 7-41.

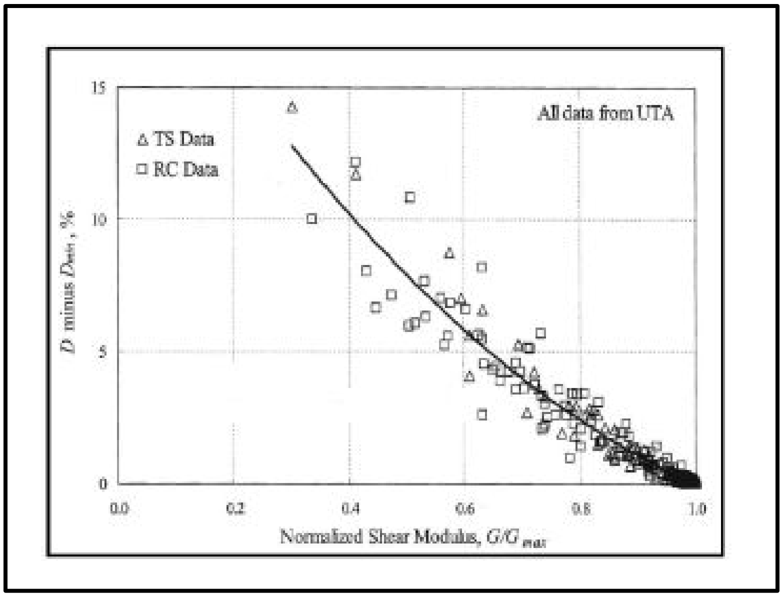

Note: D = λ

Figure 7-41, ($\lambda - \lambda_{min}$) vs. (G/G_{max}) Relationship (Andrus, et al. (2003))

Equation 7-137 represents a best-fit equation (UTA Correlation) of the observed relationship of ($\lambda - \lambda_{min}$) vs. (G/G_{max}) indicated below:

Equation 7-138

$$\lambda - \lambda_{min} = 12.2 * \left(\frac{G}{G_{max}}\right)^2 - 34.2 * \left(\frac{G}{G_{max}}\right) + 22.0$$

If we substitute Equation 7-134 into Equation 7-138 and solve for the damping ratio, λ, the Equivalent Viscous Damping Ratio curves can be generated using the following equation.

Equation 7-139

$$\lambda = \lambda_{min} + 12.2 * \left[\frac{1}{1 + \left(\frac{\gamma_c}{\gamma_{cr}}\right)^{\alpha}}\right]^2 - 34.2 * \left[\frac{1}{1 + \left(\frac{\gamma_c}{\gamma_{cr}}\right)^{\alpha}}\right] + 22.0$$

Where values of reference strain, γ_{cr}, are computed using Equation 7-135.

The procedures for using Equation 7-139 are provided in Table 7-32.

Table 7-32, Procedure for Computing Damping Ratio

Step	Procedure Description
1	Perform a geotechnical subsurface exploration and identify subsurface soil geologic units, approximate age, and formation.
2	Develop soil profiles based on geologic units, soil types, average PI, and soil density. Subdivide major geologic units to reflect significant changes in PI and soil density. Identify design ground water table based on seasonal fluctuations and artesian pressures.
3	Calculate the average σ'_m and determine the corresponding $\pm$50% range of σ'_m for each major geologic unit using Equation 7-136.
4	Calculate σ'_m for each layer within each major geologic unit. If the values for σ'_m of each layer are within a geologic unit's $\pm$50% range of σ'_m (Step 3) then assign the average σ'_m for the major geologic unit (Step 3) to all layers within it. If the σ'_m of each layer within a geologic unit is not within the $\pm$50% range of σ'_m for the major geologic unit, then the geologic unit needs to be "subdivided" and more than one average σ'_m needs to be used, provided the σ'_m remain within the $\pm$50% range of σ'_m for the "subdivided" geologic unit.
5	Select appropriate small-strain material Damping @ σ'_m = 1 atm, λ_{min1}, from Table 7-31 for each layer within a geologic unit.
6	Compute the small-strain material Damping, λ_{min}, for each layer within a geologic unit using Equation 7-137.
7	Select the appropriate values for each layer of cyclic reference strain, γ_{cr1}, @ σ'_m = 1atm , curvature coefficient, α, and k exponent from Table 7-29. These values may be selected by rounding to the nearest PI value in the table or by interpolating between listed PI values in the table.
8	Compute the cyclic reference strain, γ_{cr}, based on Equation 7-135 for each geologic unit that has a corresponding average σ'_m.
9	Compute the design equivalent viscous damping ratio curves (λ) for each layer by substituting cyclic reference strain, γ_{cr}, and curvature coefficient, α, and small-strain material Damping, λ_{min}, for each layer using Equation 7-139. Tabulate values of Soil Damping Ratio, λ, with corresponding cyclic shear strain, γ_c, for use in a site-specific site response analysis.

7.16.3.3 Alternate Dynamic Property Correlations

7.16.3.3.1 Soil Stiffness

The SPT and CPTu shear wave, V_s, correlations provided in Sections 7.17.2.1 and 7.17.2.2 are based on studies performed by Andrus, et al. (2009) for South Carolina soils. If the Andrus, et al. (2009) shear wave correlations are not appropriate (i.e., embankment fill) for the soils encountered at a specific project site, the GEOR can use alternate correlations. Documentation is required explaining the use of the alternate correlation and that the correlation is nationally or regionally recognized. Acceptable correlations for G_{max} that can be used are listed in Table 7-33 and may be substituted into rearranged Equation 7-112.

Table 7-33, Alternate Correlations for Determining Soil Stiffness Based on G_{max}

Reference	Correlation Equation	Units	Comments
Seed, Wong, Idriss and Tokimatsu (1986)	$G_{max} = 220 * (K_2)_{max} * (\sigma'_m)^{0.5}$ $(K_2)_{max} \approx 20 * (N_{1,60})^{0.33}$	kPa	$(K_2)_{max} \approx$ 30 for loose sands and 75 for very dense sands; $\approx$ 80-180 for dense well graded gravels; Limited to cohesionless soils
Imai and Tonouchi (1982)	$G_{max} = 15,560 * (N_{60})^{0.68}$	kPa	Limited to cohesionless soils
Hardin (1978)	$G_{max} = \left(\frac{625}{\chi}\right) * (K)^{0.5} * OCR^k$ $\chi = 0.3 + 0.7 * e_o^2$ $K = (P_a * \sigma'_m)^{0.5}$	kPa (1)	Limited to cohesive soils P_a = atmospheric pressure P_a and σ'_m in kPa
Jamiolkowski, Leroueil, and Lo Presti (1991)	$G_{max} = \left(\frac{625}{e_o^{1.3}}\right) * K * OCR^k$ $K = (P_a * \sigma'_m)^{0.5}$	kPa (1)	Limited to cohesive soils P_a and σ'_m in kPa
Mayne and Rix (1993)	$G_{max} = 99.5 * (P_a)^{0.305} * \left(\frac{q_c^{0.695}}{e_o^{1.13}}\right)$	kPa	Limited to cohesive soils P_a and q_c in kPa

(1) The parameter k is related to the plasticity index, PI, as follows:

PI	k	PI	k
0	0.00	60	0.41
20	0.18	80	0.48
40	0.30	>100	0.50

7.16.3.3.2 Shear Modulus Reduction Curves

The shear modulus reduction curves provided in Section 7.17.3.1 are based on studies performed by Andrus, et al. (2009). If the Andrus, et al. (2009) shear modulus reduction curves are not appropriate (i.e., embankment fill) for the soils encountered at a specific project site, the GEOR may use alternate shear modulus reduction curve correlations. Documentation is required explaining the use of the alternate curve and that the alternate curve is nationally or regionally recognized. Acceptable correlations that may be used are listed below:

- Andrus, Zhang, Ellis and Juang (2003)
- Seed and Idriss (1970)
- Vucetic and Dobry (1991)
- Ishibashi and Zhang (1993)
- Idriss (1990)
- Seed et al. (1986)

7.16.3.3.3 Equivalent Viscous Damping Ratio Curves

The equivalent viscous damping ratio curves provided in Section 7.17.3.2 are based on studies performed by by Andrus, et al. (2009). If the by Andrus, et al. (2009) equivalent viscous damping ratio curves are not appropriate (i.e., embankment fill) for the soils encountered at a project site the GEOR may use alternate equivalent viscous damping ratio curves. Documentation is required explaining the use of the alternate curve and that the alternate curve is nationally or regionally recognized. Acceptable correlations that may be used are listed below:

- Andrus, Zhang, Ellis and Juang (2003)
- Seed et al. (1986)
- Idriss (1990)
- Vucetic and Dobry (1991)

7.16.4 Cyclic Residual Shear Strength

Cyclic residual shear strengths are an important element in the evaluation of seismic slope stability. Two different residual shear strengths may be developed depending on whether the soils are susceptible to soil shear strength loss or not. The use of residual shear strengths in the Service or Strength limit states is not anticipated for slope stability analysis. However, the residual shear strengths discussed previously in this Chapter should be used for those soils that are not susceptible to soil shear strength loss, but are anticipated to undergo significant movement (typically greater than 10 inches) caused by the induced seismic motion. Typically these soils are anticipated to be above the groundwater level. Chapter 13 provides the methods for determining the residual shear strength of soils that will undergo shear strength losses. Chapter 14 provides the discussion of when to use these residual shear strengths.

7.17 ROCK DYNAMIC PROPERTIES

According to Kavazanjian, et al. (2011):

> In a seismic analysis, rock may be treated as either a linear elastic material with a constant shear modulus and no damping or as an equivalent linear material with an initial small strain modulus, a slight potential for modulus degradation, and a small amount of damping. The elastic modulus for the rock mass is generally based upon either shear wave velocity measurements or, in cases where the value of the modulus is not critical (i.e., when the modulus is merely used to characterize the impedance contrast at the bottom of a soil column), using typical properties. Modulus reduction and damping typically based upon generic equivalent linear modulus reduction and damping curves (e.g., the generic curves for soft rock from Silva, et al. (1996)).

7.18 ELECTRO-CHEMICAL PROPERTIES

The GEOR is required to test soil and water, both surface and subsurface as required, to determine the electro-chemical properties of the respective materials. Two general environments are established:

- Aggressive
- Non-aggressive

The SCDOT BDM (2006) defines the substructure “as any component or element located below the bearings.” The superstructure is defined as the “bearings and all of the components and elements resting upon them.” For superstructures the environmental classification will be determined by the SEOR. Substructures and ERSs are classified as indicated in Table 7-34.

Table 7-34, Criteria for Substructure and ERS Environmental Classifications

Environmental Classification	Electro-Chemical Component	Units	Soil	Water
Aggressive (if any of these conditions exist)	pH	-	< 5.5	< 5.5
	Cl	ppm[1]	> 500	> 500
	SO_4	ppm[1]	> 1,000	> 500
	Resistivity	Ohm-cm	< 2,000	< 5,000
Non-aggressive	This classification must be used at all sites not meeting the requirements for Aggressive Environments			
pH = acidity ($-\log_{10}H^+$; potential of hydrogen); Cl = chloride content; SO_4 = sulfate content				

[1]ppm (part per million) = mg/L (milligram per liter)

These criteria do not apply to the reinforced fill materials of MSE walls, RSSs or reinforced embankments; see the appropriate STS.

7.19 SATURATION

Soils exist in one of two states in nature either fully saturated or partially saturated. Spangler and Handy (1982) define saturation as the volume of water to the volume of voids.

$$S = \frac{V_w}{V_v} * 100 \qquad \textbf{Equation 7-140}$$

Where:

V_w = Volume of water, ft^3

V_v = Volume of voids, ft^3

Determining the degree of saturation is extremely difficult even using laboratory testing procedures; however, soils that are partially saturated will behave differently than soils that are fully saturated. For instance Clay-Like soils that are partially saturated may not take as long to settle as fully saturated soils and partially saturated Sand-Like soils may not undergo SSL as readily if at all. Therefore determining the degree of saturation can have serious consequence to SCDOT projects. In using this approach the GEOR should take into account the local soils condition as well as the regional geology.

As indicated previously, determining the degree of saturation is difficult. Because of this difficulty Skempton (1954) developed 2 pore pressure parameters that related the change in pore pressure (Δu) to the changes in the principle stresses ($\Delta\sigma_1$ and $\Delta\sigma_3$). Skempton (1954) designated these parameters as A and B. The pore pressure coefficient B is directly related to saturation, such that when B is 1 (B =1) the soil is saturated and when B is 0 (B = 0) the soil is unsaturated. The pore pressure coefficient B is typically determined in the laboratory; however, Kokusho (2000) has related V_p and B. Kokusho (2000) indicates that when a soil is completely saturated V_p will be approximately 4,600 feet per second and B is 1 (i.e., V_p = 4,600 feet per second therefore B = 1). Kokusho (2000) recommended that soil with a V_p of 90 percent of the Vp of water (i.e., V_p = 4,600 feet per second) that a B-value of 0.95 be assumed to be fully saturated. In other words if V_p = 4,140 feet per second, then B = 0.95. Therefore, this Manual will consider a soil to be fully saturated if the V_p is greater than or equal to 4,150 feet per second. However, a V_p greater than 3,500 feet per second will be anticipated to undergo SSL.

7.20 REFERENCES

American Association of State Highway and Transportation Officials, (2020), LRFD Bridge Design Specifications Customary U.S. Units, 9th Edition, American Association of State Highway and Transportation Officials, Washington, D.C.

American Association of State Highway and Transportation Officials, (2009), Transportation Glossary, 4th Edition, American Association of State Highway and Transportation Officials, Washington, D.C.

Arneson, L. A., Zevenbergen, L. W., Lagasse, P. F., and Clooper, P. E., (2012), Evaluating Scour at Bridges, Hydraulic Engineering Circular 18, (Publication No. FHWA-HIF-12-003), 5th Edition, US Department of Transportation, Office of Bridge Technology, Federal Highway Administration, Washington, D.C.

Andrus, R. D., Hayati, H., and Mohanan, N. P., (2009), "Correcting Liquefaction Resistance for Aged Sands Using Measured to Estimated Velocity Ratio." *Journal of Geotechnical and Geoenvironmental Engineering*, ASCE, Volume 135, Issue 6, pp. 735-744.

Andrus, R. D., Zhang, J., Ellis, B. S., and Juang, C. H., (2003), "Guide for Estimating the Dynamic Properties of South Carolina Soils for Ground Response Analysis", South Carolina Department of Transportation, SC-DOT Research Project No. 623, FHWA-SC-03-07.

Boulanger, R. W. (2003), "Relating Ka to a Relative State Parameter Index." *Journal of Geotechnical and Geoenvironmental Engineering*, ASCE, Volume 129, Issue 8, pp. 770-773.

Canadian Geotechnical Society, (2006), Canadian Foundation Engineering Manual, 4th Edition.

Cetin, K. O., Seed, R. B., Der Kiureghian, A., Tokimatsu, K., Harder, L. F., Kayen, R. E. and Moss, R. E. S., (2004), "Standard Penetration Test-Based Probabilistic and Deterministic Assessment of Seismic Soil Liquefaction Potential", *Journal of Geotechnical and Geoenvironmental Engineering*, ASCE, Vol. 130, Issue 12, pp. 1314-1340.

Darendeli, M. B., (2001), Development of a New Family of Normalized Modulus Reduction and Material Damping Curves, Ph.D. Dissertation, The University of Texas at Austin, Austin, TX.

Das, B. M., (1997), Advanced Soil Mechanics, 2nd Edition, Taylor & Francis, Washington, DC.

Department of Defense, Department of the Navy, Naval Facilities Engineering Command, (1986), Soil Mechanics – Design Manual 7.1, (Publication No. NAVFAC DM-7.01), Alexandria, Virginia.

Duncan, J. M. and Buchignani, A. L., (1976), An Engineering Manual for Settlement Studies, Virginia Polytechnic Institute and State University.

Duncan, J. M. and Wright, S. G., (2005), Soil Strength and Slope Stability, John Wiley & Sons, Inc., Hoboken, New Jersey.

Duncan, J. M., Wright, S. G. and Brandon, T. L., (2014), Soil Strength and Slope Stability,2nd Edition, John Wiley & Sons, Inc., Hoboken, New Jersey.

Hardin, B. O., (1978), "The Nature of Stress-Strain Behavior of Soils", Proc. Earthquake Engineering and Soil Dynamics, ASCE, Pasadena, California, Vol. 1, pp. 3-89.

Hatanaka, M. and Uchida, A., (1996), “Empirical Correlation Between Penetration Resistance and Internal Friction Angle of Sandy Soils”*, Soils and Foundations*, Japanese Geotechnical Society, Volume 36, No. 4, pp. 1-9.

Hoek, E., (2007), Practical Rock Engineering, Rocscience, Available at: http://www.rocscience.com/education,hoeks_corner.

Hoek, E., Carranza-Torres, C., and Corkum, B., (2002), “Hoek-Brown Failure Criterion – 2002 Edition,” Mining and Tunnelling Innovation and Opportunity: Proceedings of the 5th North American Rock Mechanics Symposium and the 17th Tunnelling Association of Canada Conference : NARMS-TAC 2002, Toronto, Ontario, Canada.

Holtz, R. D. and Kovacs, W. D., (1981), An Introduction to Geotechnical Engineering, Prentice Hall, New Jersey.

Hunt, R. E., (2005), "Geotechnical Engineering Investigation Handbook”, 2nd Edition, Taylor & Francis, Boca Raton, Florida.

Idriss, I. M., (1990), "Response of Soft Soil Sites During Earthquakes", H. Bolton Seed Memorial Symposium Proceedings, Volume 2, BiTech, Vancouver, British Columbia, Canada.

Idriss, I.M. and Boulanger, R.W., (2008), “Soil Liquefaction During Earthquakes.” Earthquake Engineering Research Institute (EERI), EERI Monograph MNO-12.

Imai, T. and Tonouchi, K., (1982), "Correlation of N-Value with S-Wave Velocity and Shear Modulus", Proc. 2nd European Symposium on Penetration Testing, Amsterdam, The Netherlands, pp. 67-72.

Ishibashi, I. and Zhang, X. J., (1993), “Unified Dynamic Shear Moduli and Damping Ratios of Sand and Clay”, *Soils and Foundations,* Japanese Society of Soil Mechanics and Foundation Engineering, Volume 33, No. 1, pp. 182-191.

Jamiolkowski, M., Ladd, C. C., Germaine, J., and Lancellotta, R., (1985), “New Developments in Field and Lab Testing of Soils”, 11th International Conference on Soil Mechanics and Foundations Engineering Proceedings, Volume 1.

Jamiolkowski, M., Leroueil, S. and Lo Presti, D. C. F. (1991), "Theme Lecture: Design Parameters from Theory to Practice", Proc. Geo-Coast '91, Yokohama, Japan, pp. 1-41.

Jefferies, M. G. and Davies, M. P., (1993), “Use of CPTu to Estimate SPT N_{60},” Geotechnical Testing Journal, ASTM, Volume 16, Number 4, pp. 458-468.

Kavazanjian, E., Wang, J-N. J., Martin, G. R., Shamsabadi, A., Lam, I., Dickenson. S. E., and Hung, C. H., (2011), LRFD Seismic Analysis and Design of Transportation Geotechnical Features and Structural Foundations, Geotechnical Engineering Circular No. 3, (Publication No. FHWA-

NHI-11-032), US Department of Transportation, Office of Bridge Technology, Federal Highway Administration, Washington, D.C.

Kokushho, T. (2000), “Correlation of Pore-Pressure B-Value with P-Wave Velocity and Poisson’s Ratio for Imperfectly Saturated Sand or Gravel”, Soils and Foundations, Japanese Geotechnical Society, Vol. 40, No. 4., pp. 95 – 102.

Kramer, S. L., (1996), Geotechnical Earthquake Engineering, Prentice Hall, New Jersey.

Ladd, C. C., (1973), “Settlement Analysis of Cohesive Soils,” Research Report 71-2, No. 272, Department of Civil Engineering, MIT, Cambridge, MA.

Ladd, C. C., Foot, R., Ishihara, K., Schlosser, F., and Poulos, H. G. (1977). “Stress Deformation and Strength Characteristics.” Proceedings 9th International Conference on Soil Mechanics and Foundation Engineering, Volume 2, Tokyo, Japan.

Liao, S. S. C. and Whitman, R. V., (1986), “Overburden Correction Factors for SPT in Sand”, *Journal of Geotechnical Engineering*, ASCE, Volume 112, Issue 3, pp. 373-377.

Marchetti, S. (1997). “The Flat Dilatometer: Design Applications.” Proceedings, 3rd International Geotechnical Engineering Conference, Soil Mechanics and Foundations Research Laboratory, Cairo University, Egypt.

Marchetti, S., Monaco, P., Totani, G., and Calabrese, M., (2001) “The Flat Dilatometer Test (DMT) in soil investigations, A Report by the ISSMGE Committee TC16,” Proceedings In-Situ 2001, International Conference on In Situ Measurement of Soil Properties, Bali, Indonesia.

Marinos, P. and Hoek, E., (2000), “GSI: A Geologically Friendly Tool for Rock Mass Strength Estimation,” Proceedings, Geo-Engineering 2000, International Conference on Geotechnical and Geological Engineering, Melbourne, Australia.

Mayne, P. W. (2007), Cone Penetration Testing, NCHRP Synthesis 368, National Cooperative Highway Research Program, Transportation Research Board, Washington, DC.

Mayne, P. W. and Rix, G. J., (1993), "G_{max}-q_c, Relationships for Clays", *Geotechnical Testing Journal*, ASTM, Volume 16, No. 1, pp. 54-60.

Mayne, P. W., Christopher, B. R., and DeJong, J., (2002), Subsurface Investigations - Geotechnical Site Characterization, (Publication No. FHWA-NHI-01-031), US Department of Transportation, National Highway Institute, Federal Highway Administration, Washington, D.C.

McGregor, J. A. and Duncan, J. M., (1998) Performance and Use of the Standard Penetration Test in Geotechnical Engineering Practice, Virginia Polytechnic Institute and State University.

Mitchell, J. K., (1993), Fundamentals of Soil Behavior, 2nd Edition, John Wiley and Sons, Inc.

Munfakh, G., Arman, A., Samtani, N., and Castelli, R., (1997), Subsurface Investigations, (Publication No. FHWA-HI-97-021), US Department of Transportation, National Highway Institute, Federal Highway Administration, Washington D.C.

Munfakh, G., Kavazanjian, E., Matasovic, N., Hadj-Hamou, T., and Wang, J., (1998), Geotechnical Earthquake Engineering, Reference Manual, NHI Course No. 13239, (Publication No. FHWA HI-99-012), U.S. Department of Transportation, National Highway Institute, Federal Highway Administration, Arlington, Virginia.

Rausche, F., Thendean, G., Abou-matar, H., Linkins, G. E., and Goble, G. G., (1997), Determination of Pile Driveability and Capacity from Penetration Tests – Volume I: Final Report, (Report No. FHWA-RD-96-179), U. S. Department of Transportation, Office of Engineering R&D, Federal Highway Administration, McLean, Virginia.

Robertson, P. K., and Campanella, R. G., (1983), *Interpretation of Cone Penetration Tests, Canadian Geotechnical Journal*, Volume 20, Issue 4, pp. 718-745.

Roberston, P. K. and Cabal (Roberston) K. L., (2015), Guide to Cone Penetration Testing for Geotechnical Engineering, 6th Edition, Gregg Drilling and Testing, Signal Hill, California.

Sabatini, P. J., Bachus, R. C., Mayne, P. W., Schneider, J. A., and Zettler, T. E., (2002), Evaluation of Soil and Rock Properties, Geotechnical Engineering Circular No. 5, (Publication No. FHWA-IF-02-034). US Department of Transportation, Office of Bridge Technology, Federal Highway Administration, Washington, D.C.

Seed, H. B., and Idriss, I. M., (1970), “Soil Moduli and Damping Factors for Dynamic Response Analysis”, Report EERC 70-10, Earthquake Engineering Research Institute, Berkeley, CA.

Seed, H. B., Wong, R. T., Idirss, I. M., and Tokimatsu, K., (1986), “Moduli and Damping Factors for Dynamic Analysis of Cohesionless Soils”, *Journal of the Geotechnical Engineering Division,* ASCE, Volume 112, Issue 11, pp. 1016-1031.

Silva, W., Abrahamson, N. A., Toro, G. R., and Constantino, C., (1996), “Description and Validation of the Stochastic Ground Motion Model”, Report prepared for the Engineering Research and Applications Division, Department of Nuclear Energy, Pacific Engineering and Analysis, El Cerrito, California.

Skempton, A. W., (1954), “The Pore-Pressure Coefficients A and B”, Géotechnique, Volume 4, pp. 143-147

Sorensen, H. K. and Okkels, N., (2013), “Correlation between drained shear strength and plasticity index of undisturbed overconsolidated clays”, Challenges and Innovations in Geotechnics, Proceedings of the 18th International Conference on Soil Mechanics and Geotechnical Engineering, Paris, France.

South Carolina Department of Transportation, (2009), Requirements for Hydraulic Design Studies, South Carolina Department of Transportation, http://www.scdot.org/doing/technicalPDFs/hydraulic/requirements2009.pdf.

Spangler, M. G. and Handy, R. L., (1982), Soil Engineering, 4th Edition, Harper & Row.

Stark, T. D. and Eid, H. T., (1994), “Drained Residual Strength of Cohesive Soil”, *Journal of Geotechnical Engineering*, ASCE, Volume 120, Issue 5, pp. 856-871.

Stark, T. D. and Eid, H. T., (1997), "Slope Stability Analyses in Stiff Fissured Clays", *Journal of Geotechnical and Geoenvironmental Engineering*, ASCE, Volume 123, Issue 4, pp. 335-343.

Stark, T. D. and Hussain M., (2013), "Empirical Correlations: Drained Shear Strength for Slope Stability Analyses", *Journal of Geotechnical and Geoenvironmental Engineering*, ASCE, Volume 139, Issue 6, pp. 853-862.

Stokoe, K. H., II, Hwang, S. K., Darendeli, M. B., and Lee, N. J., (1995), "Correlation Study of Nonlinear Dynamic Soils Properties", final report to Westinghouse Savannah River Company, The University of Texas at Austin, Austin, TX.

Stokoe, K. H., II, Darendeli, M. B., Andrus, R. D., and Brown, L. T., (1999). "Dynamic Soil Properties: Laboratory, Field and Correlation Studies", *Proceedings, 2nd International Conference on Earthquake Geotechnical Engineering,* Vol. 3, Lisbon, Portugal, 811-845.

Terzaghi, K., Peck, R. B., and Mesri, G., (1996), Soil Mechanics In Engineering Practice, 3rd Edition, John Wiley & Sons, Inc., New York.

Tiwari, B. and Ajmera, B., (2012), "New Correlation Equations for Compression Index of Remolded Clays", *Journal of Geotechnical and Geoenvironmental Engineering*, ASCE, Volume 138, Issue 6, pp. 757-762.

Turner, J., (2006), Rock-Socketed Shafts for Highway Structure Foundations, NCHRP Synthesis 360, National Cooperative Highway Research Program, Transportation Research Board, Washington, D.C.

Vucetic, M., and Dobry, R., (1991), "Dynamic Effect of Soil Plasticity on Cyclic Response", *Journal of Geotechnical Engineering*, ASCE, Volume 117, No. 1, pp. 89-107.